KANSAS GEOLOGICAL SURVEY
OPEN-FILE REPORT 87-1

Interpretation of State-wide Gravity Survey of Kansas

by

Chi Kin Lam

KANSAS GEOLOGICAL SURVEY
1930 Constant Avenue
University of Kansas
Lawrence, KS 66047

INTERPRETATION OF STATE-WIDE GRAVITY SURVEY OF KANSAS

by
CHI KIN LAM
B.Sc., University of Hong Kong, 1975
M.S., Pittsburg State University, 1979

Submitted to
the Department of Physics
and Astronomy and the Faculty
of the Graduate School of the
University of Kansas in partial
fulfillment of the requirements for
the degree of Doctor of Philosophy.

Dissertation Committee:

Harold J. Yarger
Chairman

Carl McCamy

K-H-C-J

Dissertation defended:
September 5, 1986

ACKNOWLEDGMENT

I would like to thank my thesis advisor, Harold Yarger, for his patient guidance, support, and tolerance over the past few years. Many students carried out the gravity field work and their names are listed in the Kansas Geological Survey open file map, 'Bouguer Gravity Map of Kansas'. Robert Simpson of the USGS gave me a copy of the 'AIRYROOT' program, for which I am grateful. I appreciate very much the valuable time Drs. Ling, McEwlee, Stahl, and Wong spent on serving on my dissertation committee. The gravity survey of Kansas was supported principally by the Kansas Geological Survey, and in part by the Department of Energy under grant number DE-AS07-19E T27204, by the Nuclear Regulatory Commission under contract number AT (49-24)-2056, and by Three-D gravity, Inc. Yan Zhao, a Visiting Research Associate from the South China Sea Institute of Oceanology, Academia Sinica, also participated in the gravity field work.

TABLE OF CONTENTS

LIST OF TABLES

LIST OF FIGURES

LIST OF PLATES

ABSTRACT

Over 27,000 gravity stations were occupied throughout eastern and northwestern Kansas in this regional gravity survey. These gravity data were reduced using standard methods and some new quality control procedures. The resultant Bouguer gravity values were gridded and a map, contoured at a 1 mgal interval, was produced. Interpretation and data enhancement techniques such as trend surface analysis, spectral filtering, synthetic illumination, and computer forward modeling were applied to the data. Isostatic correction and combined analysis of gravity and magnetic data using Poisson's theorem were also carried out. The Midcontinent Geophysical Anomaly (MGA) in central Kansas clearly extends to at least the Oklahoma border and is underlain by a thinned crust and lithosphere. The abrupt decrease in amplitude, going from north to south, of the mid-continent gravity high in central Kansas is due to the more ductile character of the lithosphere in southern Kansas. The upper crust in eastern Kansas is anomalously thick giving rise to a broad negative isostatic and free-air anomaly. The correlation coefficients and derived magnetization to density contrasts for short wavelength gravity and magnetic anomalies show that the shallow basement rocks in northern and southern Kansas are quite distinct, which corresponds to the different basement age terranes. Analysis of long wavelength anomalies suggests an almost homogeneous crust at depth with no distinct age terranes. Many other local anomalies are identified and discussed.

CHAPTER ONE

INTRODUCTION

PURPOSE

The Kansas Geological Survey (KGS) has been conducting a regional gravity survey of the state for the past few years. This new gravity data supplements the Kansas regional aeromagnetic data and yields more information on the geology, crustal structure and early geologic history of the state.

Almost all of the surficial rocks found in Kansas are Phanerozoic sedimentary rocks. Underneath this thin layer (170 to 3300 meters) of younger sediments is the Precambrian basement, which is made up of predominantly igneous intrusives and clastic sediments. A regional gravity survey is sensitive to lateral density contrasts caused by structures and different rock types within the basement. The overlying sediments are in essence 'transparent' to the gravity field because of the following reasons. The sediments were generally deposited on a near-horizontal surface resulting in strata with little lateral density contrast. Within each stratum, the density is nearly uniform because the type of sedimentary deposition is largely influenced by the prevalent geologic environment. For contemporaneous sediments of the same type, the density is almost the same. This layer cake condition is sometimes perturbed by post-deposition crustal movement. It results in two sources of lateral density contrast, which are the sediment/sediment and sediment/basement contrasts. Because the density contrast

between the basement rocks and the sediments is usually larger than that between two different kinds of sediments, the resulting gravity anomaly caused by crustal movement can be attributed almost entirely to the basement relief (table 1 lists the densities of several common rocks).

Another common geologic event that would cause a lateral density contrast is when molten rock migrates upward from deep within the crust and is emplaced at or near the basement surface. It usually results in a sharp lateral density contrast between the intruded and host rock. Lateral changes in density due to different basement rock types are the source for most anomalies on a regional gravity map.

There may exist a few large amplitude localized anomalies caused by the sediments. However, these are usually of short wavelength and are largely filtered out by the large sampling distance ($\geqslant$1.6 km) in the present survey. Slowly varying sediment thickness may contribute a low amplitude long wavelength component to the regional gravity trend. Regional gravity measurements can be very effective in identifying basement faults because of the density contrast on either side of the fault.

INTRODUCTION TO METHODS OF INTERPRETATION

Although the Kansas gravity measurements are very accurate (one part in ten billion), it is sometimes difficult to discern subtle features on the gravity map. To aid in the interpretation, I have applied special processing techniques to enhance certain low

ROCK TYPE	DENSITY, GM/CC
Sedimentary rocks	
Shale	2.00 - 2.65
Limestone	2.25 - 2.80
Sandstone	2.20 - 2.70
Igneous rocks	
Granite	2.65 - 2.75
Diorite	2.70 - 2.95
Gabbro	2.80 - 3.10
Dunite	3.20 - 3.30

Table 1. Densities of rocks (after Garland, 1979).

amplitude features. These enhancement methods do not create any additional information that is not already in the data. They merely help to improve the signal-to-noise ratio and focus on the interesting geologic content of the signal.

In the following I give a brief account of the enhancement methods and the difficulties they help to overcome. These will be discussed in more detail in chapter five. There are two main problems that make gravity interpretation difficult. First, there are many density anomalies present and they give rise to interfering signals. It is essential to separate the desired signal from the 'noise'. I use trend surface fitting and spectral filtering techniques for anomaly separation. Second, there is a problem with displaying gravity measurements. A rectangular grid of the data is usually needed before any contour and/or color map can be generated. This gridding procedure invariably involves smoothing and interpolating the original data. Useful information may be obscured or lost in these processes. There are typically only a limited number of color intervals available on a color map. Small anomalies are sometimes embedded within one color interval and overlooked. The difficulty with displaying the data is partially alleviated by the removal of a regional trend using a trend surface fitting method. Synthetic illumination of the gravity data also helps to reveal subtle trends and lineaments.

After identifying an anomaly, computer forward modeling can be used to characterize the size, shape and density contrast of the causative body. A moving window application of Poisson's theorem to

gravity and magnetic data derives the ratio of the magnetization to density contrast of the anomalous body. Lastly, applying isostatic correction to the data removes the gravitational attraction of hypothetical crustal roots, which according to the Airy model, compensate for the surface topographic load. The readers may refer to Paterson and Reeves (1985), and Hinze (1985) for a review of the state-of-the-art of the gravity and magnetic methods.

THE GRAVITY METHOD

In the following paragraphs, I outline the underlying physical principles of the gravity method.

The average gravitational acceleration on the surface of the earth is approximately 980,000 mgals (1 gal = 1 cm/sec^2 = 1,000 mgals). Spatial and temporal variations of gravity are affected by latitude, elevation, local geology, density and temperature anomalies deep within the earth, flow of viscous mantle material, gravitational attraction of extra-terrestrial bodies (mainly the sun and the moon), solid earth tide, and others.

Newton's law of universal gravitation specifies the gravitation acceleration, g, on the surface of a rotating sphere of uniform density as,

$$g = (GM/|\vec{r}|^3)\,\vec{r} - \vec{w} \times (\vec{w} \times \vec{r})$$

where G is the gravitational constant,

M is the mass of the sphere,

$\vec{w}$ is the angular velocity of the sphere,

$\vec{r}$ is the radius vector of the sphere.

The actual gravitational field on the surface of the earth deviates somewhat from this simple relation for the following reasons. The figure of the earth is approximately an ellipsoid flattened at the poles. Due to the shorter distance to the center of mass of the earth, and a smaller centrifugal force with increasing latitude, gravity generally increases with latitude. Gravity usually

decreases with elevation because of its inverse squared dependency on $\vec{r}$. Gravity measurements taken at the surface of the earth are sensitive to lateral density changes within the earth. Therefore any geologic structures such as igneous plutons, rock terrane boundaries, salt domes, faults or dikes which result in a lateral density contrast, will give rise to a gravity anomaly detectable on the ground surface. A modern gravimeter is capable of measuring an anomaly as small as 5 microgals, although 100 microgals (0.1 mgal) is the limit of accuracy in most regional surveys because of uncertainties in elevation and location. The anomalies I discuss in this report are typically greater than 1.0 mgal.

Corrections as outlined below are applied to the gravity measurements to isolate the gravity signal caused by geologic structures. A reference gravity field of an ellipsoidal earth (International Association of Geodesy, 1967) is subtracted from the gravity measurement to account for the latitude effect. This simplistic earth model is used because the sole purpose here is to isolate the anomalies of geologic interest. A more refined reference field model will not significantly improve the definition of such anomalies, which are of much shorter wavelength than those of the reference field. Gravity measurements are adjusted to a sea level datum (free-air and Bouguer corrections). Chapter 4 discusses more quantitatively the corrections applied in the reduction of gravity data.

Limitations of the gravity method are as follows. Gravity measurements taken at x km spacing on the ground surface are capable

of discerning anomalies at least x km wide. In the present survey the east-west and north-south gravity station spacings vary between 1.6-3.2 and between 3.2-9.6 km respectively. For anomalous sources in the upper several kilometers of the crust, these values also represent the limiting size of anomalous bodies detectable. For a 1.6 km diameter spherical body buried 1 km beneath the ground, the minimum density contrast needed to produce a detectable (1 mgal peak) gravity signal is 0.07 gm/cc (Nettleton page 189, 1976).

Since the gravity method measures only the gravitational attraction caused by density anomalies in the subsurface, it does not provide a direct indication of the rock type. Many different types of rock may have the same density, while the same rock type may have different densities (see Table 1). Densities are affected by porosity, temperature, water and gas saturation, and relative abundance of minor minerals. Moreover, density anomalies depend on the densities of both the anomalous body and the surrounding host rock.

Furthermore, there are an infinite number of possible solutions to a given set of gravity measurements because of the intrinsic non-uniqueness of the potential field problem. For instance, a small dense body may give rise to the same gravity anomaly as a larger, but less dense body at shallower depth. Therefore the interpretation of gravity data and its correlation to geology have to be done in collaboration with other information obtained from geologic, seismic, and magnetic studies, as well as drill logs and cores. This additional information helps to constrain the depth, size, shape,

rock type and density of the source, thus reducing the number of feasible solutions to a few.

EPILOGUE

The new Kansas gravity data in this report has been collected as part of a large state-wide gravity survey project. Its goal is to compile a comprehensive, more accurate, and updated gravity data base for the better understanding of the state's geology. It also provides auxiliary information for use in the exploration and exploitation of the natural resources of Kansas.

CHAPTER TWO

GEOLOGIC SETTING

The Phanerozoic rocks in Kansas form a thin veneer covering the Precambrian basement, which is 1000 to 6000 feet below sea level, except near Nemaha county, where uplifted basement is about 560 feet above sea level (fig. 1). The only occurrence of Precambrian rocks at the surface are large granite xenoliths found in peridotites near Rose in Woodson county (Bickford and others, 1971) and small xenoliths found in kimberlite pipes in Riley county (Brookins, 1970). Major basement structural provinces in Kansas are shown in figure 2. The central Kansas uplift continues northwesterly into Nebraska as the Cambridge arch, while the Nemaha ridge, a basement uplift that formed in late Mississippian to early Pennsylvanian time, extends north northeasterly to Nebraska and Iowa, and into Oklahoma on the other end. Recent micro-seismic activity (Steeples, 1980, 1981) along these basement highs indicate continued tectonic activity. The southern extension of the Salina basin in northcentral Kansas is bounded by the Nemaha ridge and the central Kansas uplift on the east and west respectively. In northeastern Kansas is the southwestern corner of the Forest City basin, which together with the Salina basin, were part of the ancestral North Kansas basin that is now separated by the Nemaha ridge. The Bourbon arch, a small east-west trending basement high, separates the northern extension of the Cherokee basin from the Forest City basin. The Sedgwick basin in southcentral Kansas, the Hugoton embayment of the Anadarko basin

Figure 1. Configuration of the top of the Precambrian rocks in Kansas. Bold contour intervals are 1000 feet relative to sea level. After Cole (1976). Adapted from Yarger (1985).

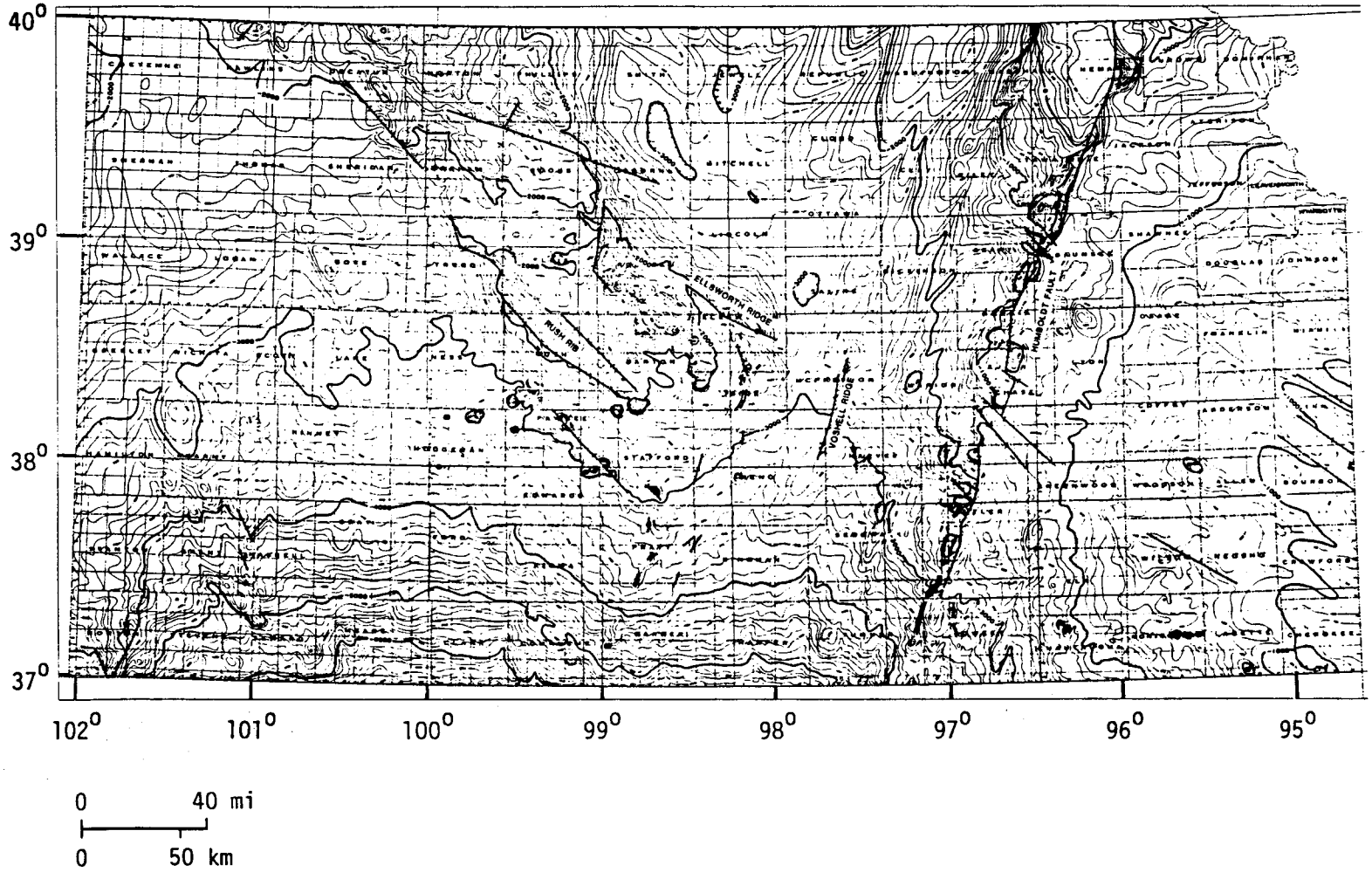

Configuration of the top of Precambrian rocks in Kansas. After Cole (1976).

Figure 2. Generalized structure map of the Precambrian in Kansas. After Merriam (1963). Adapted from Yarger (1985).

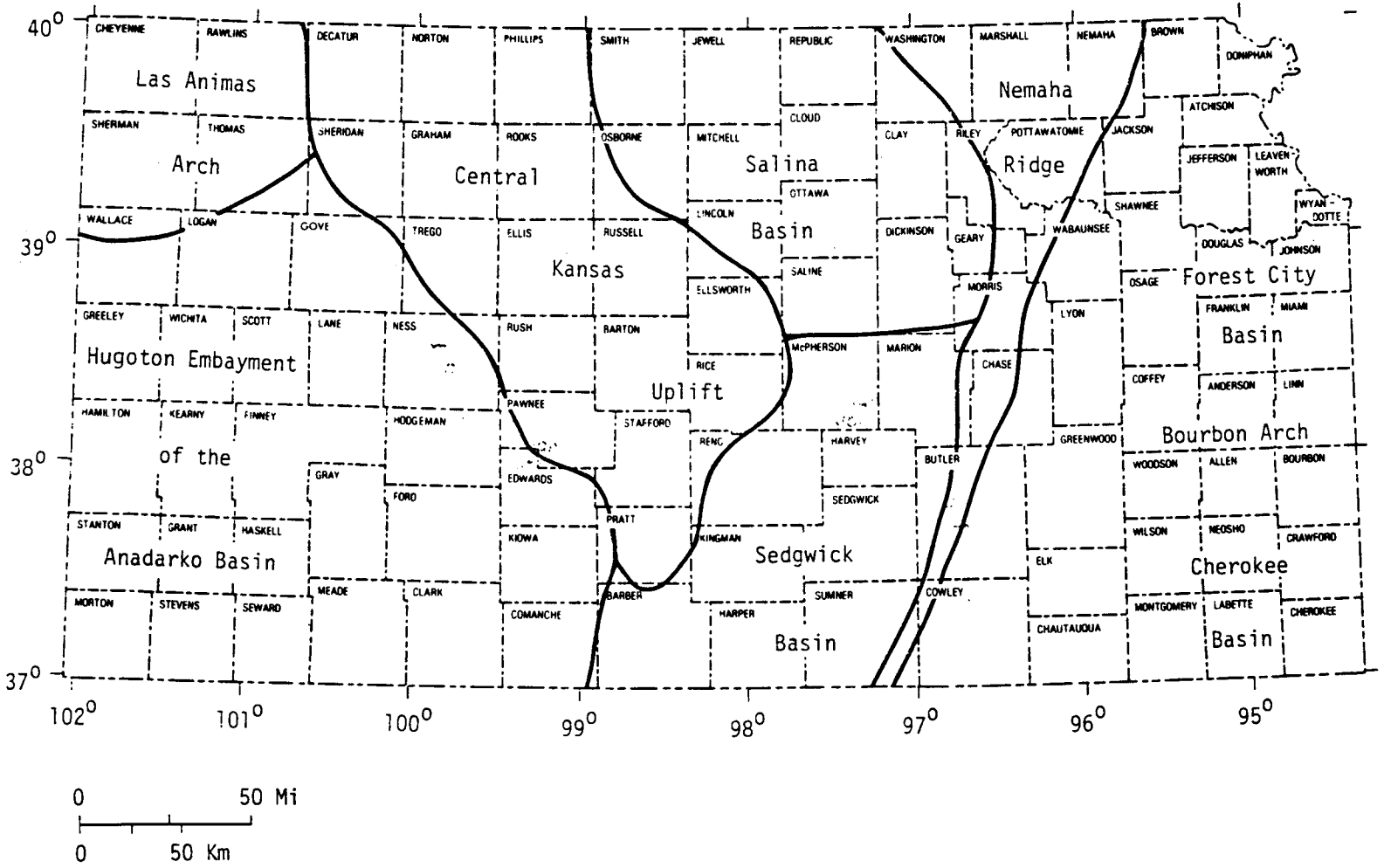

Generalized structural map of the Precambrian in Kansas. After Merriam (1963).

and the Las Animas arch in western Kansas round out the major structural elements in the state.

Figure 3 shows a generalized geologic map of surface rocks in Kansas. The oldest rocks, Pennsylvanian in age, outcrop in eastern Kansas near the Missouri border. The exposed rocks become progressively younger toward the west. Glacial drift deposits in the northeastern corner of the state indicate the approximate southern limit of the Kansan glacier. Central Kansas is dominated by Cretaceous rocks in the north, and a combination of river valley deposits, sand dunes and Permian rocks in the south. Tertiary rocks and river valley deposits are abundant in northwestern Kansas, while southwestern Kansas outcrops are mostly sand dunes and river valley deposits. Profile SS', shown in figure 3, is a typical east-west cross section of the sedimentary rocks. The Phanerozoic sedimentary column is about 670 m thick near the Missouri border, and it thickens almost linearly to the west to reach a total thickness of 2000 m near the Colorado border.

The basement-rock types in Kansas are discussed below and illustrated in figure 4. The Kansas basement is divided into an older (1.6 b.y.) terrane of sheared granite in the north and a younger (1.4 b.y.) granite-rhyolite southern terrane (Bickford and others, 1981; Thomas and others, 1984; Denison and others, 1984; Van Schmus and others, 1986). Mafic igneous rocks and flanking arkosic sandstones are found along the trend of the Midcontinent geophysical anomaly (MGA), which is a linear gravity and magnetic high with flanking lows that extends north northeasterly to the Lake

Figure 3. Geologic map of Kansas. After Kansas Geological Survey map 1 (1964).

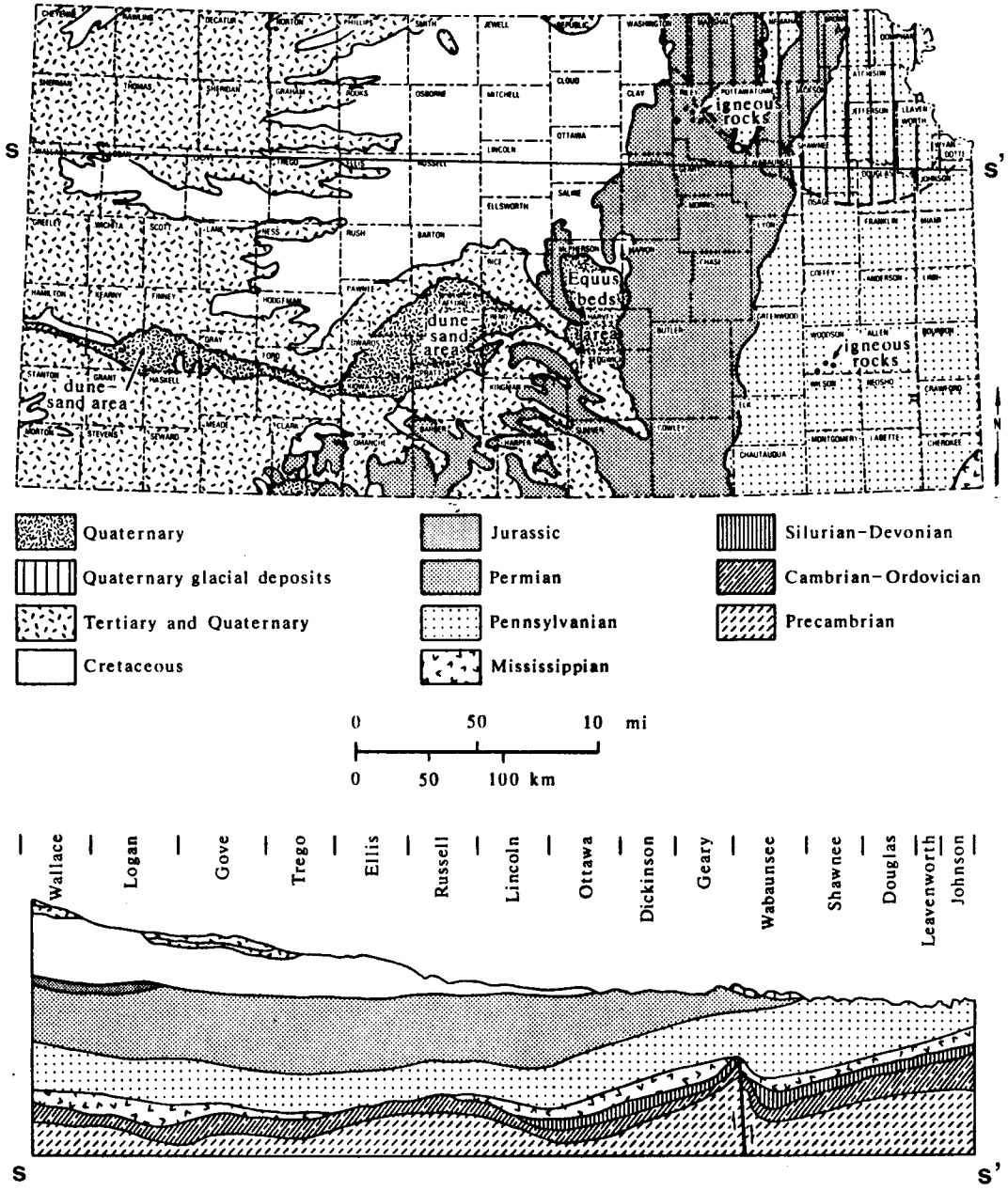
S
S'
igneous rocks
Equus beds area
dune-sand area
dune-sand area
igneous rocks
Quaternary
Quaternary glacial deposits
Tertiary and Quaternary
Cretaceous
Jurassic
Permian
Pennsylvanian
Mississippian
Silurian-Devonian
Cambrian-Ordovician
Precambrian
0 50 10 mi
0 50 100 km
Wallace
Logan
Gove
Trego
Ellis
Russell
Lincoln
Ottawa
Dickinson
Geary
Wabaunsee
Shawnee
Douglas
Leavenworth
Johnson
S
S'

Figure 4. Map of basement-rock types in the central Midcontinent region. After Bickford and others (1981).

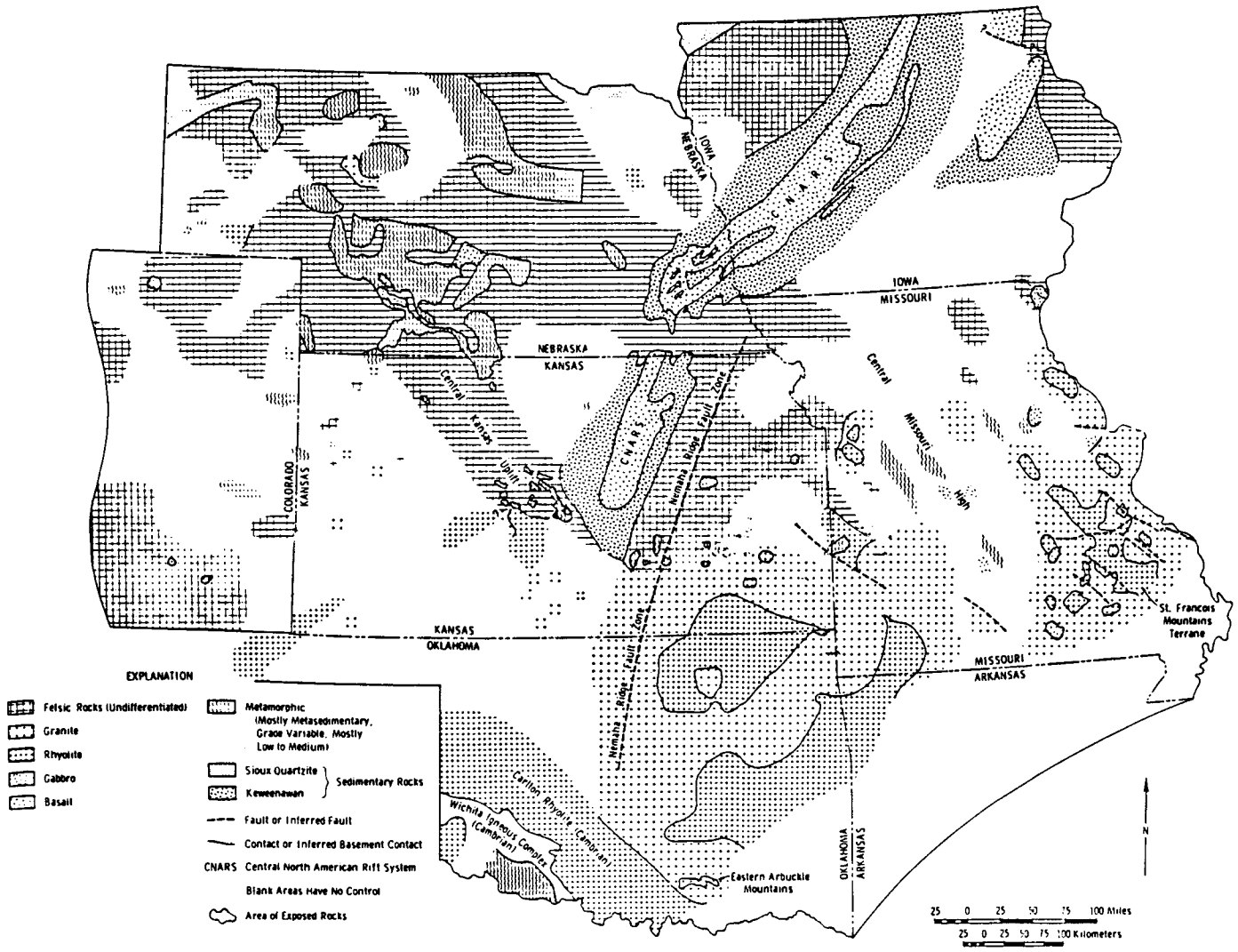
IOWA
NEBRASKA
CNARS
IOWA
MISSOURI
NEBRASKA
KANSAS
Central
Kansas
Uplift
CNARS
Nemaha Ridge Fault Zone
Central
Missouri
High
COLORADO
KANSAS
KANSAS
OKLAHOMA
Nemaha Ridge Fault Zone
MISSOURI
ARKANSAS
St. Francois
Mountains
Terrane
Carrion Rhyolite (Cambrian)
Wichita Igneous Complex (Cambrian)
Eastern Arbuckle Mountains
OKLAHOMA
ARKANSAS
N
25 0 25 50 75 100 Miles
25 0 25 50 75 100 Kilometers
EXPLANATION
Felsic Rocks (Undifferentiated)
Granite
Rhyolite
Gabbro
Basalt
Metamorphic
(Mostly Metasedimentary, Grade Variable, Mostly Low to Medium)
Sioux Quartzite
Keweenawan
Sedimentary Rocks
Fault or Inferred Fault
Contact or Inferred Basement Contact
CNARS Central North American Rift System
Blank Areas Have No Control
Area of Exposed Rocks

Superior region. The MGA has been interpreted as a late Precambrian aborted rift (Chase and Gilmer, 1973; Ocola and Meyer, 1973; Van Schmus and Hinze, 1985), which is sometimes called the Central North American rift system (CNARS). Several small (~15 km) circular undeformed intrusive plutons of 1.35 b.y. epizonal granite, which contain about two percent magnetite by weight, are scattered throughout northeastern Kansas and around the boundary of the northern and southern terranes (Steeples and Bickford, 1981; Yarger, 1983,1985; Van Schmus and others, 1986). Substantial amount of metasedimentary rocks containing mostly quartzite were found on basement highs near the southeastern end of the central Kansas uplift (Bickford and others, 1979), and in northern Rawlins, Sedgwick and Lyon counties.

CHAPTER THREE

DATA COLLECTION

INSTRUMENTS

In the earliest stage of the gravity survey in northeastern Kansas, a Worden gravimeter with 0.01 mgal/division precision was used. LaCoste and Romberg (L&R) model G gravimeters G-245, G-111 and G-68 on loan to the KGS, were used in surveying southeastern, southcentral and northwestern Kansas. KGS owned L&R model D meters D71 and D72 were used in northwestern Kansas. The nominal drift rates for the L&R gravimeters were 1 mgal/month. The accuracy for model G meters is 0.01 mgal, while that of the model D meter is 0.005 mgal (Instrument Manual for LaCoste and Romberg gravity meter).

The L&R gravimeter is a relative instrument, which measures the difference in gravity between two stations. The absolute gravity value of a station is established by comparison with a reference station, which has a known gravity value. The absolute gravity value at a reference station is determined by a pendulum meter. The Department of Defense has established several reference stations in Kansas.

The L&R gravimeter uses a "zero length" elastic spring suspended in a metastable equilibrium state. The restoring force on an ordinary spring is proportional to the amount of extension of the spring. Whereas a zero length spring's restoring force is proportional to the total length of the spring, s. The zero length

Figure 5. LaCoste and Romberg gravimeter.

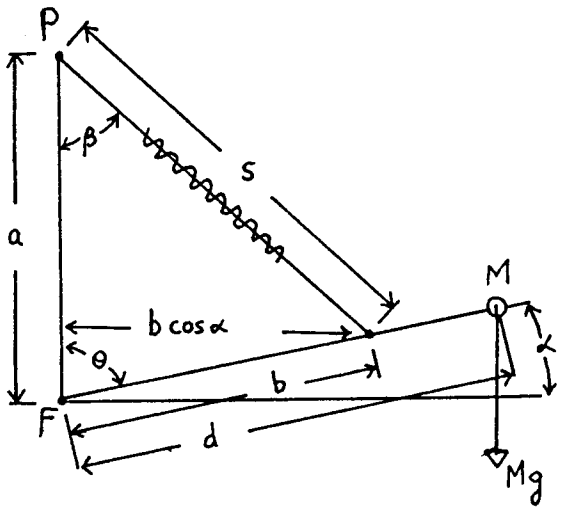

FIG. 5a

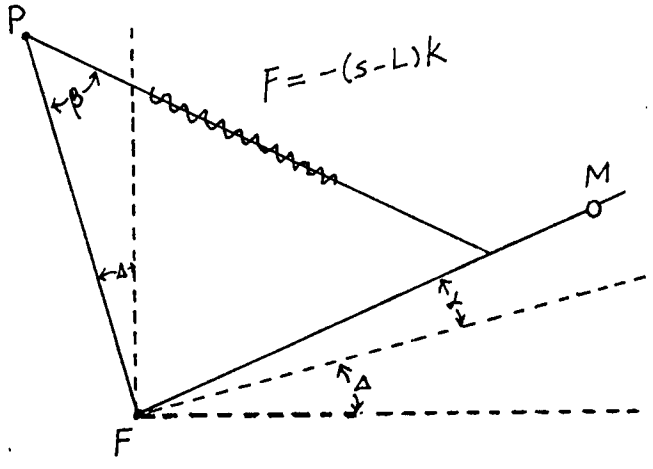

FIG. 5b

spring is suspended in a slant position making an angle to the vertical (fig. 5a). In making a gravity measurement, the vertical distance (fig. 5a) between the fulcrum, F, and the point of suspension of the spring, P, is adjusted by turning a screw connecting P to the top of the meter. The meter is 'nulled' when the suspended mass returns to its neutral position. The gravity reading is read from a dial and a counter connected to the measuring screw.

The ideal condition illustrated in figure 5a is not used in practice. The arm FP (fig. 5b) generally deviates from the vertical by a small angle, and a truly zero length spring is very rare. Usually the restoring force of the spring is proportional to (s-L), where L is small compare to s. With the notations in figure 5b, the equilibrium state is attained if the sum of moments about F is zero, that is,

$$mgd \sin(\theta-\Delta) = kba \sin\theta - Lka \sin\beta$$

If we assume $\theta=90$, L=0, and $\Delta^2=0$, then δg is linearly related to δa and $\delta\theta$ as shown below,

$$\delta\theta = \delta g \{mg/kba\Delta\}$$

$$\delta g = \delta a \{kb/md \cos\Delta\}$$

For $L\neq 0$, δg is still linearly related to δa, but the equation is more complicated.

I shall outline the most common sources of error for the L&R gravimeters. For a thorough discussion of the performance of L&R gravimeters, the reader may refer to Woollard (1963). Because the spring constant of the zero length spring changes with temperature, it is essential to maintain a constant gravimeter temperature. The L&R gravimeter is housed in a thermally insulated case. Its temperature is maintained constant (around 50°C for most L&R gravimeters) by a heating element and thermostat. A small 12 volt rechargeable battery provides the electrical power. During the field work for this project the air temperature, on occasion, rose above 38°C during a hot summer day. The gravimeter failed to regulate its temperature because of the excessive heat transmitted to it from the hot pavement. Measurements were not taken when the meter overheated. The gravimeter temperature also dropped below its operating temperature on a few occasions. This was caused by a loose electrical connection between the battery and the gravimeter, or a run-down battery. A sudden change in ambient temperature, as described above, or violent motion caused by travelling on a bumpy road, affects the performance of the gravimeter. A 'meter tare', or a sudden jump in gravimeter reading results. These undesirable conditions were watched for by using repeated base readings during the day. Stations affected by these conditions were re-measured.

FIELD PROCEDURE

Gravity stations were normally located at the corner of a 1.6 km (1 mi) section, usually at a road intersection or fence line.

When a particular section corner was not accessible by vehicle, a nearby replacement point was taken instead. The average north-south station spacing is 9.6 km in northeastern Kansas, 6.4 km in southeastern and southcentral Kansas, and 3.2 km in northwestern Kansas. Except for some stations in northeastern Kansas, which are 3.2 km apart, the average stations are spaced 1.6 km apart in the east-west direction (see fig. 6). Approximately 27,500 gravity measurements were taken in this study. The entire state was divided into rectangular blocks of approximately 26 by 40 km (16 by 25 mi). A KGS base station was established at a central location within each block. These KGS base stations were, in turn, tied to a nearby Department of Defense (DOD) base station, which was referenced to the International Gravity Standardization Net 1971 (Morelli and others, 1974).

The International Gravity Standardization Net 1971 (IGSN71) is a world-wide net of reference gravity stations with established absolute gravity values. A subset of the DOD base stations belong to the IGSN71, with the rest being an extension of the net in the United States. Typical accuracy of the DOD base stations used in this study is 0.1 mgal. A few DOD bases have an uncertainty as large as 0.5 mgal (e.g. one located near Red Cloud, Nebraska).

The KGS base stations used in this survey are an extension of the DOD base station net. Because actual DOD base stations are so sparse, many KGS base stations were established for logistical reasons. To monitor gravimeter behavior, it is necessary to re-occupy the reference base station every three to four hours.

Figure 6. Gravity stations in Kansas. Average east-west station spacing is 1.6 km (except for some stations spaced 3.2 km apart in northeastern Kansas). Average north-south spacing is 9.6, 6.4, 6.4, and 3.2 km in northeastern, southeastern, southcentral, and northwestern Kansas respectively.

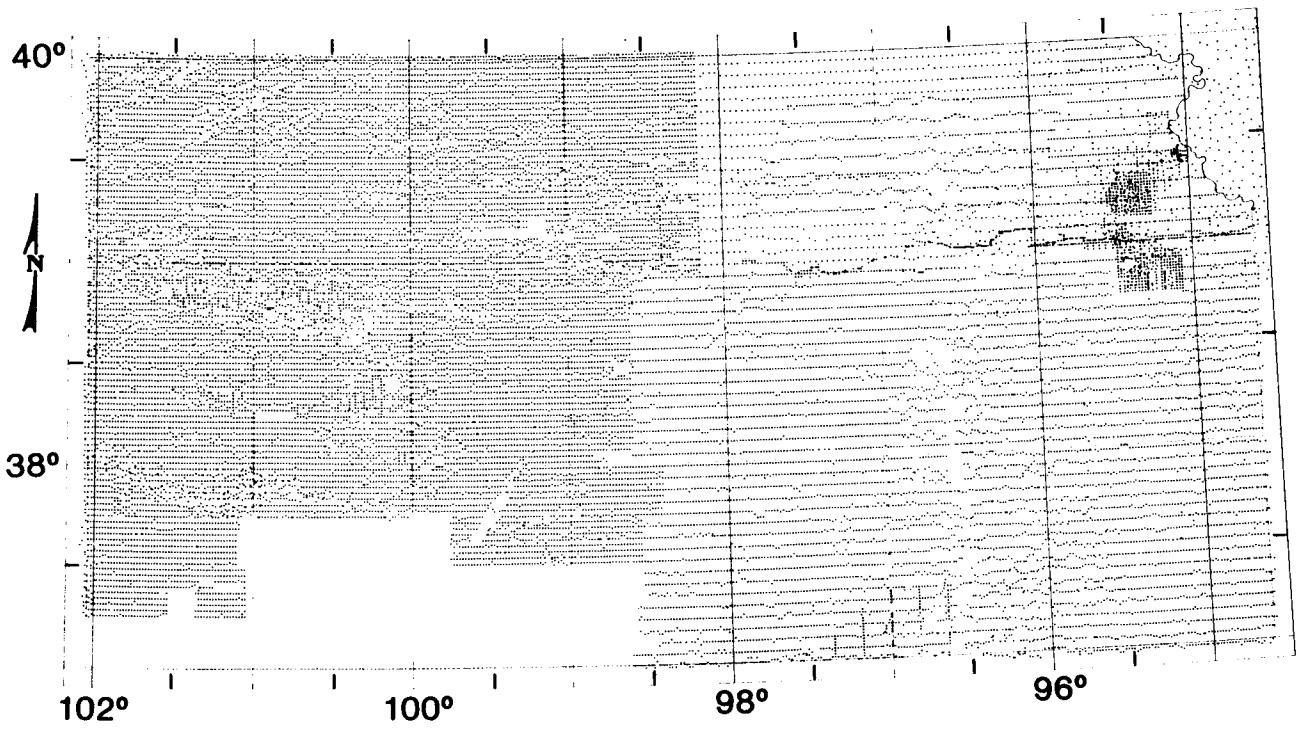

GRAVITY STATIONS IN KANSAS

Approximately twenty-five regular gravity stations, with about one station per section (1.6 km) in the east-west direction, were occupied in four hours on a normal day. A KGS base station was located approximately every 40 km (25 mi) in the east-west direction and 26 km (16 mi) in the north-south direction. Stations along the eastern and western boundaries of each block were occupied twice. These are called overlap stations. This four percent redundancy allowed for error checking and quality control. Because it was desirable to have at least one overlap station between successive base readings, one overlap station for every twenty-five measurements was the minimum needed.

United States Geological Survey (USGS) 7.5 minute topographic maps were used in navigation and determining the station elevation. These maps cover an area 7.5' longitude by 7.5' latitude, i.e. 7 by 8.5 miles or 11 by 13.5 km. Roads, landmarks and section lines are also shown on these maps. They are contoured at 10 feet intervals with elevations (accurate to the nearest foot) labelled at section corners, midway between two adjacent section corners, as well as on benchmarks. Once in a while, elevation was not labelled on the map at a gravity station. In that case, the elevation was estimated by interpolating between contour lines.

To monitor meter behavior, a base station was occupied three times during the day, with three to four hours separating successive readings. The first meter reading was taken at the beginning of the work day in the morning, again in the middle of the day, and at the conclusion of the day. To ensure the gravimeter performed properly,

these base readings were checked on site against theoretical tidal drift calculated using Longman's (1959) algorithm.

The temporal variation of gravity is due mainly to the gravitational attraction of the sun and the moon (the earth tide), as well as the resulting deformation of the earth (the solid earth tide). Longman's algorithm determines the positions of the sun and the moon at a certain time, and calculates the earth tide at the gravity station. The earth tide is quite sensitive to time. It could vary by as much as 0.3 mgals in six hours. The solid earth tide is approximately 20% of the earth tide, and is acting in the opposite sense. The computer was programmed to calculate the combined effects of the earth and solid earth tide, and to generate a chart of tidal gravity variation with time.

CHAPTER FOUR

DATA REDUCTION

THEORY

The gravity meter reading was multiplied by a meter calibration factor (about 1.0) to convert to the mgal unit. After subtracting the theoretical tidal acceleration from each measurement, the remaining time dependent variation in gravity was lumped under 'meter drift', which actually contained the true meter drift and experimental errors caused by imperfect leveling of the meter and uncertainty in nulling the meter. The maximum and average 'meter drift' of data collected using the Lacoste & Romberg meters was 0.05 and 0.01 mgal/hour respectively. This 'meter drift' was corrected by linearly distributing the error to points between successive base readings.

The Bouguer anomaly was calculated by subtracting the reference field and the Bouguer correction, and by adding the free-air correction to the measured absolute gravity value of a station.

The theoretical gravity value of the reference field was determined using the 1967 International Gravity Formula (International Association of Geodesy, 1967). This reference field is given, accurate to within 0.01 mgal (Mittermayer, 1969), by,

$$g_r = 978031.85 * (1 + 0.005278895*\sin^2\phi + 0.000023462*\sin^4\phi) \text{ mgal},$$

where ϕ is the north latitude.

The free-air correction accounts for the deviation of the gravity station's altitude from sea level. The reference field is calculated assuming the earth has a perfect ellipsoidal shape. The actual sea level shape of the earth, called the geoid, deviates slightly from this assumption. This deviation is very small (for example 2.7 meters or 2 mgal in western United States, Simpson and others, 1986), and is of very long wavelength. It is therefore acceptable here to use the elevation above sea level in the free-air and Bouguer corrections. To zero order of approximation, the gravity field g is,

$$g = G * M / (R+h)^2,$$

where G is the gravitation constant,

M is the mass of the earth,

h is the station elevation,

R is the radius of the earth at the station.

Therefore the vertical gradient of g is $- 2GM/(R+h)^3$ at the station. Taking only the zero order term of h/R, it becomes -2*g/R. After substituting in the numerical values for the mean values of g and R, the free-air correction is -0.3086*h mgal/m.

The error in ignoring the higher order term in the h/R expansion is approximately -0.03% of the main term for the highest station in Kansas (approximately 1300 m above sea level). Since g and R at the gravity station should be used instead of the mean values, this approximation resulted in an error of +0.07% of the

main term. The zero order approximation in the h/R expansion results in a larger gravity gradient. While the use of the mean values of g and R, results in an under-estimation of the gravity gradient. The combined net error is about +0.04%, or 0.16 mgal for the highest station in the state. Heiskanen and Vening Meinesz (1958), and Lambert (1930) obtained the same values using the older formulas for g and R.

The Bouguer correction corrects for the gravitational attraction of the rock mass between the station and sea level. A uniform slab, extending horizontally to infinity, with a density d and thickness equal to the station elevation h, is assumed. It can be shown that (see for example Garland, 1979),

$$\text{Bouguer correction} = 2*\pi*G*d*h$$
$$= 0.04193*d*h \text{ mgals/m.}$$

For a density of 2.67 gm/cc, the Bouguer correction is 0.11195*h mgals/m.

The terrain correction improves the uniform slab approximation used in the Bouguer correction by accounting for the surrounding topography. Even with the aid of a computer, it is a very tedious process (Kane, 1962). Because of the gentle relief in Kansas, this correction was not needed for most stations.

Combining the above corrections, Bouguer gravity is defined as the following,

$$g_b = g_a - g_r - 0.3086 * h + 0.04193 * d * h$$

For d=2.67 gm/cc, it becomes,

$$g_b = g_a - g_r - 0.19665 * h$$

where g_b is the Bouguer gravity,

g_a is the measured absolute gravity,

g_r is the reference gravity field,

h is the elevation in meters,

d is the upper crustal density in gm/cc.

FLOW OF DATA

Gravity data written on the field data sheets were entered into the computer by keyboard. A computer program "DFTT" was run for quality control and error checking purposes. It calculated the approximate longitude and latitude based on a section labelling system used to identify stations. The x and y labels indicate approximately the number of sections from the Missouri and Nebraska borders respectively. "DFTT" also calculated the approximate Bouguer gravity and theoretical tidal acceleration of each data point. Two graphs were generated: an east-west profile of the day's data (fig. 7), and a plot of the theoretical tidal variation with respect to time with the least square fit of the level-shifted base

Figure 7. Bouguer gravity anomaly versus east-west line number (y) for a portion of the east-west line x=179. X and y labels indicate approximately the number of one mile sections from the Kansas-Nebraska and Kansas-Missouri border. Positive x and y denote Kansas stations, while negative values indicate stations in Nebraska and Missouri respectively.

BOUGUER GRAVITY VS STATION LOCATION

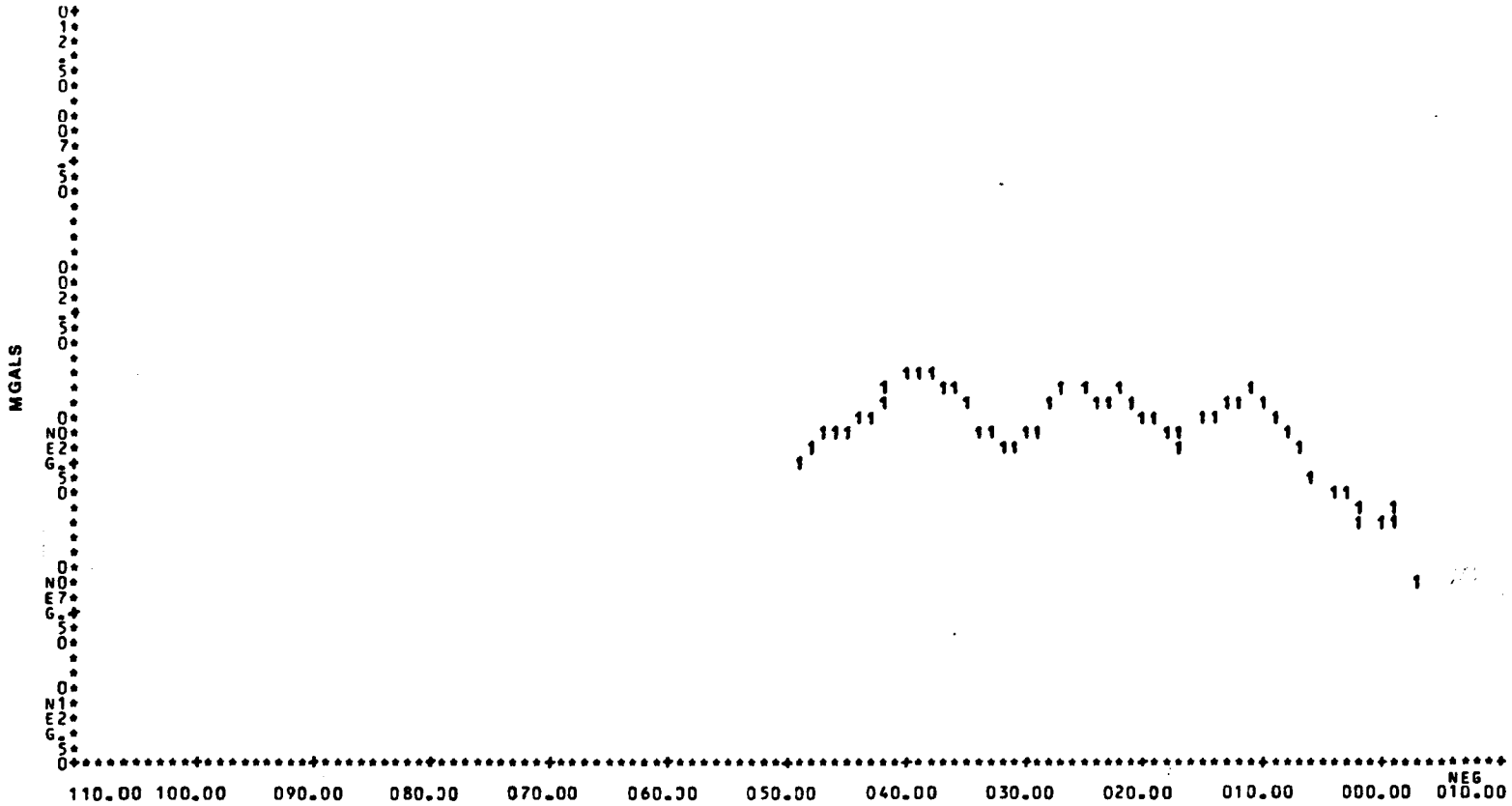

measurements superimposed (fig. 8). A typical root mean square value of this fit is about 0.05 mgal. Erroneous measurements or typographic errors show up as singularities on the profile (fig. 7), while the closeness of fit of the base readings (fig. 8) to the theoretical tidal values give an indication of the quality of the data.

The uncertainties in station elevation, location, and absolute gravity value of the reference base station are 1 foot (0.058 mgal), 0.00004 degree (0.004 mgal), and 0.1 mgal respectively. So a root mean square value on the tidal drift curve larger than 0.2 mgal was considered unacceptable. On a few occasions, an entire day's measurements were repeated because of poor meter performance indicated by a large root mean square value.

The absolute gravity value of the KGS base stations were calculated by the computer program "BASE_TIE". KGS base stations were tied into DOD base stations by two consecutive loops. The program adjusted for the tidal drift and 'meter drift', and determined an absolute gravity value for the KGS base.

The measurement station locations marked on USGS 7.5 minute topographic maps in the field were digitized to assign a longitude and latitude (accurate to within 0.00004 degree or about 4 meters) to each gravity station. This station location file was then merged with the gravity data file.

The "meter drift" between each pair of base measurements during the day was calculated and stored in a file named "DAILY". The absolute gravity value for each gravity station was calculated by

Figure 8. Theoretical tidal gravity values (smooth line on graph) for southeastern Kansas on June 12, 1980 are plotted against Greenwich mean time in hour of the day. The 24th hour indicates the beginning of another day. The level-shifted base readings (• on graph) are superimposed on the tidal gravity plot. The root-mean-square of the fit between the calculated tidal gravity and the time dependent base readings is 0.056 mgals.

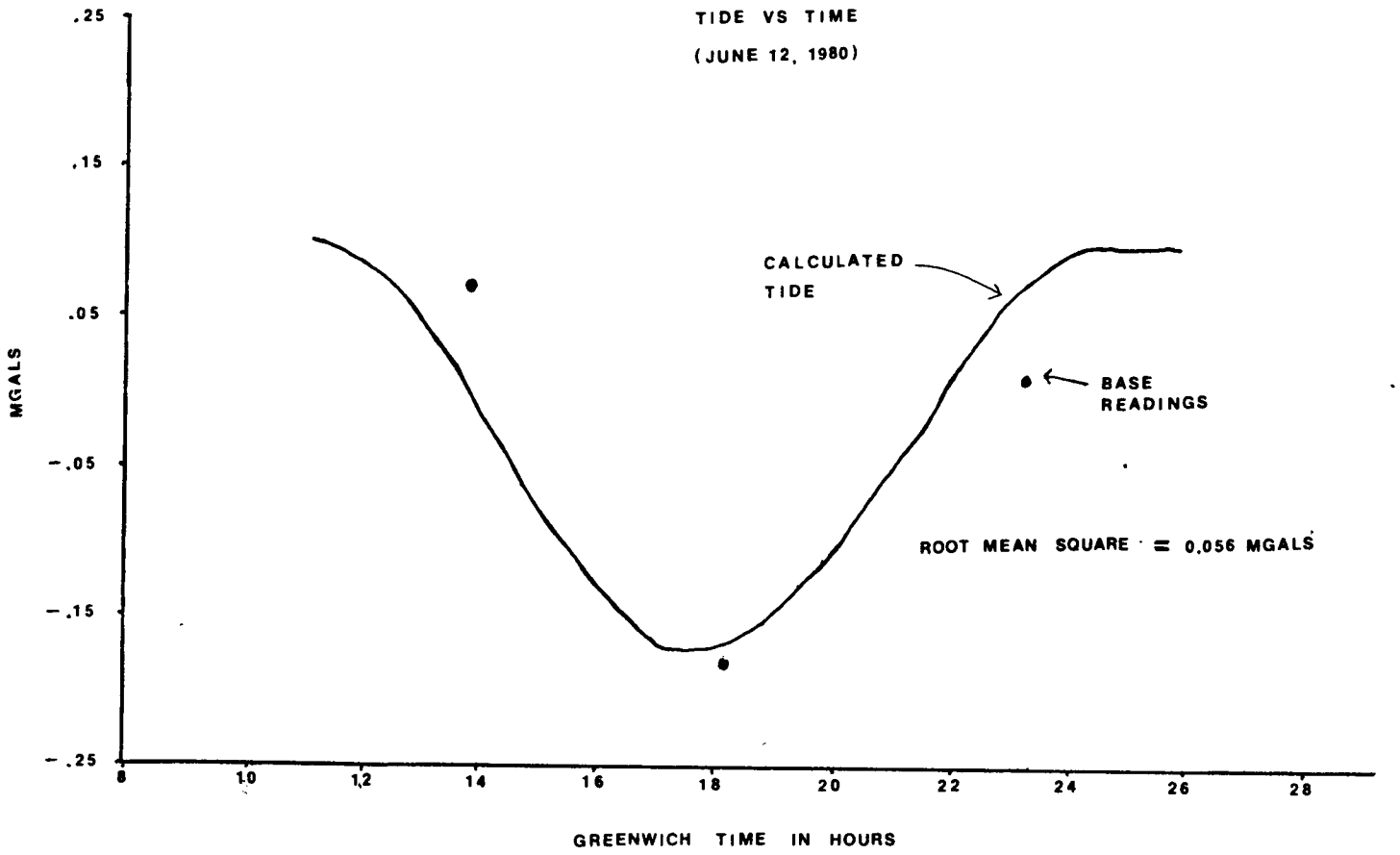
TIDE VS TIME
(JUNE 12, 1980)
.25
.15
.05
-.05
-.15
-.25
MGALS
CALCULATED
TIDE
BASE
READINGS
ROOT MEAN SQUARE = 0.056 MGALS
8
10
12
14
16
18
20
22
24
26
28
GREENWICH TIME IN HOURS

program "STATIE". The output file was sorted in the X and Y labels, and overlap pairs were picked out by the program "OVERLAP". The mismatches on the overlap stations, which averaged about 0.2 mgal, were used to level adjacent blocks by fine tuning the KGS base station absolute gravity values. After leveling, the average mismatch was 0.1 mgal, which compares favorably with the 0.1 mgal accuracy of DOD base stations. The corrected data file was then re-formatted and re-arranged by east-west lines to be read by a program "PROFILE", which generated a suite of four graphs for each line. Examples of these for western Kansas are shown in figures 9 through 12. Figure 9 is an elevation profile of line 136. The absolute gravity values in figure 10 vary approximately inversely to elevation. Figure 11 shows the free-air gravity, which is corrected to sea level. The Bouguer gravity in figure 12 is corrected for the mass of material between the station and sea level. This line is the result of combining several blocks of measurements which are referenced to several different base stations. These four graphs are the final quality check of the data.

The Bouguer gravity was gridded into 1.6 by 1.6 km cells using the Surface II (Sampson, 1978) computer program, and a map with a 1 mgal contour interval was produced (fig. 13 and plate 1). Interpretation techniques applied to this map are discussed in the following chapters.

Figure 9. Elevations versus longitude for east-west line 136 in southeastern Kansas.

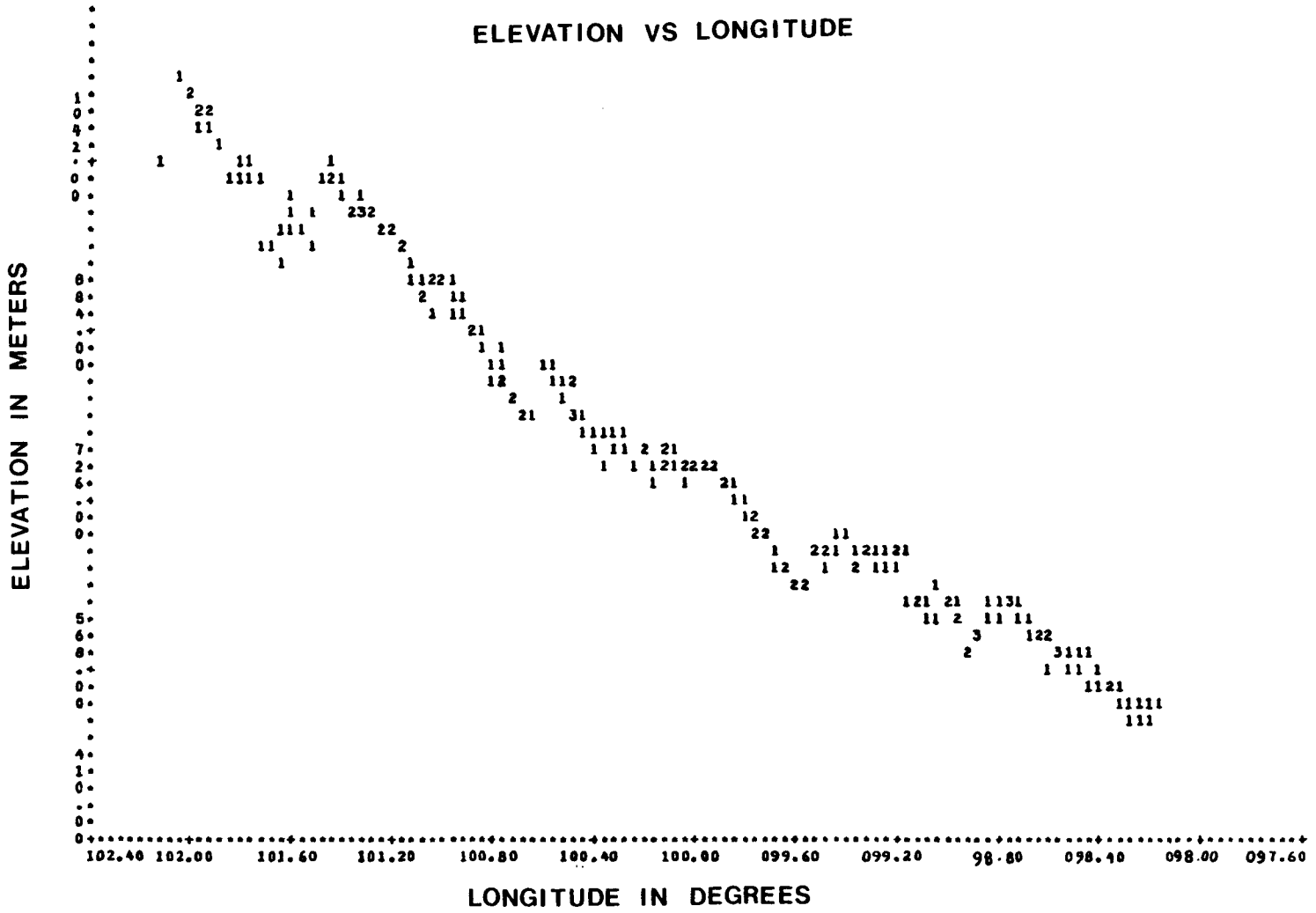
ELEVATION VS LONGITUDE
ELEVATION IN METERS
LONGITUDE IN DEGREES
102.40
102.00
101.60
101.20
100.80
100.40
100.00
099.60
099.20
98.80
098.40
098.00
097.60

Figure 10. Absolute gravity versus longitude for east-west line 136 in southeastern Kansas. A constant level of 979877.5 mgal, the average absolute gravity of these stations, has been removed.

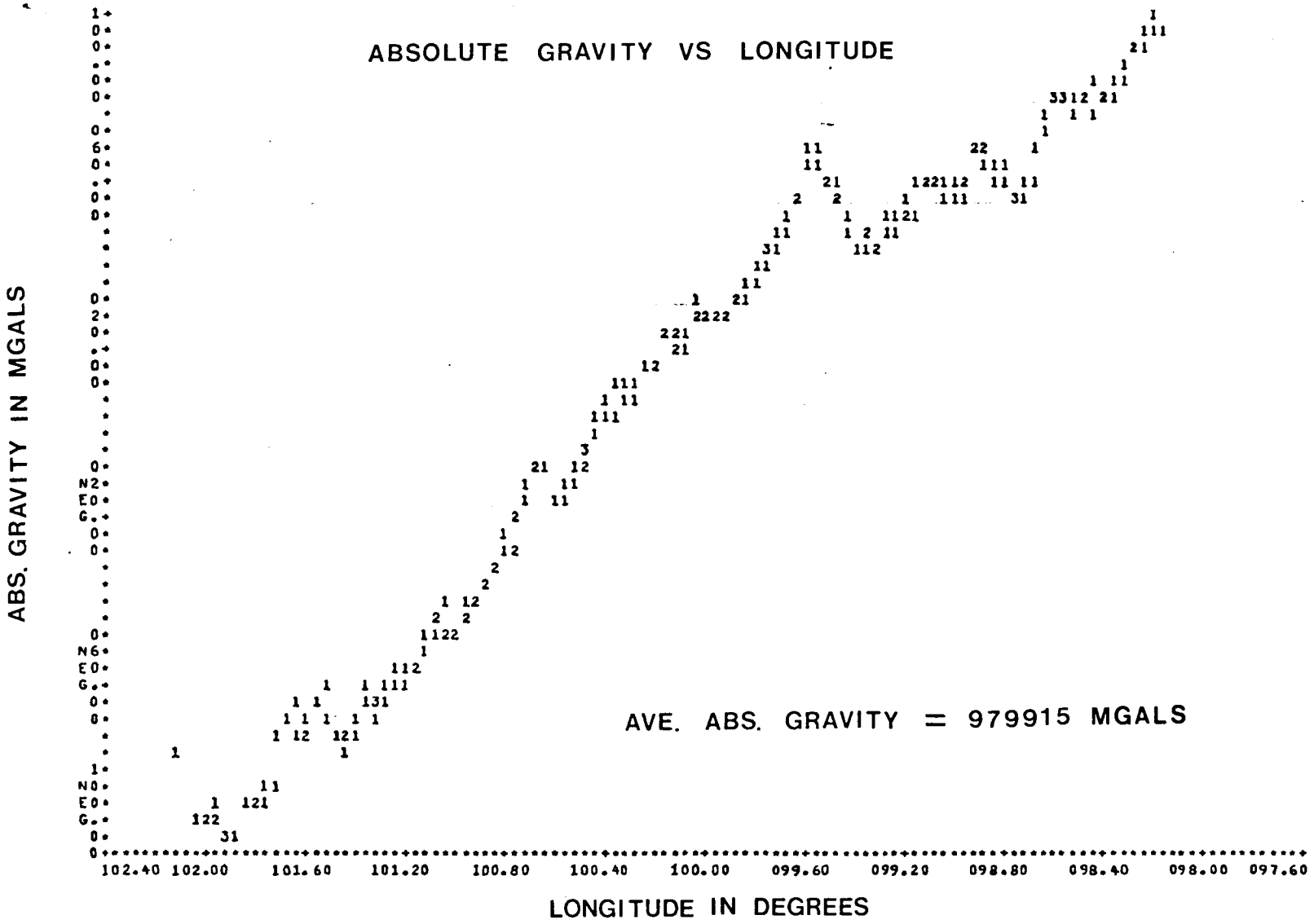
ABSOLUTE GRAVITY VS LONGITUDE
ABS. GRAVITY IN MGALS
AVE. ABS. GRAVITY = 979915 MGALS
102.40 102.00 101.60 101.20 100.80 100.40 100.00 099.60 099.20 098.80 098.40 098.00 097.60
LONGITUDE IN DEGREES

Figure 11. Free-air gravity versus longitude for east-west line 136 in southeastern Kansas.

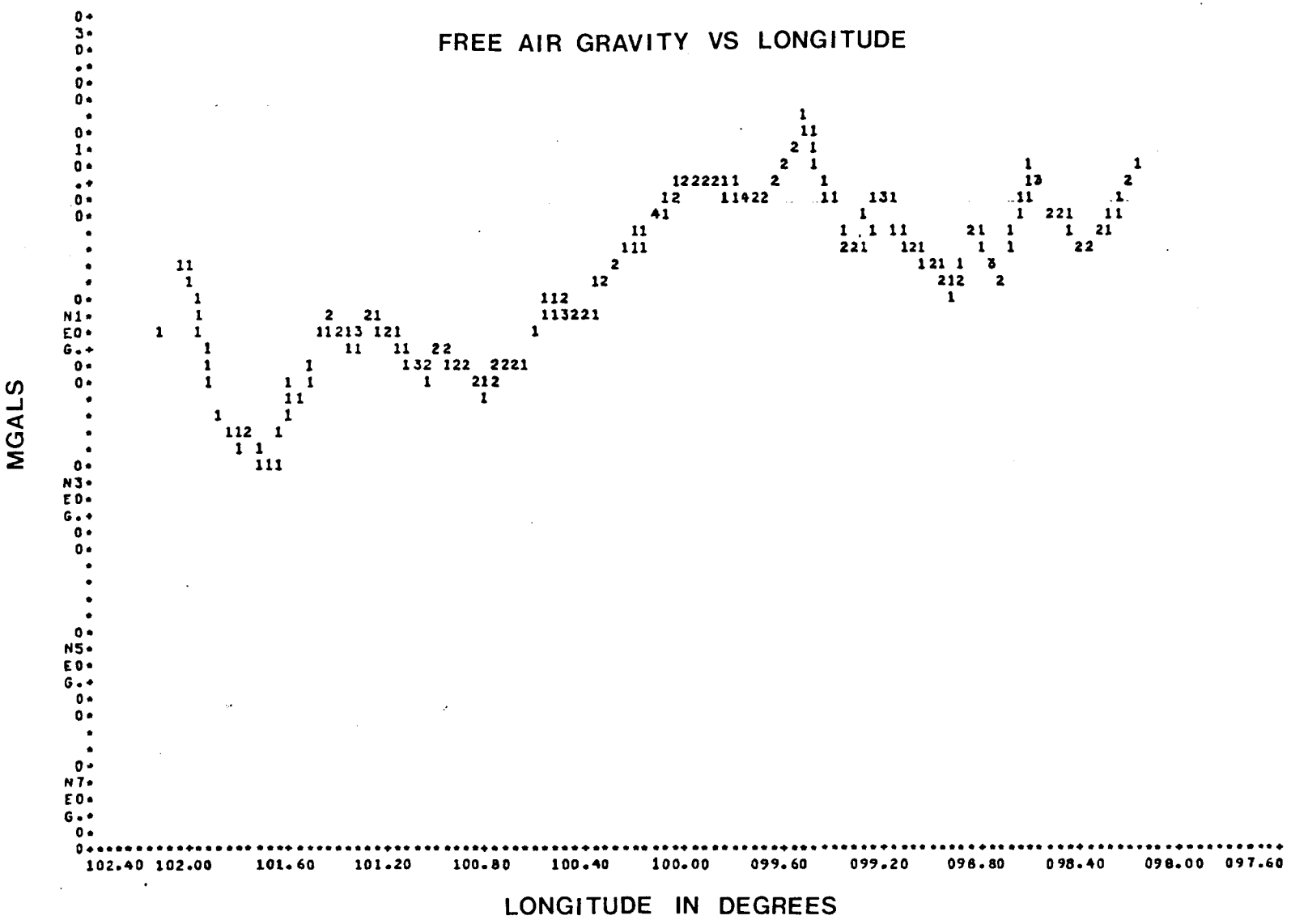
FREE AIR GRAVITY VS LONGITUDE
MGALS
0
3
0
0
0
0
0
1
0
0
0
0
0
N1
E0
G.
0
0
0
0
0
N3
E0
G.
0
0
0
0
0
N5
E0
G.
0
0
0
0
0
N7
E0
G.
0
0
102.40 102.00 101.60 101.20 100.80 100.40 100.00 099.60 099.20 098.80 098.40 098.00 097.60
LONGITUDE IN DEGREES

Figure 12. Bouguer gravity versus longitude for east-west line 136 in southeastern Kansas.

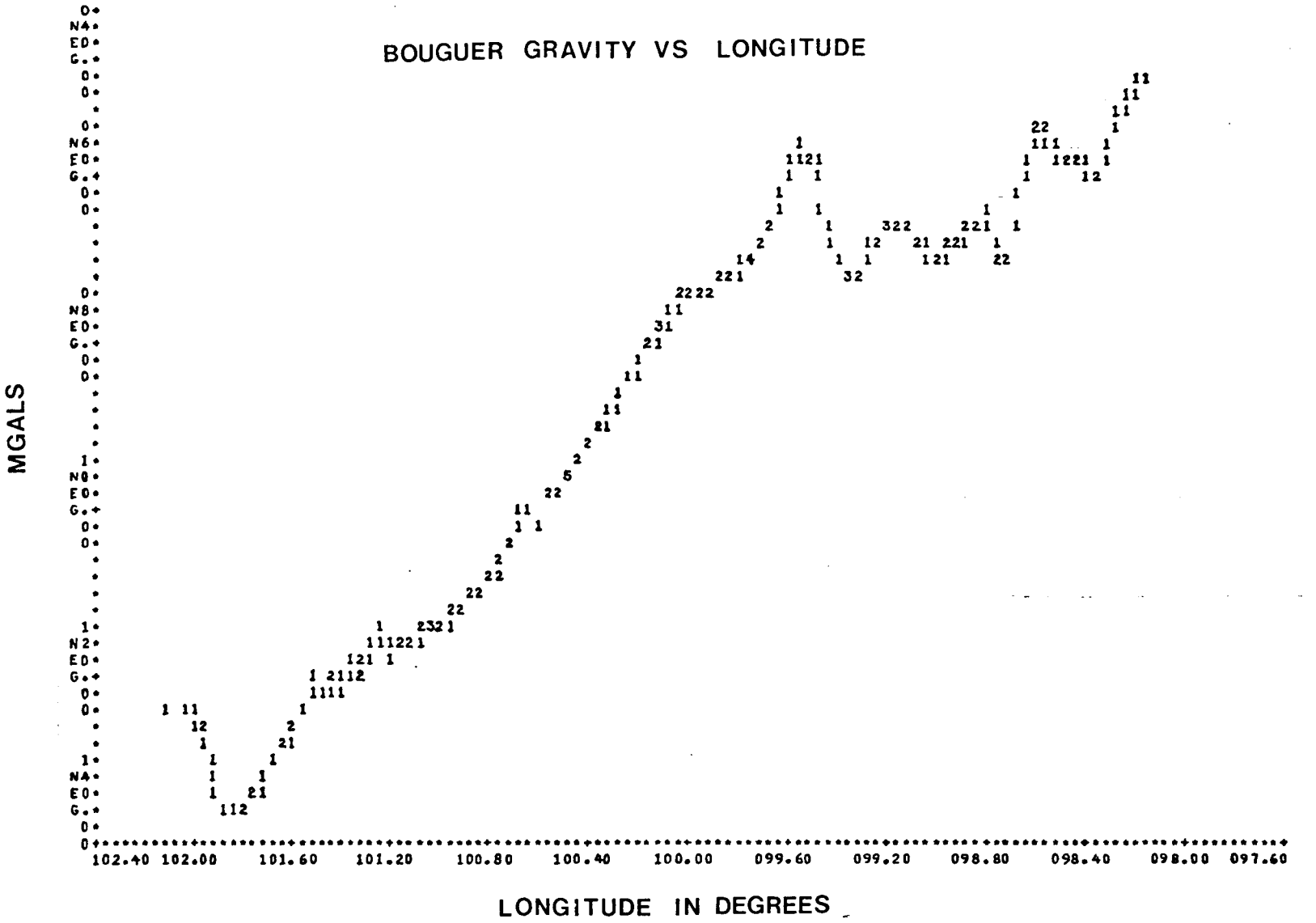
BOUGUER GRAVITY VS LONGITUDE
MGALS
LONGITUDE IN DEGREES
102.40 102.00 101.60 101.20 100.80 100.40 100.00 099.60 099.20 098.80 098.40 098.00 097.60

Figure 13. Bouguer gravity map of Kansas with 1 mgal contour interval. Bouguer gravity was calculated using gravity formula 1967 and a density of 2.67 gm/cc, and was referenced to the International Gravity Standardization Net 1971 (IGSN71). Projected using Lambert conformal projection with standard parallels at 33° and 45°.

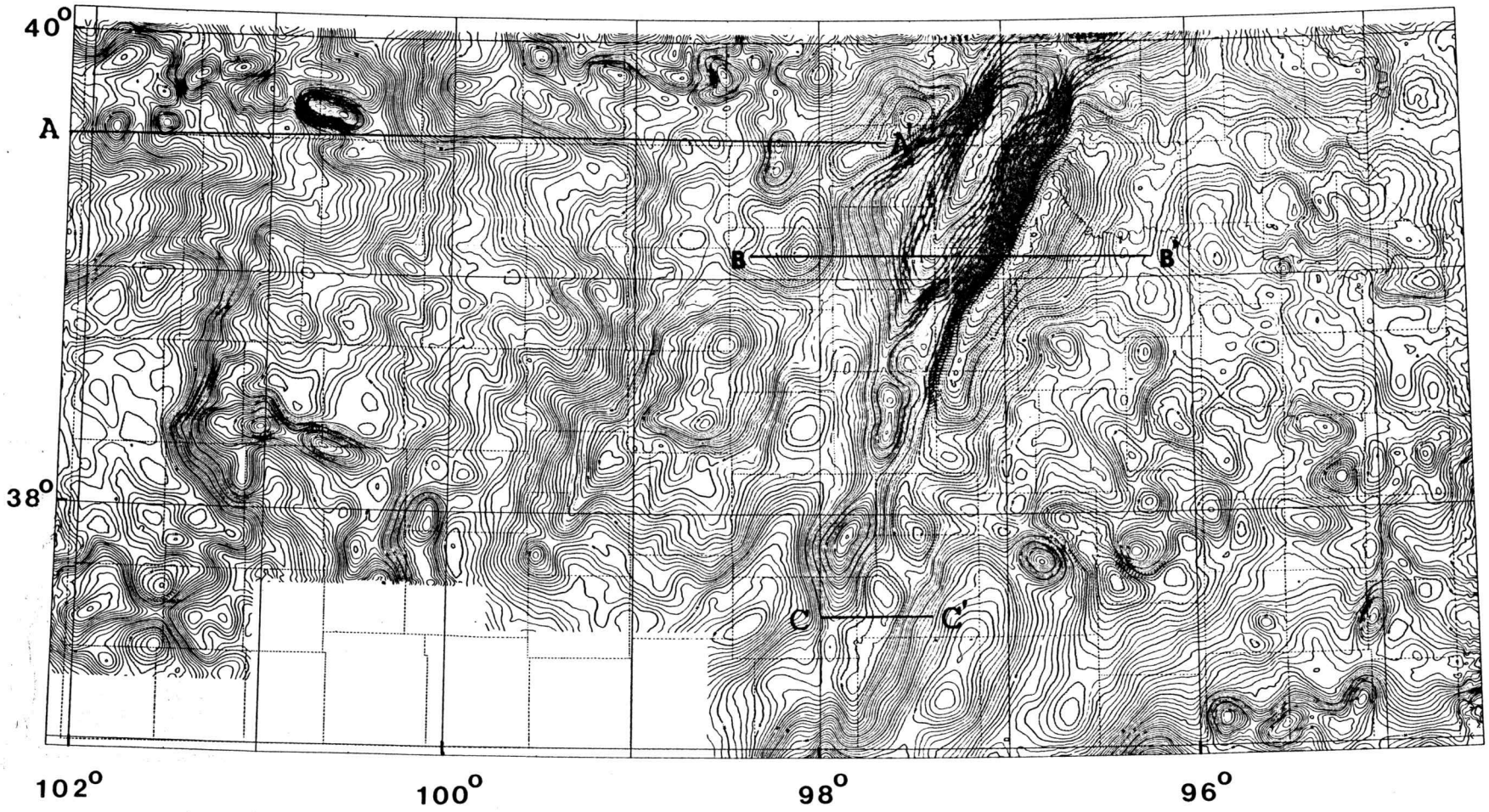
40°
38°
A
A'
B
B'
C
C'
102°
100°
98°
96°

CHAPTER FIVE

ENHANCEMENT AND INTERPRETATION METHODS

In this chapter, I discuss the data enhancement and interpretation methods used in this study. The advantages and drawbacks of each method and the underlying physical principles and mathematical development are presented. Discussions on the application of these techniques to the Kansas data and their geologic interpretations are deferred to chapter 6.

TREND SURFACE ANALYSIS

Trend surface analysis has been successfully used to separate local and regional anomalies (Van Voorhis and Davis, 1964; Coons and others, 1967). The general approach is to fit a polynomial, which represents the regional trend, to the data in the least squares sense. A residual map, representing the local anomalies, is obtained by subtracting the polynomial from the original data. The advantage of this method is that a series of low order polynomial trend and residual maps can be generated easily and the optimal set of maps for anomaly separation is chosen by visual inspection. It is also reproducible and well defined mathematically, in contrast to graphical or moving average methods. Its drawback is that it always produces a residual map that is averaged about zero mgals, essentially assuming that the average amplitude of the 'local' anomalies is zero. Moreover, the regional trend is determined by intuition rather than based on physical grounds.

I fitted the Kansas gravity data grid with n-th order polynomials of the form:

$$T(n,x,y) = \sum_{j=0}^{n} \sum_{i=0}^{j} c_{ij}\, x^{(j-i)}\, y^{i}$$

The coefficients c_{ij} were obtained by solving a system of 0.5 * (n+1) * (n+2) linear equations:

$$\frac{d}{d\, c_{ij}} \left[\sum_{\alpha=1}^{k} \sum_{\beta=1}^{l} \{T(n,x_\alpha,y_\beta) - g(x_\alpha - y_\beta)\} \right] = 0$$

where k is the row number,

l is the column number, and

$g(x_\alpha, y_\beta)$ is the gravity value at (x_α, y_β).

The computer program "POLYFIT" did the gravity trend surface fitting up to ninth order. Beyond the ninth order the program could not handle the large number of significant figures in the calculation and gave erroneous results. It solved the system of linear equations by the weighted Guassian elimination method. To alleviate round off errors, it set the origin of the grid to (0,0) and normalized the grid spacing to 0.01 in both x and y directions.

SPECTRAL FILTERING

Since the advent of the electronic digital computer and the fast Fourier transform (FFT) algorithm, spectral filtering of potential fields data has become a common technique for anomaly separation (see for example Chandler and others, 1982; Yarger, 1981, 83, 85, 86).

Convolution of two functions in the spatial domain is equivalent to multiplication of their frequency domain transforms (Brigham, 1974). Filter operations are most easily accomplished by Fourier transforming the data into the frequency domain, multiplying by a filter function, and then inverse transforming back to the spatial domain (Gunn, 1974).

The FFT algorithm of Singleton (1969) was used in this study. The speed and efficiency of the FFT algorithm is achieved by reducing the number of multiplications and additions in the calculation through factoring of the transformation matrix. For a discussion of FFT, refer to Cooley and Tukey (1965) and Brigham (1974).

High frequency pass, low frequency pass, upward continuation, downward continuation, first vertical derivative, second vertical derivative and trend pass filters were applied to the Kansas gravity grid.

Frequency band pass filters cut off all frequencies beyond the upper and lower frequency bounds. Since the frequency representation of the gravity field of a realistic anomalous body (whatever its size and depth may be) covers the whole spectrum, it would be

unphysical to use a step function to zero out all of the frequencies beyond the thresholds. Moreover an abrupt cutoff will result in the "frequency leakage" producing "ringing phenomena" on the filtered map. To alleviate these problems, a Guassian filter tail, as shown below, was used in the computer program.

$$A_{ij} = A_{ij} * \exp \{ - (R_{ij}-FREQ1)^2 /2*SIG^2 \}$$

where $R_{ij} = (u^2_i + v^2_j)^{\frac{1}{2}}$ is the radial frequency component in cycles/unit distance.

A_{ij} is the amplitude at R_{ij},

FREQ1 is the cutoff frequency, and

SIG represents the "width" of the tail.

The trend pass filter retains anomalous trends in a designated direction while cutting off trends that fall outside the desired direction. This entails calculating the bearing, arctan $\{ u_i/v_i \}$, for each frequency pair.

Continuation filters mathematically recalculate the gravity values at a different altitude h units above (or below for negative h) the observation plane. Similarly, nth order vertical derivative filters derive the nth order vertical derivative of gravity based on the gravity measurements. Following the derivations of Baranov (1975) and Gunn (1974), I derive below the continuation and vertical derivative filter operators.

Free space is defined as a region with no mass density (or

magnetic moment). In free space, the LaPlace equation for the gravitation potential, $\phi(x,y,z)$, in Cartesian coordinate is,

$$\frac{d^2\phi}{dx^2} + \frac{d^2\phi}{dy^2} + \frac{d^2\phi}{dz^2} = 0$$

such that,

$$g(x,y,z) = - \frac{d\,\phi(x,y,z)}{d\,z}$$

Where the +x axis points east, +y axis points south, and the +z axis points away from the earth.

If we assume a solution $\phi(x,y,z) = X(x) * Y(y) * Z(z)$, where X, Y, and Z each depend only on x, y, and z respectively, it is known (see for example Jackson, 1963) that,

$$\phi(x,y,z) = \sum_{u=-\infty}^{\infty} \sum_{v=-\infty}^{\infty} A(u,v)\, e^{-(u^2+v^2)^{1/2} z}\, e^{-iux - ivy}$$

[EQ 5-1]

is a solution of the LaPlace equation. These symbols, u and v, will be identified below as the wavenumbers conjugate to x and y in the

Fourier transformation. Therefore, the gravity, g(x,y,z), is given by,

$$g(x,y;z) = \sum_{u=-\infty}^{\infty} \sum_{v=-\infty}^{\infty} A(u,v)\, e^{-(u^2+v^2)^{1/2} z}\, e^{-iux-ivy}\, (u^2+v^2)^{1/2}$$

In the case of a gravity survey, the vertical derivative of the potential, g(x,y,z=0), is known on the plane, z=0, and tends to zero as z goes to infinity. These boundary conditions are obviously satisfied by the function given above by a proper choice of coefficients A(u,v). Such that,

$$g(x,y;z=0) = \left.\frac{-\partial \phi(x,y;z)}{\partial z}\right|_{z=0} = \sum_{u=-\infty}^{\infty} \sum_{v=-\infty}^{\infty} A(u,v)\, e^{-iux-ivy} (u^2+v^2)^{\frac{1}{2}}$$

Because of the Uniqueness Theorem (Kellogg, 1954; Jackson, 1963), it is also a unique solution except for a constant term. We denote the Fourier transform of a function, f, by putting a ~ on top of it. So the Fourier transform, $\tilde{\phi}(u,v;z)$ of $\phi(x,y;z)$ is,

$$\tilde{\phi}(u,v;z) = \int_X \int_Y \phi(x,y;z)\, e^{iux+ivy}\, dx\, dy$$

Inverse Fourier transform of $\tilde{\phi}(u,v;z)$ gives,

$$\phi(x,y;z) = \frac{1}{4\pi^2} \int_U \int_V \tilde{\phi}(u,v;z)\, e^{-ixu - iyv}\, du\, dv$$

or in discrete form,

$$\phi(x,y;z) = \frac{1}{4\pi^2} \sum_U \sum_V \tilde{\phi}(u,v;z)\, e^{-ixu - iyv}$$

Comparing this with the equation, EQ 5-1, above gives,

$$\tilde{\phi}(u,v;z) = 4\pi^2 A(u,v)\, e^{-(u^2+v^2)^{1/2} z}$$

[EQ 5-2]

Therefore, g(x,y;z), the vertical derivative of ϕ(x,y;z), is,

$$g(x,y;z) = -\frac{\partial \phi(x,y;z)}{\partial z}$$

$$= \int_U \int_V A(u,v)(u^2+v^2)^{1/2}\, e^{-(u^2+v^2)^{1/2} z}\, e^{-ixu - iyv}\, du\, dv$$

The Fourier transform is,

$$\tilde{g}(u,v;z) = A(u,v)\,(u^2+v^2)\,e^{-(u^2+v^2)^{\frac{1}{2}}z}$$

[EQ 5-3]

Substituting z=h and z=0 into equation EQ 5-3, we obtain,

$$\tilde{g}(u,v;z=h) = A(u,v)\,(u^2+v^2)^{1/2}\,e^{-(u^2+v^2)^{\frac{1}{2}}h}$$

$$\tilde{g}(u,v;z=0) = A(u,v)\,(u^2+v^2)^{\frac{1}{2}}$$

Therefore,

$$\tilde{g}(u,v;z=h) = \tilde{g}(u,v;0)\,e^{-(u^2+v^2)^{\frac{1}{2}}h}$$

Thus continuation is easily done in the frequency domain by the multiplication of a factor $\exp\{-h*(u^2+v^2)^{1/2}\}$, where h is positive for upward continuation, and negative for downward continuation.

For calculating the nth vertical derivative in the frequency domain, we note,

$$g^n(x,y;z) = \frac{\partial^n}{\partial z^n} g(x,y;z) = -\frac{\partial^{n+1}}{\partial z^{n+1}} \phi(x,y;z)$$

$$g^n(x,y;z) = (-1)^n \int_U \int_V A(u,v)(u^2+v^2)^{\frac{n+1}{2}} e^{-(u^2+v^2)^{1/2} z} e^{-ixu-iyv}\, du\, dv$$

Therefore,

$$\tilde{g}^n(u,v;z) = (-1)^n A(u,v)(u^2+v^2)^{\frac{n+1}{2}} e^{-(u^2+v^2)^{1/2} z}$$

Therefore, comparing this with the expression for $\tilde{g}(u,v;z)$ given in EQ 5-2, gives,

$$\tilde{g}^n(u,v;z) = (-1)^n (u^2+v^2)^{\frac{n}{2}} \tilde{g}(u,v;z)$$

So the nth vertical derivative of g(u,v;z) is obtained by multiplying a factor $(-1)^n * (u^2 + v^2)^{n/2}$ to the function in the frequency domain.

It is often useful to apply a reduction to the north pole filter to magnetic data. Because both the remanent magnetic field and the ambient earth field are usually not vertically polarized, a magnetic anomaly is generally distorted such that it does not resemble the shape of the causative body. The reduction to the pole filter will re-calculate the magnetic field caused by the same anomalous body with a vertical remanent polarization, and in a vertically polarized ambient earth magnetic field. Following the development in Gunn (1974), I derive this operator in the frequency domain below.

For a single magnetic moment, $\vec{m}_a$, at (x,y,h), the scalar magnetic potential is,

$$U(x,y;h) = \vec{m}_a(\alpha,\beta,z) \cdot \vec{\nabla} \left[\frac{1}{\{(x-\alpha)^2 + (y-\beta)^2 + (z-h)^2\}^{1/2}} \right]$$

Assuming constant direction, a distribution of magnetic moments in half space z<0, produces a scalar magnetic potential,

$$U(x,y,h) = \frac{\partial}{\partial \vec{k}} \int_0^{-\infty} \int_{-\infty}^{\infty} \int_{-\infty}^{\infty} \frac{m_a(\alpha,\beta,z)\, d\alpha\, d\beta\, dz}{\{(\alpha-x)^2 + (\beta-y)^2 + (h-z)^2\}^{1/2}}$$

where $\frac{\partial}{\partial \vec{k}_o} = l\frac{\partial}{\partial x} + m\frac{\partial}{\partial y} + n\frac{\partial}{\partial z}$

l,m, and n are direction cosines, such that,

$$l = \vec{m}_a \cdot \vec{x}_1 / |\vec{m}_a| \,, \quad m = \vec{m}_a \cdot \vec{y}_1 / |\vec{m}_a| \,, \quad n = \vec{m}_a \cdot \vec{z}_1 / |\vec{m}_a|$$

x_1, y_1, and z_1 are unit vectors of the Cartesian coordinates. If we invoke the boundary condition that U (x,y,0) is defined everywhere on a infinite half plane, z=0, and is zero as z goes to infinity. We can expand the integral as a Fourier transform,

$$\int_0^{-\infty}\int_{-\infty}^{\infty}\int_{-\infty}^{\infty} \frac{m_a(\alpha,\beta,z)\, d\alpha\, d\beta\, dz}{\left\{(\alpha-x)^2 + (\beta-y)^2 + (h-z)^2\right\}^{1/2}} =$$

$$\sum_{U=-\infty}^{\infty}\sum_{V=-\infty}^{\infty} B(u,v)\, e^{-(u^2+v^2)^{1/2} z}\, e^{-iux - ivy}$$

Then,

$$U(x,y,z) = \frac{\partial}{\partial \vec{k}_o}\left(\sum_U \sum_V B(u,v)\, e^{-(u^2+v^2)^{1/2} z}\, e^{-iux - ivy}\right)$$

$$U(x,y,z) = -\sum_U \sum_V (+iul + ivm + (u^2+v^2)^{1/2} n)\, B(u,v) * e^{-(u^2+v^2)^{1/2} z}\, e^{-iux - ivy}$$

The Fourier transform is,

$$\tilde{U}(u,v;z) = -(iul + ivm + (u^2+v^2)^{1/2} n)\, B(u,v)\, e^{-(u^2+v^2)^{1/2} z}$$

[EQ 5-4]

Since the magnetic field, $\vec{H}(x,y,z)$, is defined as

$$\vec{H}(x,y,z) = -\vec{\nabla} U(x,y,z)$$

$$\therefore$$

$$\vec{H}(x,y,z) = \vec{\nabla} \left(\sum_U \sum_V (iul + ivm + (u^2+v^2)^{1/2} n) * B(u,v)\, e^{-(u^2+v^2)^{1/2} z}\, e^{-iux - ivy} \right)$$

If L,M, and N are the direction cosines of the measured magnetic field vector,

$$L = \frac{\vec{H}\cdot\vec{X}_1}{|\vec{H}|}, \quad M = \frac{\vec{H}\cdot\vec{Y}_1}{|\vec{H}|}, \quad N = \frac{\vec{H}\cdot\vec{Z}_1}{|\vec{H}|}$$

then,

$$\vec{H}(x,y,z) = -\sum_{u=-\infty}^{\infty}\sum_{v=-\infty}^{\infty} (iul + ivm + (u^2+v^2)^{1/2} n) * (iuL + ivM + (u^2+v^2)^{1/2} N) * B(u,v)\, e^{-(u^2+v^2)^{1/2} z}\, e^{-iux - ivy}$$

$$\tilde{\vec{H}}(u,v,z) = -(iul + ivm + (u^2+v^2)^{1/2} n) * (iul + ivM + (u^2+v^2)^{1/2} N) * B(u,v)\, e^{-(u^2+v^2)^{1/2} z}$$

If we denote, $\tilde{\vec{H}}_{\perp}(u,v,z)$, the magnetic field due to the same magnetic moments aligned vertically in a vertically polarized field, then

$$\tilde{\vec{H}}_{\perp}(u,v,z) = -(u^2+v^2)\, B(u,v)\, e^{-(u^2+v^2)^{1/2} z}$$

Therefore,

$$\frac{\tilde{\vec{H}}_{\perp}}{\tilde{\vec{H}}} = \frac{u^2+v^2}{(iul + ivm + (u^2+v^2)^{1/2} n)(iuL + ivM + (u^2+v^2)^{1/2} N)}$$

The expression on the right hand side of the equation above is the factor (or filter) used to multiply to the measured field in the frequency domain to give the reduced to the pole magnetic field.

Next, we develop the relationship between the magnetic and gravity potentials. From EQ 5-1, we have,

$$\frac{\partial}{\partial \vec{k}_o}\phi(x,y,z) = -\sum_U \sum_V A(u,v)\, e^{-(u^2+v^2)^{1/2} z} * e^{-iux - ivy} (iul + ivm + (u^2+v^2)^{1/2} n)$$

Therefore,

$$\frac{\partial}{\partial \vec{k}_o}\tilde{\phi}(u,v,z) = -A(u,v)\, e^{-(u^2+v^2)^{1/2} z} * \left(iul + ivm + (v^2+u^2)^{1/2} n\right)$$

Dividing the above equation by EQ 5-4, we obtain,

$$\frac{\partial}{\partial \vec{k}_o}\tilde{\phi}(u,v,z) = \frac{A(u,v)}{B(u,v)} * \tilde{U}(u,v,z)$$

If we assume a constant density and magnetization for the common source, then A(u,v)/B(u,v) should not depend on u and v, and is a constant term. To find the constant term, A(u,v)/B(u,v), we consider a small volume v at $\vec{r}'$ with density d and magnetization $\vec{m}_a$. The potentials are given by,

$$\phi(\vec{r}) = \phi(x,y,z) = \frac{G\rho\,\Delta V}{|\vec{r} - \vec{r}'|}$$

$$U(\vec{r}) = U(x,y,z) = \Delta V\, \vec{m}_a \cdot \vec{\nabla}\left(\frac{1}{|\vec{r} - \vec{r}'|}\right)$$

It is noted that,

$$\frac{\partial}{\partial \vec{k}_o} = \frac{\vec{m}_a \cdot \vec{\nabla}}{|\vec{m}_a|}$$

Therefore,

$$\frac{\partial}{\partial \vec{k}_o}\,\phi(\vec{r}) = G\rho\,\Delta V\left(\frac{\vec{m}_a\cdot\vec{\nabla}}{|\vec{m}_a|}\right)\left(\frac{1}{|\vec{r}-\vec{r}'|}\right)$$

Dividing the two equations above gives,

$$\frac{\frac{\partial}{\partial \vec{k}_o}\,\phi(\vec{r})}{U(\vec{r})} = \frac{G\rho\,\Delta V\left(\frac{\vec{m}_a\cdot\vec{\nabla}}{|\vec{m}_a|}\right)\left(\frac{1}{|\vec{r}-\vec{r}'|}\right)}{\Delta V\,\vec{m}_a\cdot\vec{\nabla}\left(\frac{1}{|\vec{r}-\vec{r}'|}\right)}$$

Therefore,

$$\frac{A(u,v)}{B(u,v)} = \frac{G\rho}{|\vec{m}_a|}$$

or,

$$\frac{\partial}{\partial \vec{k}_o}\,\phi(\vec{r}) = \frac{G\rho}{|\vec{m}_a|}\,U(\vec{r})$$

Poisson arrived at this equation in 1826 and is called Poisson's theorem.

MOVING WINDOW APPLICATION OF POISSON'S THEOREM

Chandler and others (1981) applied Poisson's theorem to a multisource magnetic and gravity data set using a small moving window. Assuming a body with a uniform magnetization and density, the gravity (ϕ) and magnetic (U) potentials are related by (as derived earlier in the discussion of spectral filtering),

$$U = \frac{1}{G}\left(\frac{\Delta m}{\Delta d}\right)\frac{\partial \phi}{\partial \vec{k}_o}$$

For the vertical component of the magnetic field, it becomes,

$$H_z = \frac{1}{G}\left(\frac{\Delta m}{\Delta d}\right)\frac{\partial g}{\partial z}$$

Generally, for a local anomaly superimposed on a regional trend, A,

$$H_z = A + \frac{1}{G}\left(\frac{\Delta m}{\Delta d}\right)\frac{\partial g}{\partial z}$$

where H_z is the magnetic field reduced to the pole,

G is the gravitation constant,

Δm is the magnetization contrast,

Δd is the density contrast,

$\vec{k}_o$ is the direction of magnetization,

$\partial g(z)/\partial z$ is the first vertical derivative of gravity.

This assumes that there is no interference from surrounding sources, and the regional field is adequately represented by the term A. That means the wavelength of the regional field is much larger than the window size. Because the vertical component of the magnetic field is usually obtained by the reduction to the north pole operation, the anomalous body must be polarized in the direction of the ambient earth field and there cannot be a remanent magnetization for this relation to hold.

Inputs are grids of magnetic field reduced to the pole and the first vertical derivative of gravity. A least square fit of the data points within a small moving window estimates the intercept A and slope ($\Delta m / \Delta d$) of the above linear equation.

Three terms, the correlation coefficient, intercept A, and slope ($\Delta m/\Delta d$) were determined on each grid node. The window was then displaced 1.6 km to the next grid node and the calculation repeated. This method allows the combined analysis of gravity and magnetic data. Values of ($\Delta m/\Delta d$) should provide clues to rock type and dimensions of the source. Interpretation of the results is limited to areas of high correlation between the gravity and magnetic fields and stable intercept values. Low correlations are assumed to come from areas with interference from nearby sources, or from areas that violate the assumption that the anomalies are caused by the same body with uniform density and uniform induced magnetization. Unstable intercept values may indicate interference from other sources or presence of a large component of remanent magnetization.

SYNTHETIC SUN ILLUMINATION

Synthetic sun illumination of map data helps to identify subtle features. The map data can be any spatially dependent physical quantity, such as elevation, gravity, or magnetic field. Many previous works describe this technique. Horn (1981) reviewed the historical development and various approaches in generating shaded-relief maps of topography. Batson and others (1975) applied the Lommel-Seeliger law to produce reflectance maps of the topography. While Guinness and others (1982) used the technique on topographic, gravity and thermal infrared image data.

Synthetic sun illumination of gravity data will allow easier perception of relief in the data, and detection of directional trends and patterns by varying the azimuth of the sun illumination. It is superior to the frequency trend pass filter, which tends to elongate anomalies in the filter direction.

Since quite different sets of trend lines are derived from the same map by different observers, one has to be cautious in interpreting each individual trend line. It is therefore more appropriate to interpret these lineaments collectively. It has been noted (for example Wise and others, 1985) that lineaments derived from topographic relief appear to divide the land surface into domains. Such that within each domain, the majority of the lineaments are more or less aligned in a certain direction distinct from that of the adjacent area. This localized swarm of lineaments may reflect the large scale domain-wide stress strain pattern and common structural grain. Categorization of the gravity lineaments

into cumulative length per ten degrees in azimuthal angle may reveal preferred directions of the trend lines and aid in the interpretation.

I used the Lommel-Seeliger law to calculate the reflectance. It states that

$$I = 1/ (1 + \cos e / \cos i)$$

where I = the intensity of the reflectance

e = the angle between the observer and the slope normal

i = the angle between the sun and the slope normal

Figure 14 illustrates the definition of the parameters. This law was empirically derived from a study of sun reflectance from various earth materials (see Batson and others, 1975).

For gravity data, the slope of a surface depends on the choice of the factor that converts gravity values to spatial dimension. Proper selection of this factor will also give optimal exaggeration to the relief. The factor 0.75 mgal/km (1.2 mgal/mile) was chosen in our case to produce a maximum slope of less that 45 degrees.

Figure 14. Lommel-Seeliger law for reflectance. The intensity of the reflectance is $1/(1+\cos(e)/\cos(i))$.

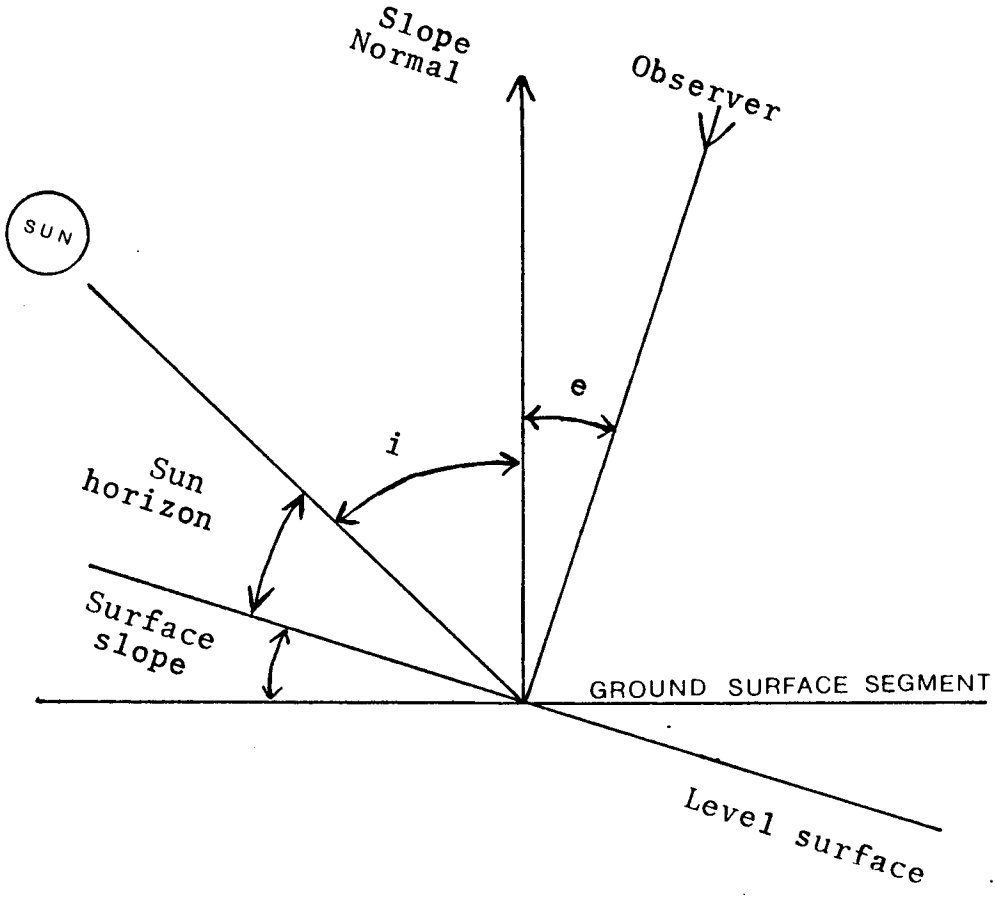
Slope
Normal
Observer
SUN
e
i
Sun
horizon
Surface
slope
GROUND SURFACE SEGMENT
Level surface

ISOSTATIC CALCULATION

It has long been noted that the Bouguer anomaly has a strong negative correlation with topography. The most commonly accepted hypotheses to explain this phenomenon were those put forth by Airy and Pratt. In the Airy model, the mass of a column of crust is maintained constant by varying the depth of a root beneath the crust, which is given by,

$$R = \frac{d_c}{d_m - d_c} * h$$

where d_c is density of crust,

d_m is density of mantle,

h is the elevation.

In the Pratt model, the density of the column of mass down to a certain depth of compensation, D, is varied so that the pressure at that depth is the same everywhere. For an elevation, h, the density, d_0, of a column at sea level is altered and is given by,

$$d_h = \frac{d_o * D}{(D + h)}$$

Modification to these simple local compensation models include horizontal redistribution of the compensating mass, i.e. regional compensation, and incorporation of the effect due to the rigidity of the crust, i.e. partial compensation.

The isostatic correction is the gravitational acceleration due to the root system, which has a density contrast of (d_m-d_c), in the Airy model; or that due to the column of mass, which has a density contrast of $-d_0*h/(h+D)$, in the Pratt model. Since the sources of the isostatic correction are at depth, it is of very long wavelength and sometimes can be regarded as the regional trend in anomaly separation. An isostatic anomaly is obtained by subtracting the isostatic correction from the Bouguer anomaly.

COMPUTER FORWARD MODELING

The modeling program uses formulae for a prism-shape body described by Goodacre (1973), and Bhattacharyya (1964). Required input prism parameters are density and/or susceptibility contrast, and the Cartesian coordinates of the four vertices at the top and bottom of the prism. The gravitational acceleration (or magnetic field) along a data profile is calculated. Comparison can be made between the modeled and measured values, then the prism parameters are modified to improve on the closeness of fit. The process is repeated until a satisfactory fit is reached. Since there can be an infinite number of possible sources that could give rise to a given anomalous field, further constraints on the model using information derived from geology, drill well data, magnetics, and seismic methods will limit the number of feasible solutions to a few.

CHAPTER SIX

INTERPRETATION

In this chapter, I discuss the application of the enhancement methods to the Kansas gravity data, and my interpretation of the enhanced maps and data. I shall present a synthesis of these findings in chapter seven.

THE BOUGUER GRAVITY MAP

A summary of the main features apparent on the Bouguer gravity map of Kansas (figures 13 and 15) follows. The gravity magnitudes range from a high of +5 mgals in northcentral Kansas (labelled 'H') to a low of -150 mgals near the Kansas/Colorado border (just north of 'L'). The most prominent features on the Bouguer gravity map of Kansas (fig. 15) are: a steep west-dipping gravity gradient in western Kansas, which is caused mainly by the thickening of the crust to the west; a northeast trending gravity high (labelled 'H') with flanking lows in northcentral Kansas, which is the gravity signal associated with a late Precambrian failed rift;, a broad gravity high in southeastern Kansas (labelled 'R'), which coincides with rhyolitic basement; and a gravity high near the southeastern end of the Central Kansas uplift (labelled 'C'). The above anomalies will be discussed in more detail in the following sections.

Figure 15. Color Bouguer gravity map of Kansas. Same as figure 13.

BOUGUER GRAVITY ANOMALY MAP OF KANSAS

REFERENCED TO IGSN71, DENSITY=2.67 GM/CC

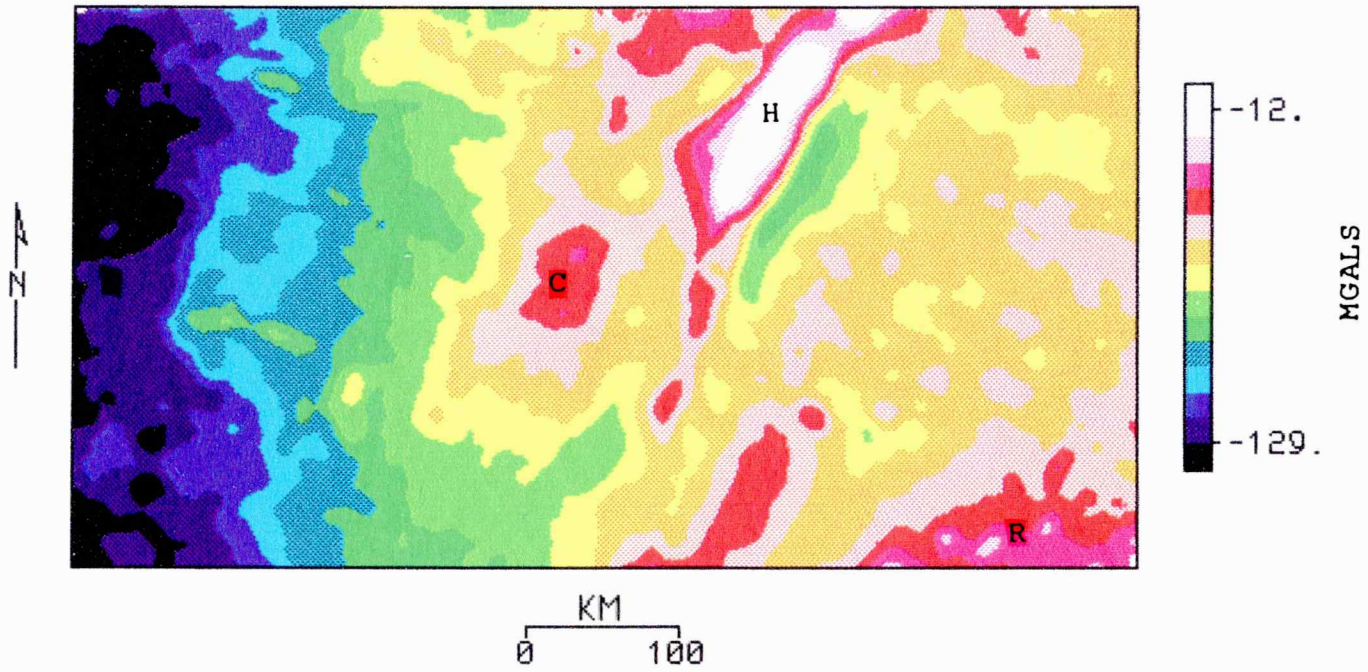

ISOSTATIC REDUCTION

It is clear that there is generally a negative correlation between Bouguer gravity (fig. 15) and elevation (fig. 16), particularly in western Kansas. As mentioned in chapter 5, this negative correlation is due to an Airy isostatic root system at the base of the crust. To better isolate the geologic signal from within the crust, it is desirable to correct for this isostatic effect.

The computer program "AIRYROOT" developed at the United States Geological Survey (USGS) by Simpson and others (1983) was adapted to calculate the gravity acceleration of the Airy root system for a region that is centered about the observation point and extends 166.7 km radially outward. The isostatic map compiled by Karki and others (1961) was used to estimate the gravity effect of the root system beyond 166.7 km. The sum of these calculations gives the total isostatic correction.

The program "AIRYROOT" takes advantage of the Parker algorithm (1972) which uses the fast Fourier transform (FFT) to calculate potential field anomalies. This efficient algorithm allowed me to experiment with different Airy isostatic models, using a range of lower crust/upper mantle (c/m) density contrasts and sea level crustal column depths. Since the Karki map used a c/m density contrast of 0.6 gm/cc and a sea level crustal column of 30 km, a different set of parameters used in the "AIRYROOT" program will give rise to a smooth, long wavelength mismatch error of several mgals, as estimated by Simpson and others (1983). It has been noted (Woollard, 1966) that the optimal thicknesses of the sea level

Figure 16. Topographic map of Kansas in meters above sea level.

TOPOGRAPHIC MAP OF KANSAS - ELEVATION IN METERS

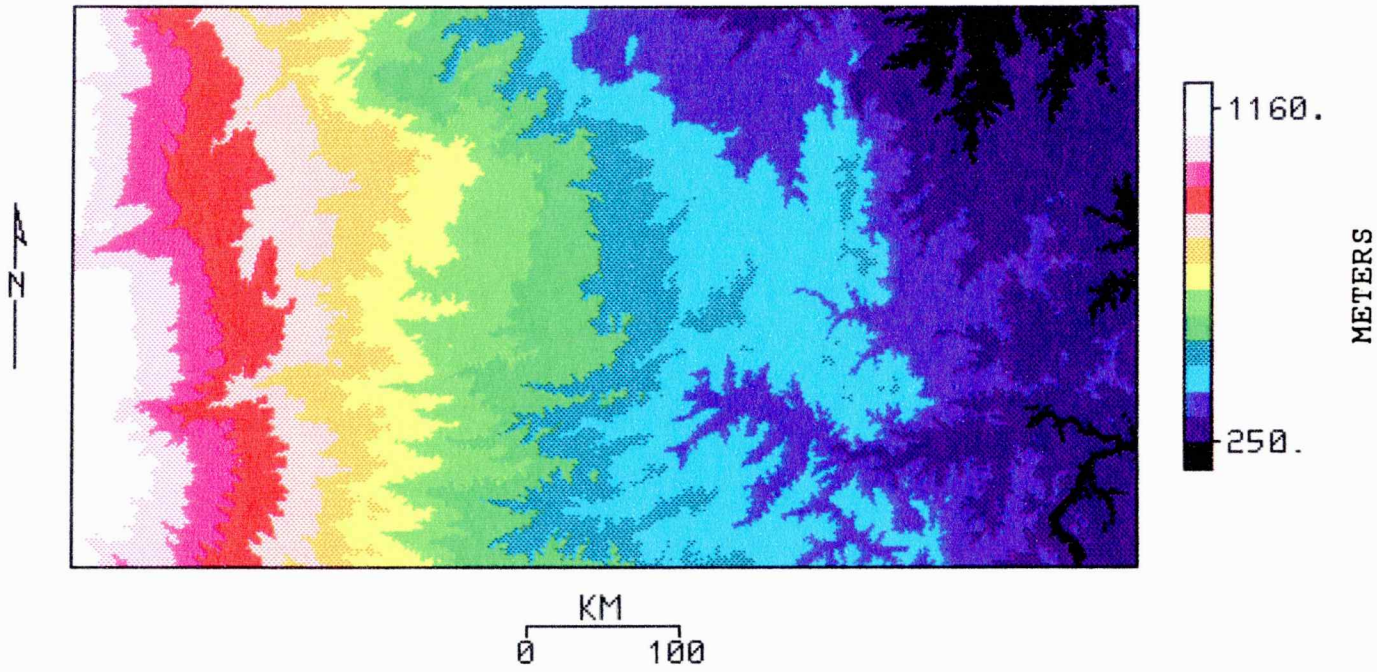

crustal columns and c/m density contrasts for isostatic calculations are not constant and depends strongly on the particular geologic province. These parameters chosen were such that they are in agreement with the seismically determined crustal thicknesses and velocities of the study area. Therefore these parameters are usually different from the Karki values given above.

Since the topographic relief in Kansas and adjacent area is relatively gentle, a 5 by 5 minute topographic data grid was good enough for calculating the root depth. The maximum errors are 1 and 3 mgals when using a 3- and 5-minute topographic grid in the isostatic calculations of the entire continental United States (Simpson, 1983). I have also calculated the isostatic corrections for a one degree by two degree area in central Kansas using a 1.6 by 1.6 km and 11.2 by 11.2 km topographic grid of the state. The average, maximum and minimum differences in the two resultant isostatic correction grids are 0.036, 0.1 and 0.00024 mgals respectively.

Since the gravity data was collected at various elevations, the Bouguer gravity map was leveled to an observation elevation of 1.28 km above sea level, which is about the highest point in the state. A leveled gravity grid is needed because the AIRYROOT program generates a correction grid at a horizontal observation plane, which was chosen to be 1.28 km above sea level in this study. The following procedure was used to prepare the leveled gravity grid.

Because our FFT program requires a grid with no undetermined values, the missing values in the gravity grid were filled in with

interpolated or estimated values. Some grid nodes have a missing value code assigned to it for the following reasons. First, the gravity data in southwestern Kansas have not been incorporated. This area was filled in with crude estimates based on the few gravity stations obtained from the Defense Mapping Agency. Second, the grid node gravity value occasionally cannot be reliably estimated from the surrounding measurements because of an insufficient number of data points. This usually happens near rivers, lakes, sand hills or open ranges. Missing values in the grid were filled in with interpolated values.

The resulting filled-in gravity grid was upward continued to seven different horizons from 150 m (500 ft) to 1050 m (3500 ft), at increments of 150 m. These grids were used later to differentially upward continue the gravity data to a common datum level. Since the original gravity data was collected at various elevations, each grid node had to be upward continued by a different amount to produce a final Bouguer gravity grid upward continued to the same level, 1280 m (4200 ft) above sea level. I assumed that the gravity data were taken at the grid nodes, and at an elevation given by the terrain grid of the state (fig. 16), which was prepared from the data provided by the National Oceanic and Atmospheric Administration (NOAA). The amount of upward continuation needed for a particular grid node is equal to the difference between the elevation there and 1280 m. The upward continued gravity value was obtained by interpolating between the grids at two adjacent horizons. For

example, a grid node at an elevation of 800 m was upward continued by 480 m, and its value was determined by interpolating between the 450 and 600-m upward continued gravity grids. Sources of error for this approach are that the gravity data were neither measured at the grid node, nor at the elevation given by the terrain grid, and the operation of upward continuation applied to data collected at differing elevations. Although this approach of point by point upward continuation is not rigorous, it at least brought the entire data grid to approximately the same level of observation, at 1.28 km above sea level (fig. 17). Almost all gravity grid nodes changes by less than 0.5 mgal per 150 meters. Therefore, the error introduced by making the above assumptions was usually less than the 0.1 mgal accuracy of the original data.

The 1.28 km upward continued isostatic correction grid, which was generated by the "AIRYROOT" program, was subtracted from the leveled Bouguer gravity map to give the isostatic residual map. A wide range of crust/mantle (c/m) density contrasts and depths for sea level crustal columns were attempted in order to come up with a set of optimal parameters for Kansas. Correlation coefficients between residual isostatic gravity and elevation were calculated in order to choose the optimal c/m density contrast.

To test these isostatic correction procedures, I first studied some hypothetical cases, assuming the same topographic relief as given by the 5 by 5 minute state grid, a homogeneous density in the upper crust and Airy root system. The resulting isostatic residual map was a flat zero mgals surface as expected, while the Bouguer

Figure 17. Bouguer gravity map of Kansas leveled at 1.28 km above sea level.

BOUGUER GRAVITY MAP OF KANSAS

LEVELED AT 1.28 KM ABOVE SEA LEVEL

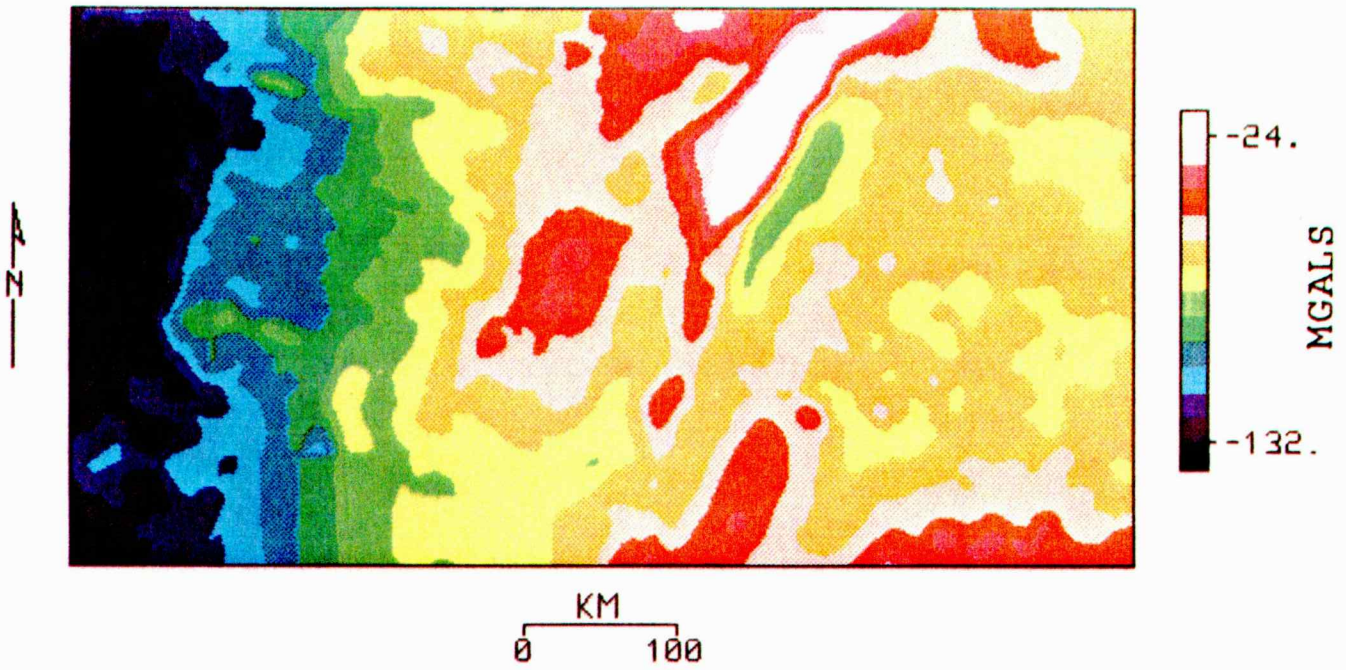

gravity map represented the gravity effect due to the Airy root system. A c/m density contrast of 0.45 gm/cc and 30 km sea level crustal column was used. Isostatic corrections corresponding to density contrasts from 0.05 to 0.99 gm/cc were applied to this hypothetical Bouguer gravity grid. The correlation coefficients for these isostatic residual grids and the topographic grid are shown in figure 18. It shows a sharp discontinuity at the correct density contrast, 0.45 gm/cc as expected.

The success in finding the optimal c/m density contrast in the hypothetical model above was encouraging. It prompted me to try out a more sophisticated hypothetical model. Random noise of 10 mgal maximum amplitude and an additional west-dipping gravity gradient of -0.01875 mgal/km in western Kansas was introduced into the ideal model above. The purpose for so doing was to simulate the actual gravity measurements in Kansas. The 10 mgals noise reflects the shallow localized density anomalies, while the -0.01875 mgal/km west-dipping gravity gradient reflects the thickening as well as the lowering of the average density of the Phanerozoic sediments to the west (Woollard, 1959). The resultant hypothetical Bouguer gravity grid was again subjected to the same isostatic corrections as discussed in the last paragraph. The residual isostatic gravity grids were then correlated with the topographic grids. The plot of the correlation coefficients against c/m density contrasts is shown in figure 19. The distinct discontinuity at 0.45 gm/cc is no longer observable. Instead, a smooth bend connects the two more or less straight lines on the two sides. Since the location of the bend is

Figure 18. Correlation coefficient versus lower-crust/upper-mantle density contrast. Surface topography was correlated with the residual isostatic gravity for various lower-crust/upper-mantle density contrasts. A homogeneous upper crust, a 40-km crustal column, and complete isostatic compensation at Moho were assumed in this hypothetical model.

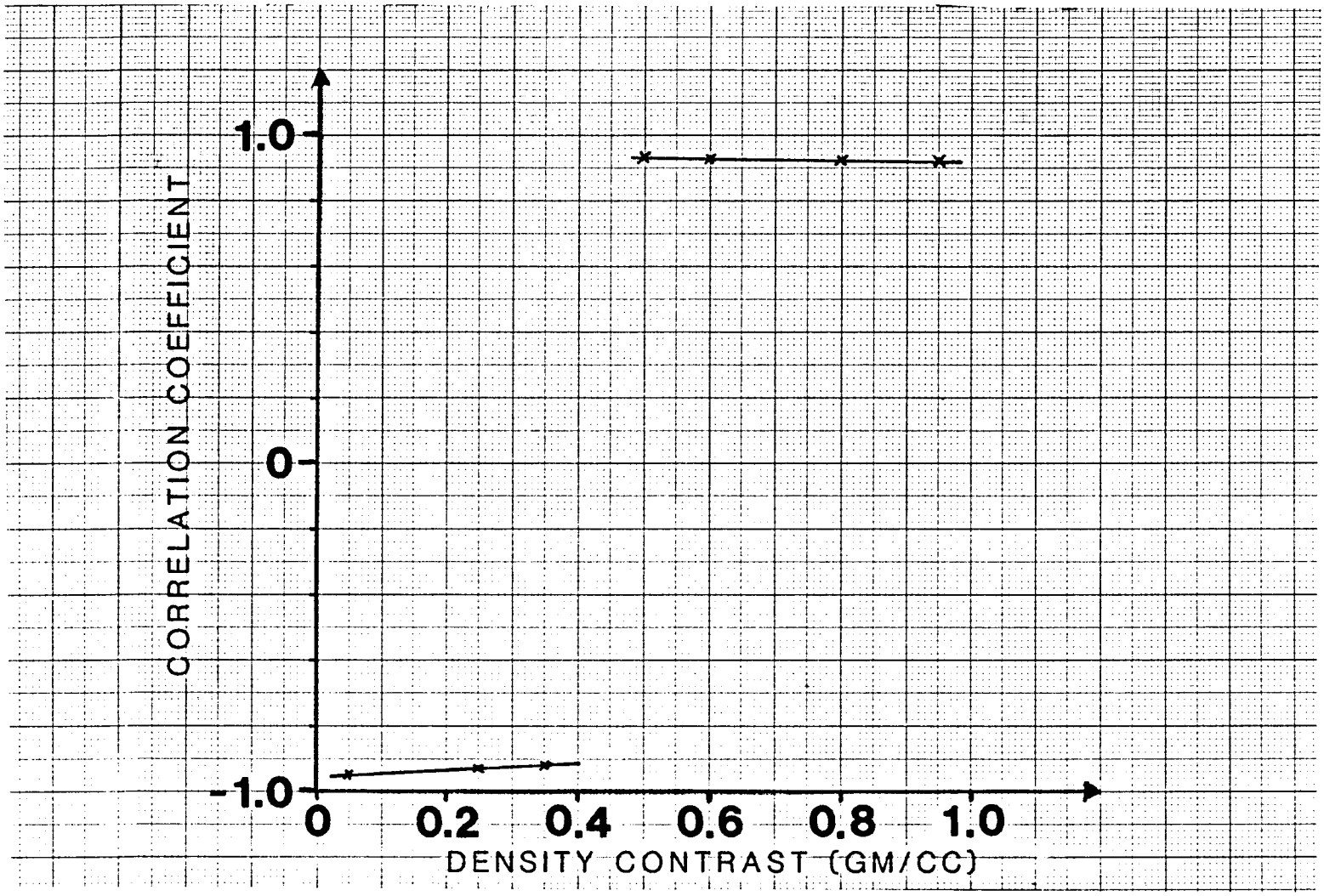
1.0
0
-1.0
CORRELATION COEFFICIENT
0
0.2
0.4
0.6
0.8
1.0
DENSITY CONTRAST (GM/CC)

Figure 19. Correlation coefficient versus lower-crust/upper-mantle density contrast. Surface topography was correlated with the residual isostatic gravity for various lower-crust/upper-mantle density contrasts. A -0.01875 mgal/km west-dipping gravity gradient in western Kansas and random noise with a 10 mgal peak were added to the hypothetical model used in figure 18.

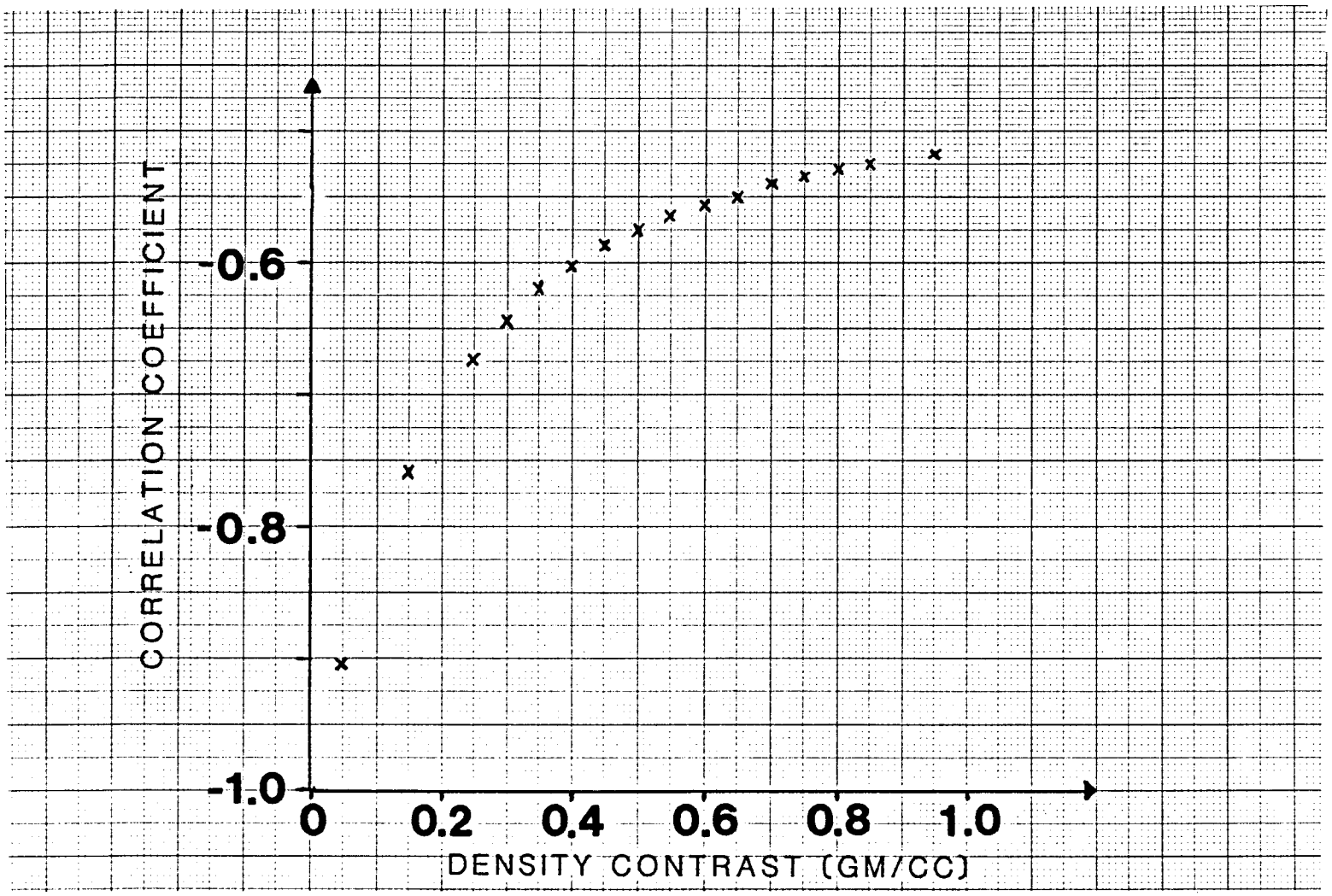
CORRELATION COEFFICIENT
-0.6
-0.8
-1.0
0
0.2
0.4
0.6
0.8
1.0
DENSITY CONTRAST (GM/CC)

not as well defined as the discontinuity in the case with no noise, only an optimal density contrast with quite large uncertainties could be determined.

One way of estimating this optimal density contrast is to fit two straight lines to the lower and higher ends of the density contrasts. The optimal range of density contrast is indicated by those points on the plot that deviate significantly from these two straight lines.

I next repeated the calculations using the actual Bouguer gravity grid. Figures 20 shows the correlation coefficients plotted against c/m density contrasts, with the sea level crustal column held constant at 40 km. A density contrast of 0.4 to 0.45 gm/cc apparently fits the Airy isostatic model best. The upper limit for the density contrast is 0.6 gm/cc. The density contrast, 0.4-0.45 gm/cc, was chosen because it also approximately agrees with the evidence from seismic refraction studies. I shall discuss this in more detail in the next section.

A similar procedure was used to estimate the optimal depth of the sea level crustal column. Figure 21 plots the correlation coefficients against sea level crustal column depths for a constant c/m density contrast of 0.45 gm/cc. The estimated optimal depth of the sea level crustal column is around 40 to 42 km. Except for an estimated crustal thickness of about 36 km near Concordia in central Kansas, these values are in agreement with the crustal thickness of Kansas determined from seismic refractions (Steeples, 1981; Stewart, 1968).

Figure 20. Correlation coefficient versus lower-crust/upper-mantle density contrast. Surface topography was correlated with the residual isostatic gravity for various lower-crust/upper-mantle density contrasts. Actual gravity data (fig. 17) was used. A 40-km crustal column was assumed.

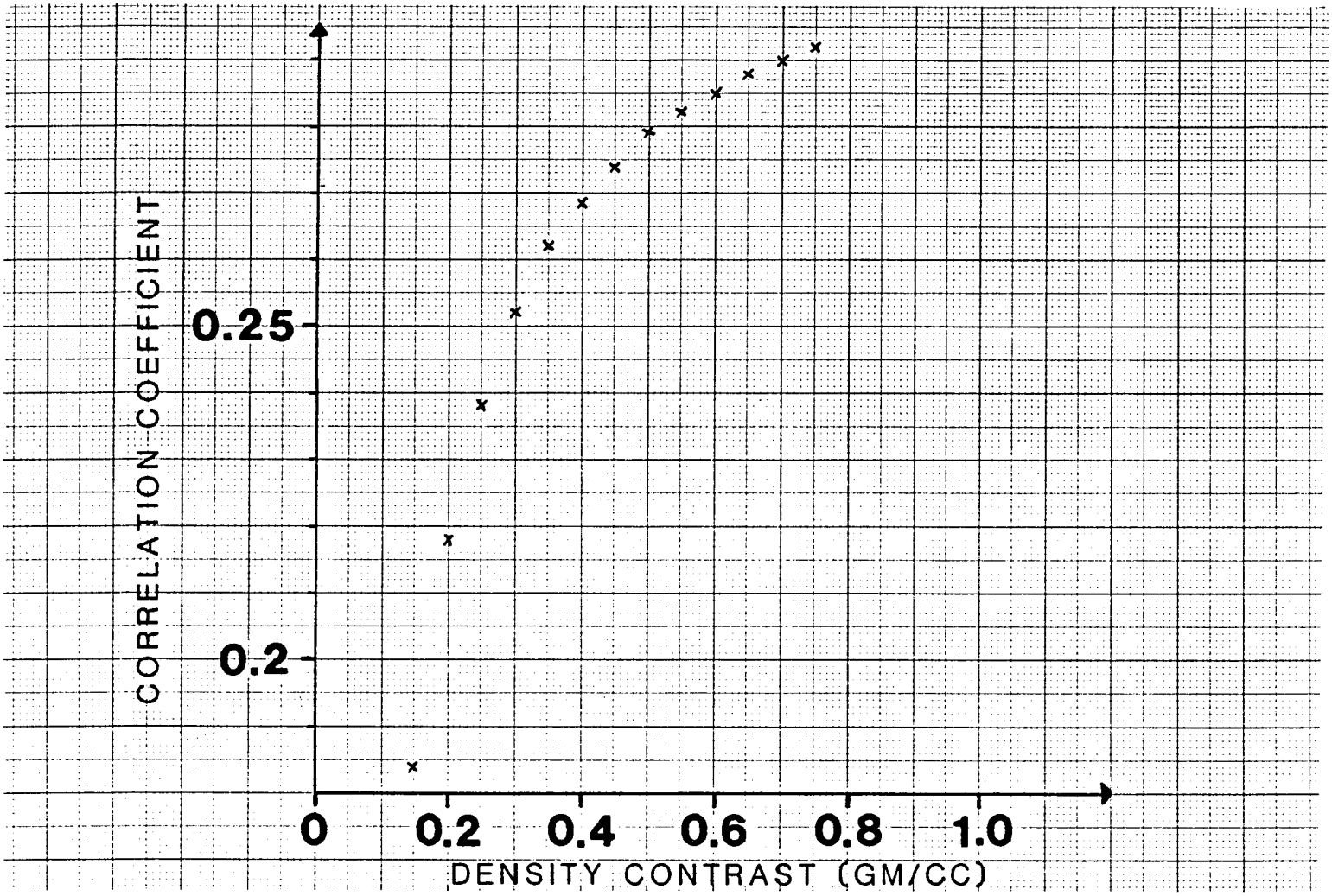
CORRELATION COEFFICIENT
0.25
0.2
0
0.2
0.4
0.6
0.8
1.0
DENSITY CONTRAST (GM/CC)

Figure 21. Correlation coefficient versus crustal column depths. Surface topography was correlated with residual isostatic gravity for various crustal column depths. Actual gravity data (fig. 17) was used. A lower-crust/upper-mantle density contrast of 0.45 gm/cc was assumed.

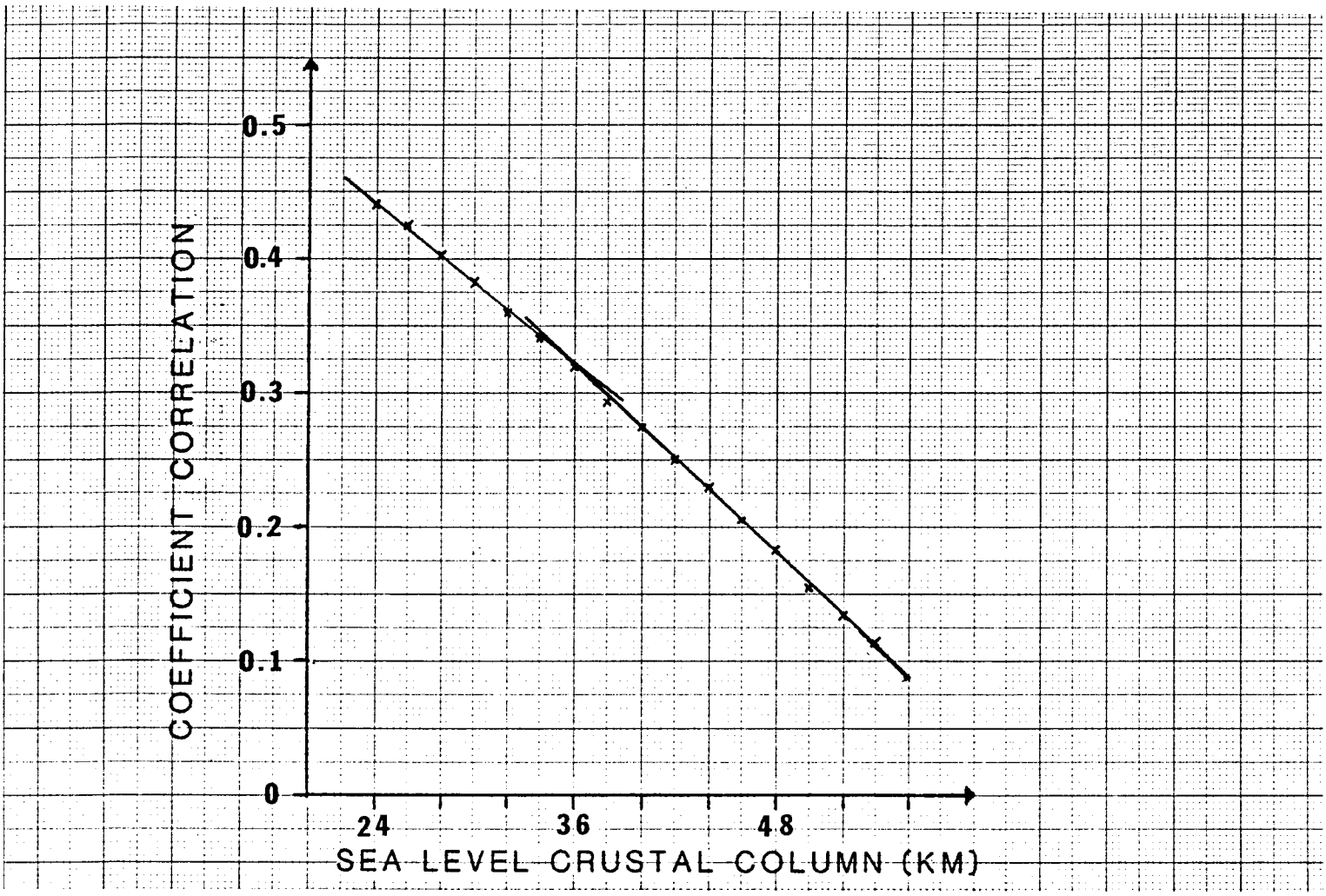
COEFFICIENT CORRELATION
0.5
0.4
0.3
0.2
0.1
0
24
36
48
SEA LEVEL CRUSTAL COLUMN (KM)

Although this method of correlating residual isostatic anomalies with the topography was very promising for the first hypothetical case, it failed to yield any significant new information about the optimal c/m density contrast and depth of the sea level crustal column for the actual measured data. The range of c/m values estimated by this method was about the same as previously suggested in the literature (see for example, Woollard, 1966). The estimated range of the depth of the sea level crustal column was 32 to 42 km.

Since the isostatic correction is smooth and of very long wavelength, the resultant isostatic residual maps using any reasonable density contrast and sea level crustal depth do not differ significantly from one another. Figures 22 and 23 show the isostatic correction and residual maps for a density contrast of 0.45 gm/cc and a 40 km deep crustal column.

The isostatic correction map (fig. 22) shows a west dipping gravity gradient, which is steeper in western (0.18 mgals/km) than eastern (0.05 mgals/km) Kansas. Except for a small gravity high in southeastern Kansas, the monotonous east-west gravity gradient dominates this map. If the isostatic root system is a true representation of the crustal thickness, then the Moho has a gentle relief in eastern Kansas, and dips almost linearly to the west in western Kansas.

The residual isostatic gravity map (fig. 23), compared to the Bouguer map (fig. 17), reveals more details of the local anomalies, particularly in western Kansas. But there are still very long

Figure 22. Airy isostatic correction gravity grid of Kansas. A 0.45 gm/cc lower-crust/upper-mantle density contrast and a 40-km crustal column were assumed.

AIRY ISOSTATIC CORRECTION MAP OF KANSAS, UPPER CRUST DENSITY = 2.67 GM/CC

NORMAL CRUSTAL COLUMN = 40 KM, C/M DENSITY CONTRAST = 0.45 GM/CC

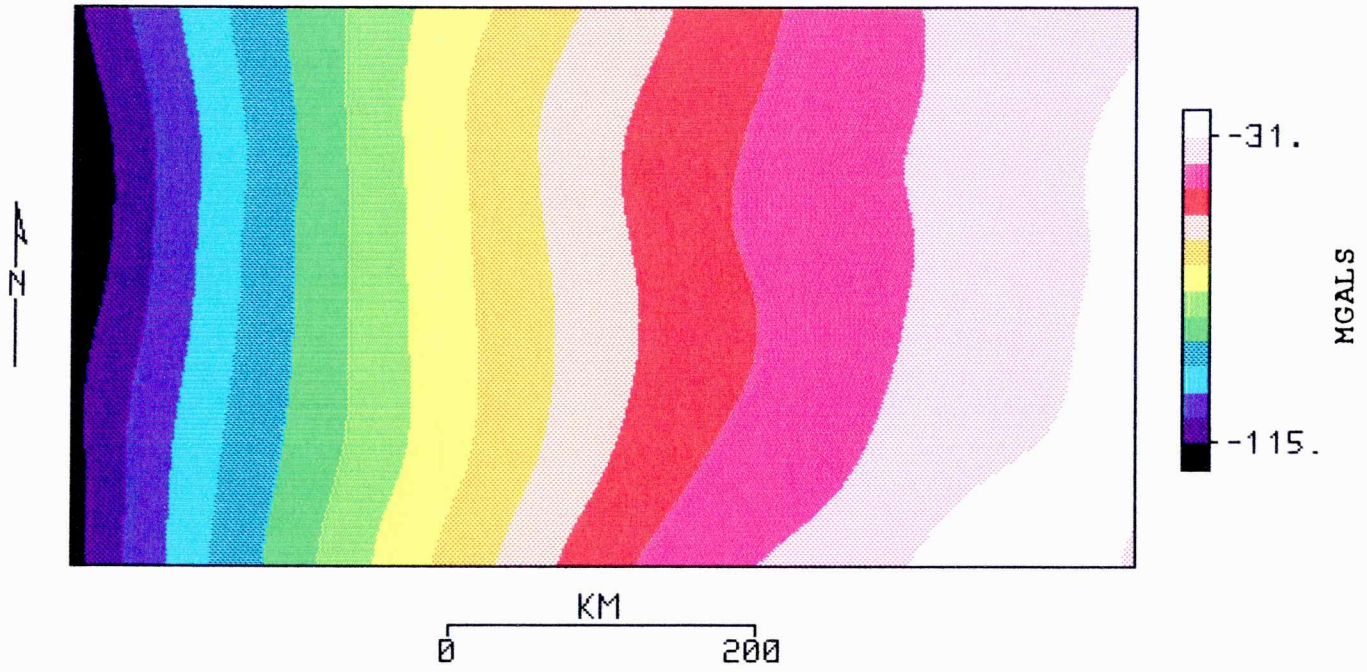

Figure 23. Airy isostatic residual gravity grid of Kansas. A 0.45 gm/cc lower-crust/upper-mantle density contrast and a 40-km crustal column were assumed.

AIRY ISOSTATIC RESIDUAL MAP OF KANSAS, UPPER CRUST DENSITY = 2.67 GM/CC

NORMAL CRUSTAL COLUMN= 40 KM, C/M DENSITY CONTRAST = 0.45 GM/CC

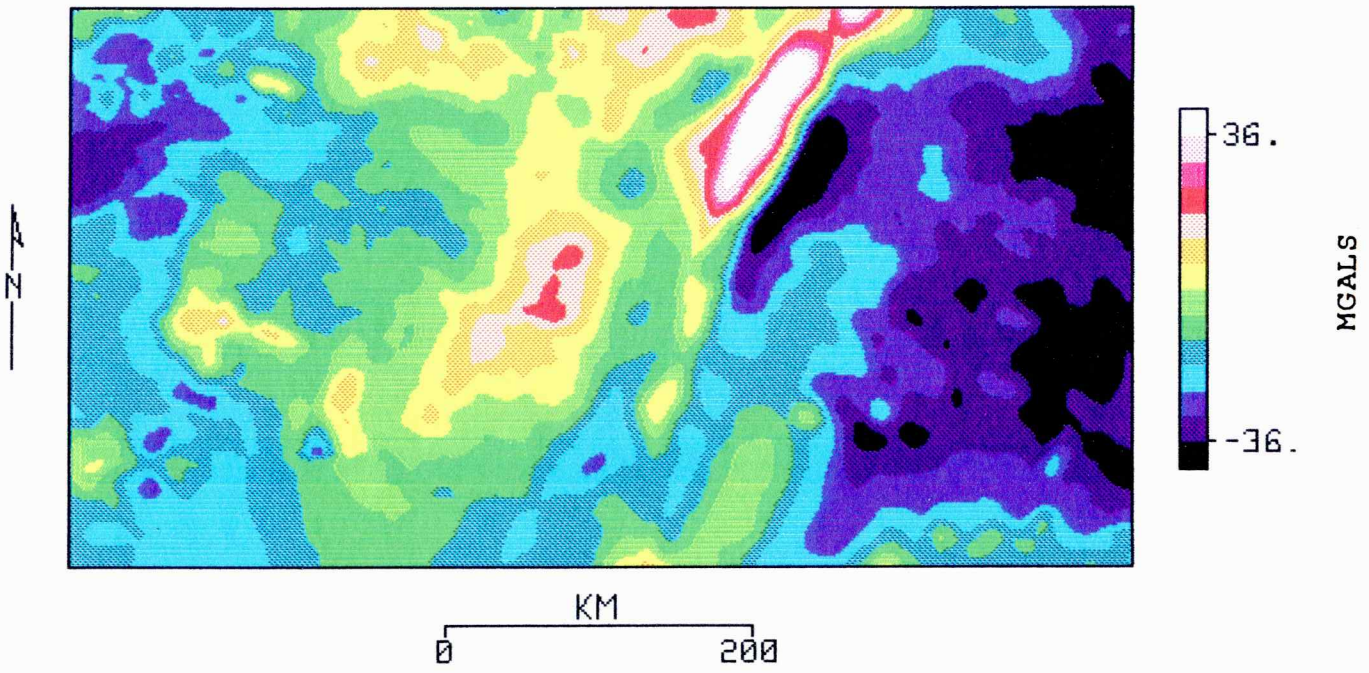

wavelength anomalies that are not removed by the isostatic correction. Broad negative anomalies in eastern and western Kansas, and a large gravity high in central Kansas could be caused by large intra-crustal or sub-crustal density anomalies, or non-Airy root behavior of the crust.

The -30 to -40 negative anomaly (fig. 23) in the east coincides with a negative free-air anomaly (fig. 24) of similar magnitude. McGinnis and others' (1979) free-air gravity map of the United States shows this anomaly is part of a larger anomaly that extends into western Missouri. This in turn is one of a chain of free-air gravity lows that extends from Wisconsin, Iowa and into Texas on a long wavelength free-air gravity map.

Free-air gravity anomalies are calculated without correcting for the mass of the rocks between the observation point and sea level, as well as the hypothetical isostatic roots at the bottom of the crust. Long wavelength free-air negative gravity anomalies reveal regional mass deficiencies in the underlying crust-mantle column.

Rather than attribute the cause of the regional isostatic low in eastern Kansas to an exceptionally thick crust (which would also account for the mass deficiency indicated on the free-air map). I prefer the explanation as depicted in figure 25. It shows an east-west cross section of the crust before and after rifting. The east dipping horizon at about 15 km below sea level is the bottom of the zone of low reflected energy observed by Brown and others (1983) in their COCORP seismic reflection line in northeastern Kansas. I

Figure 24. Free-air gravity map of Kansas.

FREE-AIR GRAVITY ANOMALY MAP OF KANSAS

REFERENCED TO IGSN71

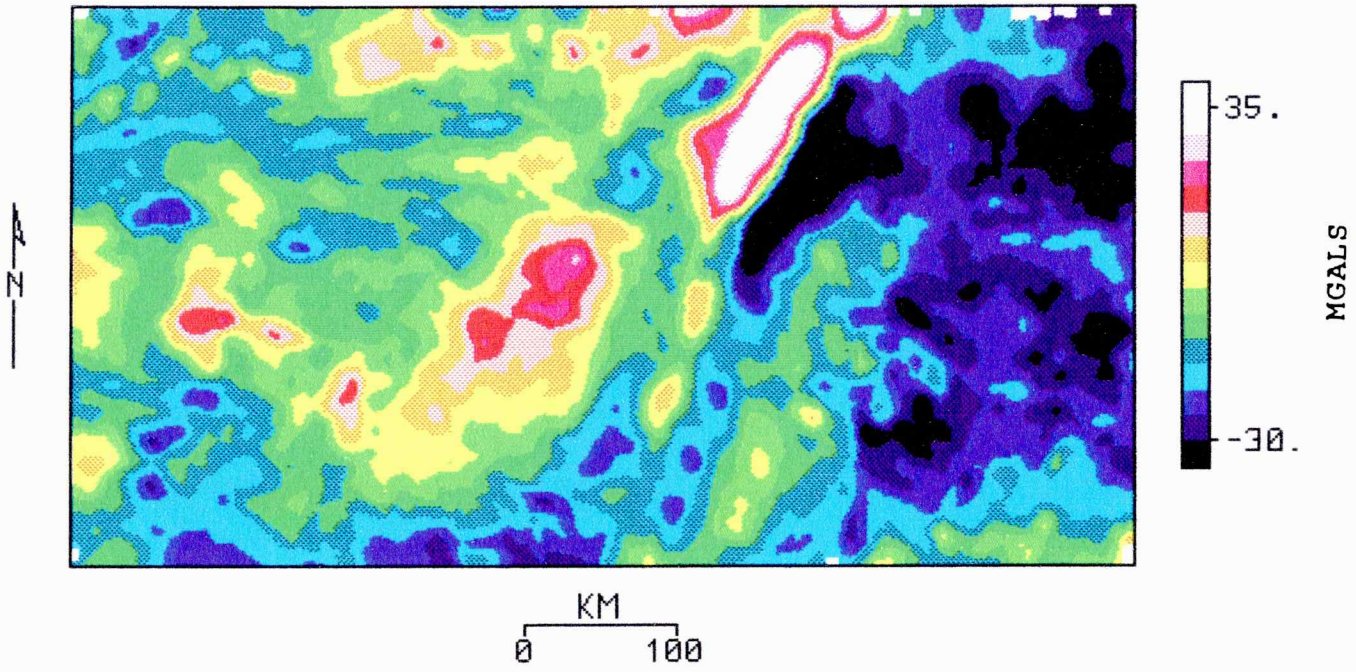

Figure 25. Cross sectional model of the crust in eastern Kansas before and after rifting in late Precambrian time.

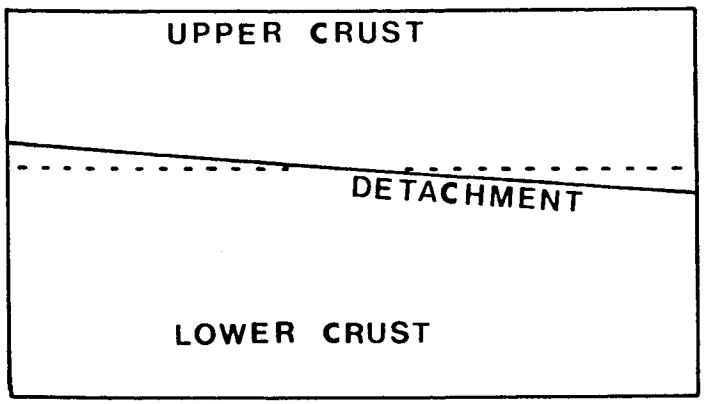

BEFORE RIFTING

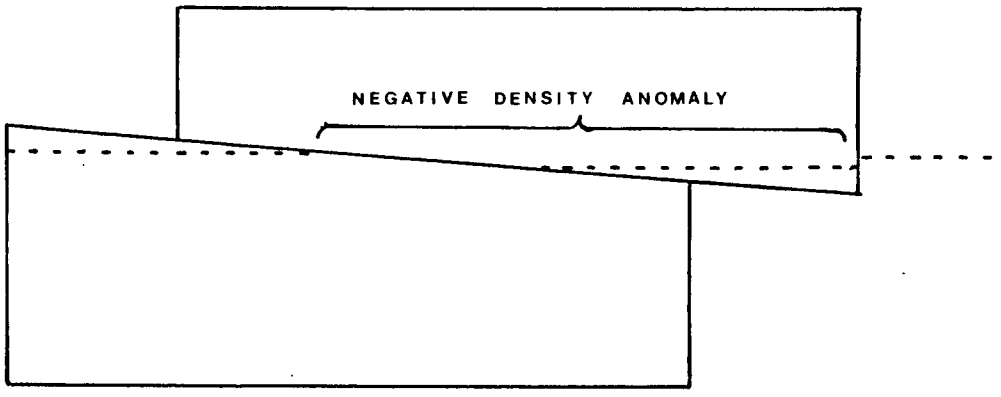

AFTER RIFTING

assume that this is a detachment (Wernicke and Burchfiel, 1982) that separates the brittle upper crust from the more ductile lower crust. Relative motion between the upper and the lower crust caused by rifting resulted in a net eastward translation of the upper crust. Assuming increasing density with depth (the dash line indicates rocks of equal density), this eastward translation resulted in a negative density anomaly at the mid-crust level. Because the surface elevation of this block of translated upper crust was relatively lower than the 'undisturbed' crust farther to the east, it eroded less and consequently ended up with a thicker upper crust. I have assumed that the rate of isostatic rebound/compensation was slower than the rate of erosion. I should emphasis that eastern Kansas is now in isostatic equilibrium in spite of the negative isostatic anomaly observed. In general, a compensated negative (positive) density anomaly in the upper crust will give rise to a negative (positive) isostatic anomaly because the gravitational attraction of the Airy root is smaller (it depends on the inverse square of distance) than that of the density anomaly in the upper crust.

The -15 mgal broad gravity low in western Kansas (fig. 23) is partly due to the thickening of the lower density Phanerozoic sedimentary rocks toward the west, which is not accounted for in the isostatic correction. Woollard (1959) estimated this effect to be about -6 mgals. The remaining unexplained -9 mgals appears to be a level shift for the entire state that is caused by a deep low density source. In summary, the isostatic correction calculated

using an Airy model fails to account for all the long wavelength anomalies, and is inadequate for purpose of anomaly separation.

Next, I consider the question of crustal thickness in central and western Kansas by comparing gravity results to a seismic refraction survey. To model the gravity gradient in western Kansas, a first order trend surface was fitted to the western Kansas Bouguer gravity grid (profile A-A' is shown on figure 13). A west-dipping gradient of 0.255 mgal/km was obtained (fig. 26). Steeples (1976) evaluated a refraction profile shot by the USGS between Agate, Colorado and Concordia, Kansas and derived a crustal thickness of 48 km at Agate and 38 km at Concordia. I used this seismically determined dipping Moho to model the regional gravity gradient in western Kansas. Since a small part of the Bouguer gravity gradient is due to the thickening (about 600 m) of the sedimentary cover to the west (Cole, 1976; Zeller, 1968; Merriam, 1963), a correction for the lower density Phanerozoic rocks is needed. From Vargas (1983), the average density of shale and limestone in a normal Pennsylvanian section was calculated to be 2.27 gm/cc and 2.51 gm/cc respectively. If we assume these densities are representative of the entire Phanerozoic section, the average density is estimated to be 2.43 gm/cc. This assumes that the Phanerozoic section consists of approximately one third shale and two third limestone (as estimated from Plate 1 in Zeller, 1968). This is 0.24 less than the density 2.67 used in the Bouguer correction, and corresponds to a 6-mgal difference in the gravity gradient on AA'. Woollard (1959) obtained a similar value in his "geologic correction", which assumes a

Figure 26. Gravity model of the Moho in western Kansas along AA' (fig. 13). Depth to Moho was determined by seismic refraction (Steeples, 1976). Density contrast between the lower crust and upper mantle was varied to fit the observed gravity gradient.

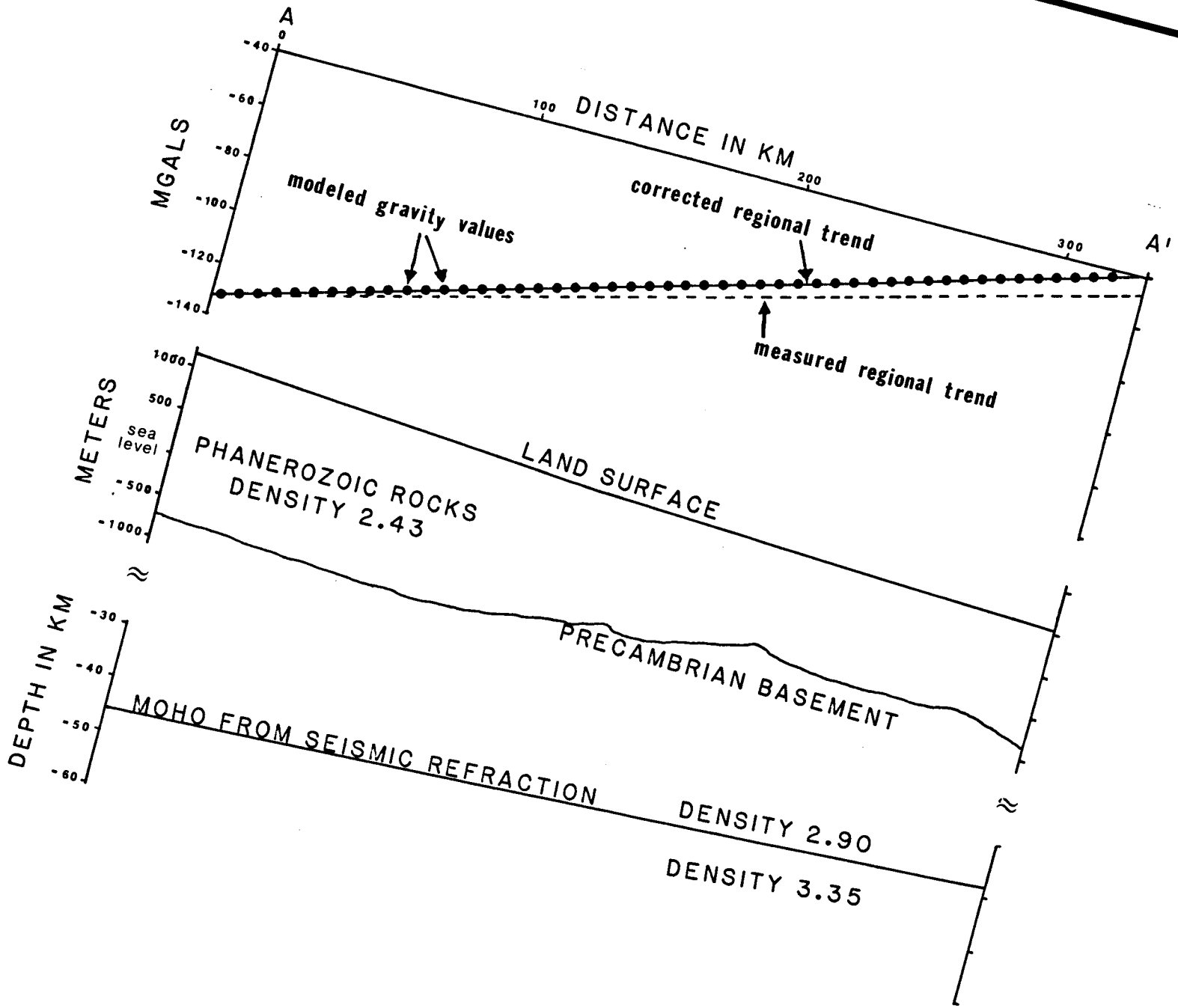
A
0
-40
-60
-80
-100
-120
-140
MGALS
100
DISTANCE IN KM
200
300
A'
modeled gravity values
corrected regional trend
measured regional trend
1000
500
sea level
-500
-1000
METERS
PHANEROZOIC ROCKS
DENSITY 2.43
LAND SURFACE
PRECAMBRIAN BASEMENT
-30
-40
-50
-60
DEPTH IN KM
MOHO FROM SEISMIC REFRACTION
DENSITY 2.90
DENSITY 3.35

lateral density change on AA'. This correction was applied to the Bouguer gravity gradient and is shown in figure 26. The density contrast at the Moho (between the crust and mantle) was varied until the modeled gradient matched the corrected Bouguer gravity gradient. A density contrast of -0.45 gm/cc was found to give the best fit. This result is consistent with density values of 2.9 gm/cc in the lower crust and 3.35 gm/cc in the upper mantle, which are normal values for continental crust in stable cratons (see for example Fleitout and Froidevaux, 1983; Hinze and others, 1982).

This 10 km crustal thickening to the west, as indicated by gravity and seismic data, is not predicted by the Airy hypothesis of isostasy. Using elevations of 0.48 km (1600 ft) at Concordia, 1.09 km (3600 ft) at Agate, an upper crustal density of 2.67, and a crust-mantle density contrast of 0.45 gm/cc (as derived earlier) the predicted Airy crustal thickening is approximately 4 km.

Using the crustal thicknesses derived from refraction studies and assuming the Airy hypothesis is correct, the equivalent sea level crustal column thicknesses at Agate, Concordia, and near the Kansas/Missouri border were derived and are shown in table 2. It is obvious that the crust is thinner by five to six kilometers at Concordia in northcentral Kansas. It is most unlikely that isostatic equilibrium has not been attained after 1.1 b.y. Quite possibly, the topography is compensated partially at the Moho level and also at the base of the lithosphere, where a large low density body may be present. Evidence for such a body near the lithosphere/asthenoshere boundary was reported by Hahn (1982). He detected a large low

	CRUSTAL THICKNESS (KM)	ELEVATION (KM)	AIRY ROOT (KM)	SEA LEVEL CRUSTAL COLUMN (KM)
AGATE, CO	48*	1.09	6.47	41.53
CONCORDIA, KS	38*	0.45	2.67	35.33
KS/MS BORDER	42▪	0.30	1.78	42.22

Table 2. Crustal thicknesses, elevations, and derived Airy isostatic roots at Agate, Concordia, and the Kansas/ Missouri border.
(* from Steeples, 1976; ▪ from Stewart, 1968)

velocity body in the upper mantle beneath central Kansas using teleseismic P-wave residuals. Velocity and density of rocks generally are positively correlated (Clark, 1966).

TREND SURFACE ANALYSIS - REGIONAL

A second order trend surface fit (fig. 27) to the gravity map (fig. 15) is a good representation of the regional trend within the state. This was judged by visually inspecting the first through ninth order residual gravity maps, as well as examining the closeness of fit via the root mean square (RMS) values. RMS values for the first through seventh order fit were 16.59, 11.01, 10.01, 9.36, 9.13, 8.93, and 8.82 mgals. Raising the order of fit from the first to second improved the fit by more than 5 mgals, while successively higher order fit only gave a moderately better fit.

The second order trend surface (fig. 27) shows a steep west-dipping gradient in western Kansas and almost no gradient in eastern Kansas. It crudely resembles the isostatic correction map in figure 22. They both have a relatively steep west-dipping gradient in western Kansas, and becomes more gentle in the eastern half of the state. But the isostatic correction in the west and east border of the state are -120 and -32 mgals respectively; which are quite different from the corresponding values of -135 and -59 mgals for the second order trend of the Bouguer gravity map. While the second order residual map essential levels the entire data set about zero mgal, the isostatic residual map leaves a broad gravity low in both eastern and western edges of the state (or a broad gravity high in central Kansas).

Figure 27. Second order trend of the Bouguer gravity map shown in figure 13. Root mean square of the fit is 11 mgals. Note the steep west-dipping gradient in western Kansas.

BOUGUER GRAVITY MAP OF KANSAS

SECOND ORDER TREND

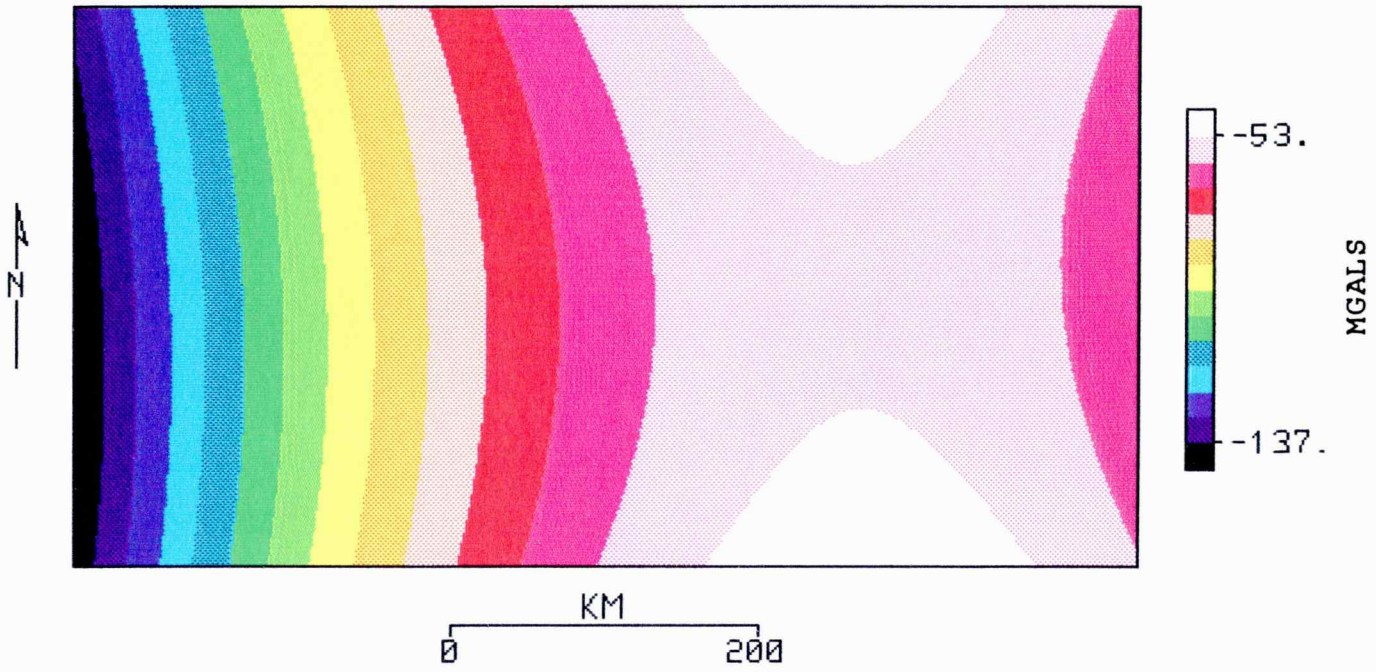

TREND SURFACE ANALYSIS - LOCAL ANOMALIES

For the following discussion in this section, please refer to figure 2 for basement provinces and use plastic overlay with county names and boundaries (in back pocket of this volume).

To emphasis the local anomalies, a residual map (Fig. 28) was obtained by removal of the regional field which is best represented by a second order trend surface. The most prominent feature on this map, which we call the Midcontinent geophysical anomaly (MGA), is a gravity high with flanking lows, that trends southwest through the state from Marshall county at the Kansas-Nebraska border, to Harper county at the Kansas-Oklahoma border. Numerous previous investigators (see for example Van Schmus and Hinze, 1985 for a good source of references) have interpreted this feature, which also has a magnetic expression (fig. 29) and extends northeasterly to the Great Lakes region, as an aborted late Precambrian rift. The central gravity high and flanking lows are due, at least in part, to a rift basin filled with Precambrian arkosic sandstone which includes a central trough of basalt.

Previous investigators have developed a variety of cross-sectional models for the MGA. King and Zietz (1971), based on simultaneous gravity and magnetic modeling across the Iowa portion of the MGA, suggest a fairly shallow basin (8 km deep) filled with basalt that subcrops at the present Precambrian surface. Ocala and Meyer (1973), based on gravity modeling controlled by seismic refraction results, suggest that a large part of the gravity high is due to the presence of a high density rock intruded into the upper

Figure 28. Second order residual gravity map of Kansas.

SECOND ORDER RESIDUAL GRAVITY MAP OF KANSAS

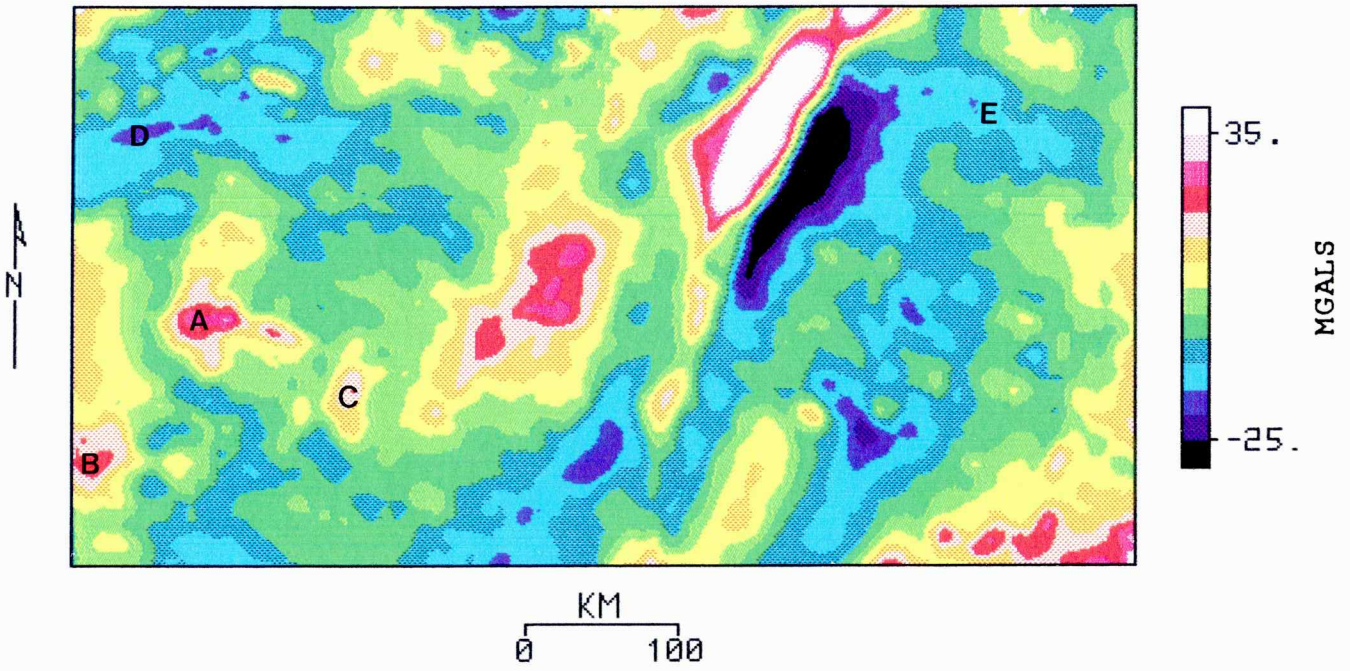

Figure 29. Aeromagnetic map of Kansas.

MAGNETIC MAP OF KANSAS

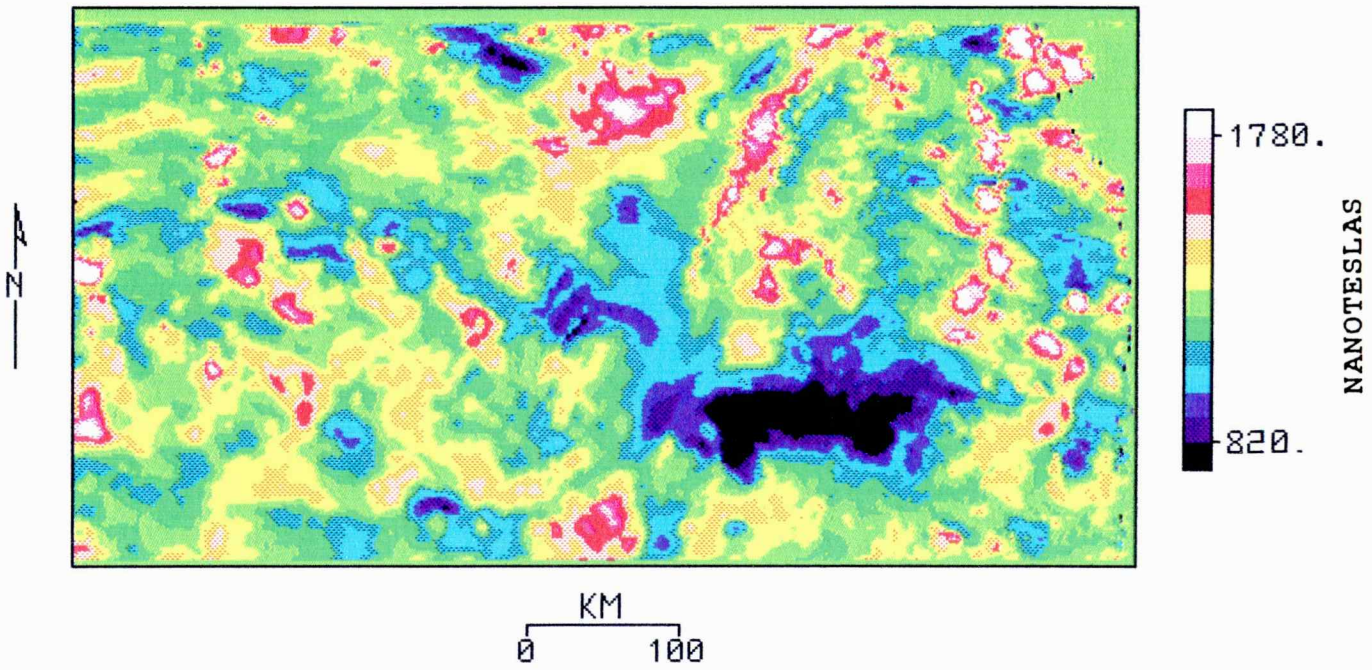

crust. The cross sectional shape is also roughly that of a symmetrical basin with depth of 25-35 km. Chase and Gilmer (1973) suggest a vertical prism of mafic material extending to great depth into the upper mantle. More recently, Serpa and others (1984), based on a deep seismic COCORP line (fig. 30) in northeastern Kansas, suggest that the basalt occurs in an asymmetrical basin. The top of this basalt is some 4 km below the present Precambrian surface and is overlain by several kilometers of arkosic sandstone. Somanas (1984) reprocessed the COCORP seismic line and derived a model using constraints from gravity, magnetic and drill data. He suggests a rift basin filled with interbedded basalt and clastic rocks at 2-6 km beneath sea level, and flanked by two bodies of Precambrian clastic rocks. A thin dike of intrusive rock cutting through the clastic rock body in the east accounts for the secondary magnetic high there. Three moderately magnetic to non-magnetic deep bodies at 16-30 km contribute the remaining portion of the gravity and magnetic signals.

Although the afore-mentioned models are thought provoking and have some attractive features, they are not without weaknesses and do not exclude alternative interpretations. For instance, although the COCORP line passes near a well located near the crest of the gravity high that encountered Precambrian arkosic rocks, most of the rocks found in wells to the Precambrian along the gravity high in Kansas are gabbroic. Arkosic rocks are found predominantly over the flanking gravity lows. Somanas' model suggests that the central trough of gabbro is physically separated from the flanking wedges of

Figure 30. Location of COCORP seismic line 1 in northeastern Kansas overlain on the Bouguer gravity map. R, M, and ⊙ indicate location of wells encountering Precambrian Rice formation, mafic rocks, and granite respectively.

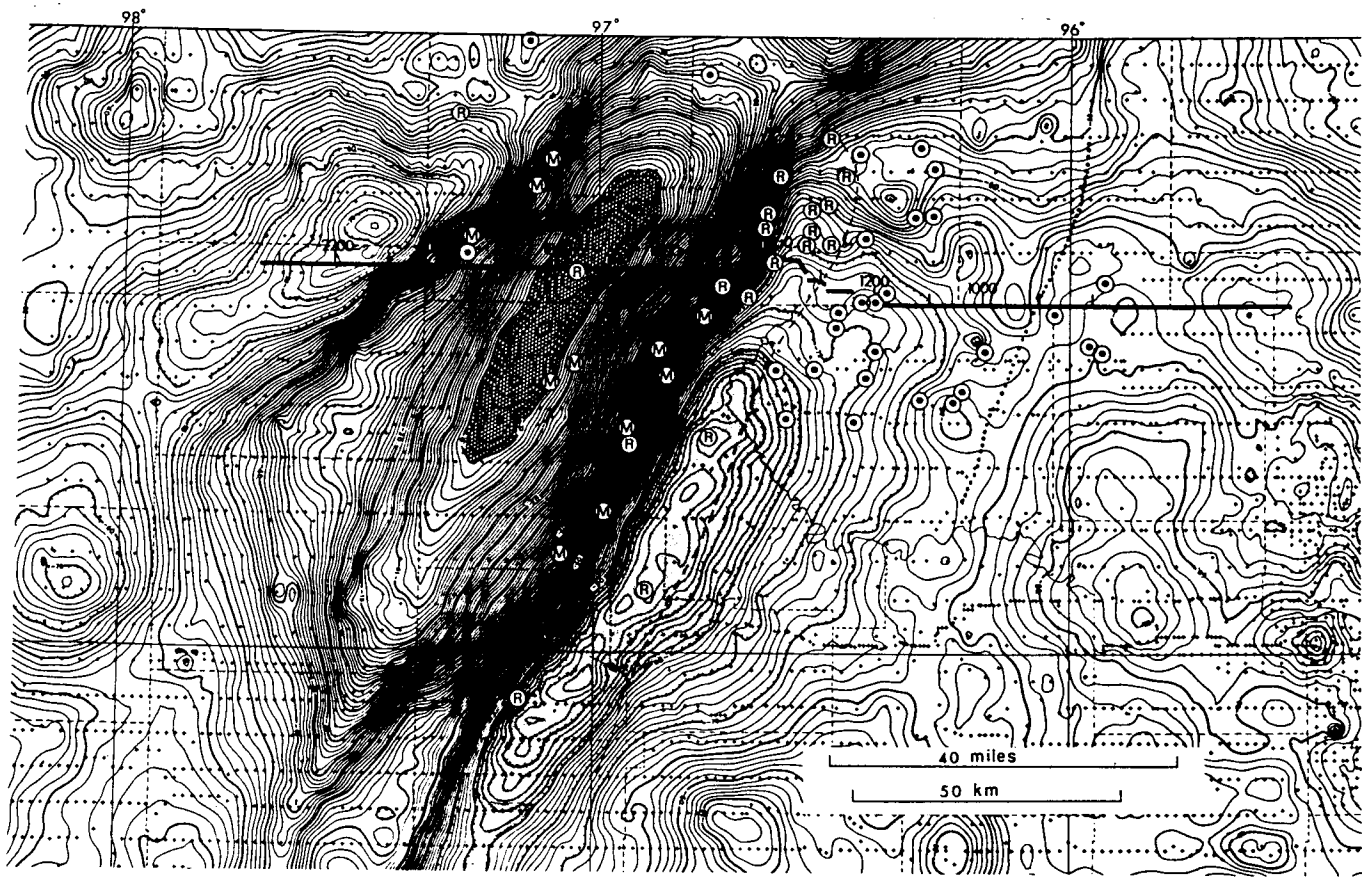
98°
97°
96°
1200
1200
1000
40 miles
50 km

arkose. Why these bodies are not in contact, but separated, presumably by granitic rocks is unclear. Further work is needed to distinguish between the various proposed cross-sectional models of the MGA.

A simple cross-sectional model (fig. 31) derived from the east-west gravity profile BB' (fig. 13), is useful for estimating the minimum amount of basalt and arkose within the rift zone. The cross-sectional area of the basalt and sandstone obtained from the model were multiplied by the estimated length of the prism, 350 km, to arrive at the volume of each. Using density contrasts of +0.3 gm/cc and -0.3 gm/cc for basalt and sandstone, respectively. The minimum volume of basalt and sandstone in northern Kansas were found to be 36,000 cu km and 16,000 cu km respectively. This considerable volume of Precambrian sandstone may contain giant hydrocarbon reservoirs and is of great interest to oil companies.

The MGA is characterized in northern Kansas by a 60 mgal gravity high. Although this positive gravity feature is easily traced southwesterly to the Kansas-Oklahoma border (fig. 28), its amplitude abruptly decreases to approximately 20 mgals in Saline county. An east-west gravity profile (CC' in Fig. 13) across the MGA in southern Kansas was also studied (fig. 32). A regional trend, indicated by the dashed line in figure 32, was first subtracted from the Bouguer gravity profile before modeling. This regional trend is due to the adjacent Nemaha ridge and is not directly related to the rift. The resulting cross-sectional model is shown in figure 33. The predicted minimum amounts of basalt and sandstone in southern Kansas

Figure 31. Cross-sectional gravity model of MGA along latitude 39.01° in northcentral Kansas (BB' in figure 13).

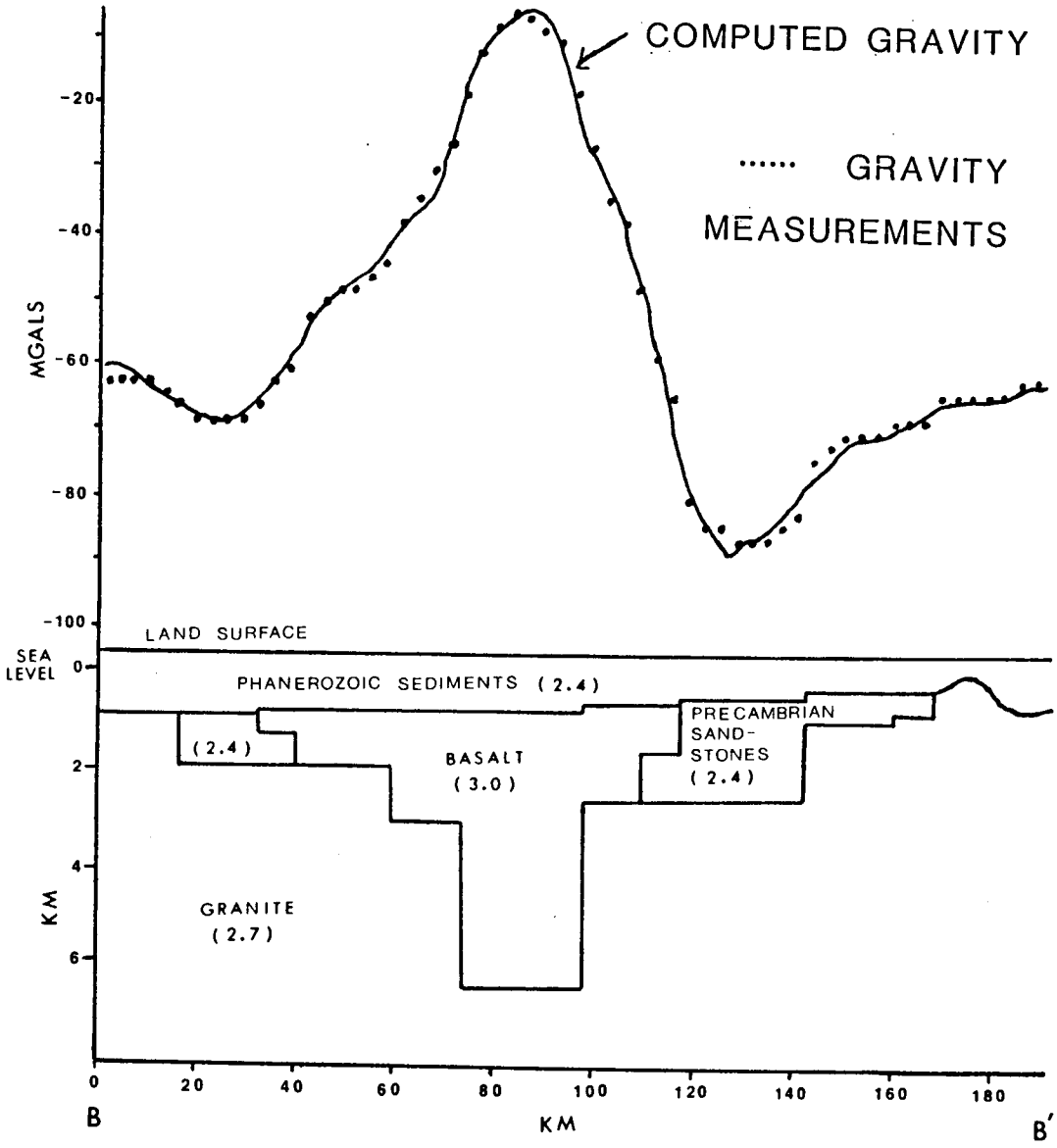
COMPUTED GRAVITY
GRAVITY MEASUREMENTS
MGALS
-20
-40
-60
-80
-100
LAND SURFACE
SEA LEVEL
0
PHANEROZOIC SEDIMENTS (2.4)
(2.4)
BASALT (3.0)
PRECAMBRIAN SAND-STONES (2.4)
GRANITE (2.7)
KM
2
4
6
0
20
40
60
80
100
120
140
160
180
B
KM
B'

Figure 32. The regional gravity anomaly along CC' (fig. 13) in southcentral Kansas along latitude 37.5° was subtracted to extract the gravity signal related to the MGA.

Figure 33. Cross-sectional gravity model of MGA along CC' (fig. 13). Regional gravity anomaly was subtracted from the Bouguer gravity profile as shown in figure 32.

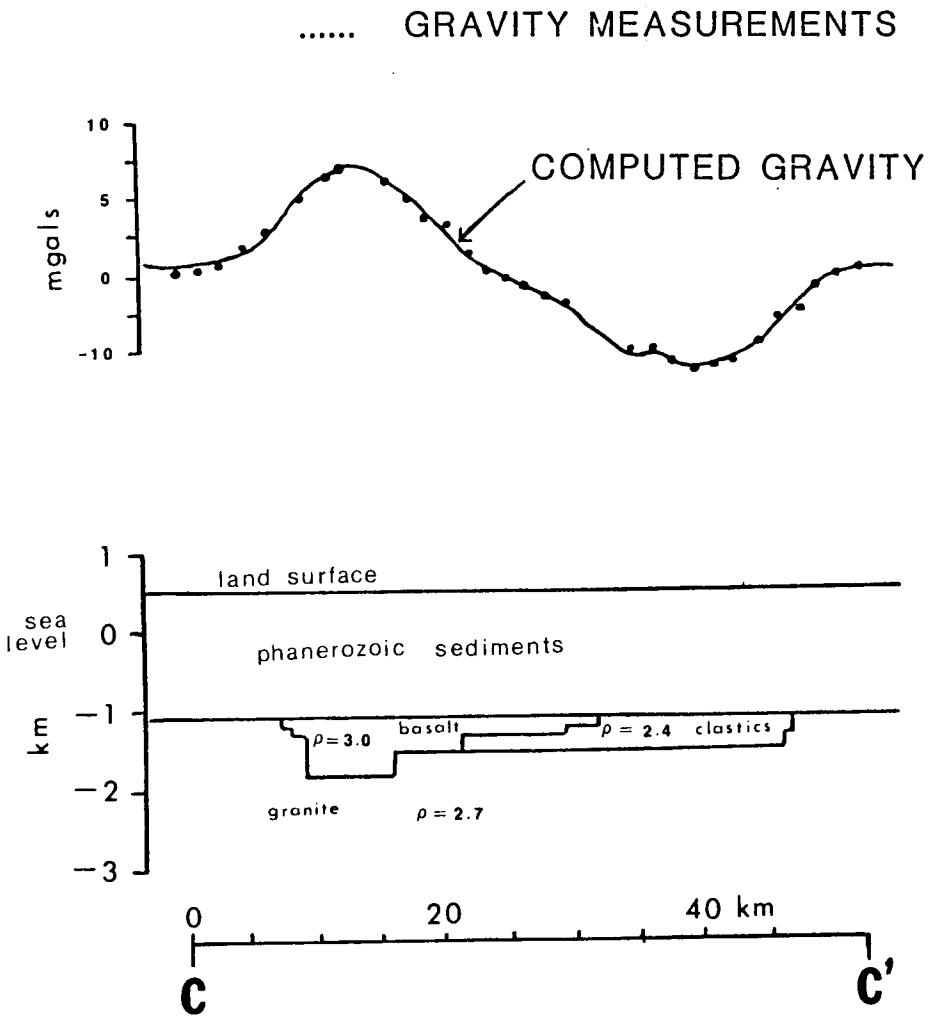
..... GRAVITY MEASUREMENTS
COMPUTED GRAVITY
mgals
10
5
0
-10
land surface
sea level
phanerozoic sediments
km
1
0
−1
−2
−3
basalt
ρ = 3.0
ρ = 2.4 clastics
granite
ρ = 2.7
0
20
40 km
C
C'

were approximately 1500 cu km for each.

A broad +30 mgal anomaly (fig. 28) containing several positive closures is present in extreme southeastern Kansas in the counties of Montgomery, Labette and Cherokee. These small circular features may be depicting magma feeder pipes which supplied the rhyolite that makes up the basement in this area (Bickford and others, 1979). It is unlikely that the actual sources for these positive anomalies are rhyolitic rocks, because rhyolite is generally less dense than granite (Clark, 1966). These anomalies may represent a more mafic phase of the magma at depth (McLelland, 1986) or possibly a later intrusive event.

The Nemaha ridge shown bounded by the Humboldt fault in northeastern Kansas (fig. 1), has little gravity expression (fig. 28). This is probably due to the lack of density contrast between the uplifted basement rock and the surrounding sedimentary rocks (Woollard, 1959). Also the proximity of the MGA may mask any small signal the Nemaha ridge might produce. In southcentral Kansas, a +15 mgal northeast trending anomaly in Sumner, Sedgwick and Butler counties overlies the Nemaha ridge. This anomaly is located on the western part of the Wichita magnetic low, a large pronounced magnetic low in the region (fig. 29).

To the east of the Nemaha ridge gravity high in southcentral Kansas, but still within the Wichita magnetic low, is a triangular shaped (-20 mgal) low in Greenwood county. The source for these gravity anomalies is poorly understood. The change in gravity anomaly polarity within the uniform magnetic low suggests a complex

Precambrian geologic history in this region.

A small positive closure in extreme northeastern Kansas (Doniphan county) has a corresponding magnetic high, indicating a mafic source body in the basement. Basement mafic rock underlying the Salina basin west of the MGA in northcentral Kansas (Republic, Jewell, Smith, and Mitchell Counties) is the probable source for the +15 mgal anomaly in this region. This could be related to an intrusive event that led to the formation of the Salina basin as has been suggested for other basins in the midcontinent (e.g. McGinnis, 1970).

A broad +25 mgal high in Barton county and a +15 mgal high in Norton county correlate with the southeastern and northwestern ends of the Central Kansas uplift. A +15 mgal high coincident with the Norton and Phillips county line suggest an intra-basement mafic body in this region. This body also gives rise to a positive magnetic anomaly. A positive anomaly with a very steep gradient along the Rawlins/Decatur county line, in northwestern Kansas, suggests a fairly shallow basement intrusive body.

Other significant anomalies include a 130 km by 100 km "L"-shaped +25 mgal high centered in Wichita and Grant counties (anomaly A in figure 28), +20 mgal high in Stanton county (anomaly B), +15 mgal high in southwestern Hodgeman county (anomaly C), A -15 mgal east-west trending low in Sherman and Thomas counties (anomaly D in northwestern Kansas), and a -15 mgal northwest trending low in Jackson, Jefferson and Johnson counties (anomaly E in northeastern Kansas). Anomaly E is the northwestern end of the Missouri gravity

low, which is probably a failed Precambrian rift (Guinness and others, 1982).

TREND SURFACE ANALYSIS - SEVENTH ORDER RESIDUAL

To better study the shallow basement sources responsible for the gravity anomalies and trends, a seventh order trend surface was removed from the original map (fig. 15) resulting in the residual map shown in figure 34. The symmetrical nature of the MGA (a central high with its flanking lows in central Kansas) and the continuation of the anomaly to the Oklahoma border show up more distinctly (labelled 'MGA' in figure 34). The northeast trending positive gravity anomaly of the Nemaha ridge (labelled 'N') extends further to the northeast then on previous maps. The southeastern end of the Central Kansas uplift (labelled 'C') and the southern end of the Nemaha ridge (labelled 'N') are situated symmetrically about the MGA. Could they have been one entity before 1.1 b.y. ago and then separated during rifting? The right lateral offset of the Central Kansas uplift anomaly along a northwest trend at the concurrence of Rush, Barton, and Pawnee counties (labelled C) coincides with the trend of basement faulting in the area (Cole, 1976). An extensive northwest-trending lineament that passes through the state (RR' in figure 34) suggests the existence of an ancient (pre 1.1 b.y.) cross-state fracture zone.

Figure 34. Seventh order residual of the gravity map in figure 13.

BOUGUER GRAVITY ANOMALY MAP OF KANSAS

SEVENTH ORDER TREND REMOVED

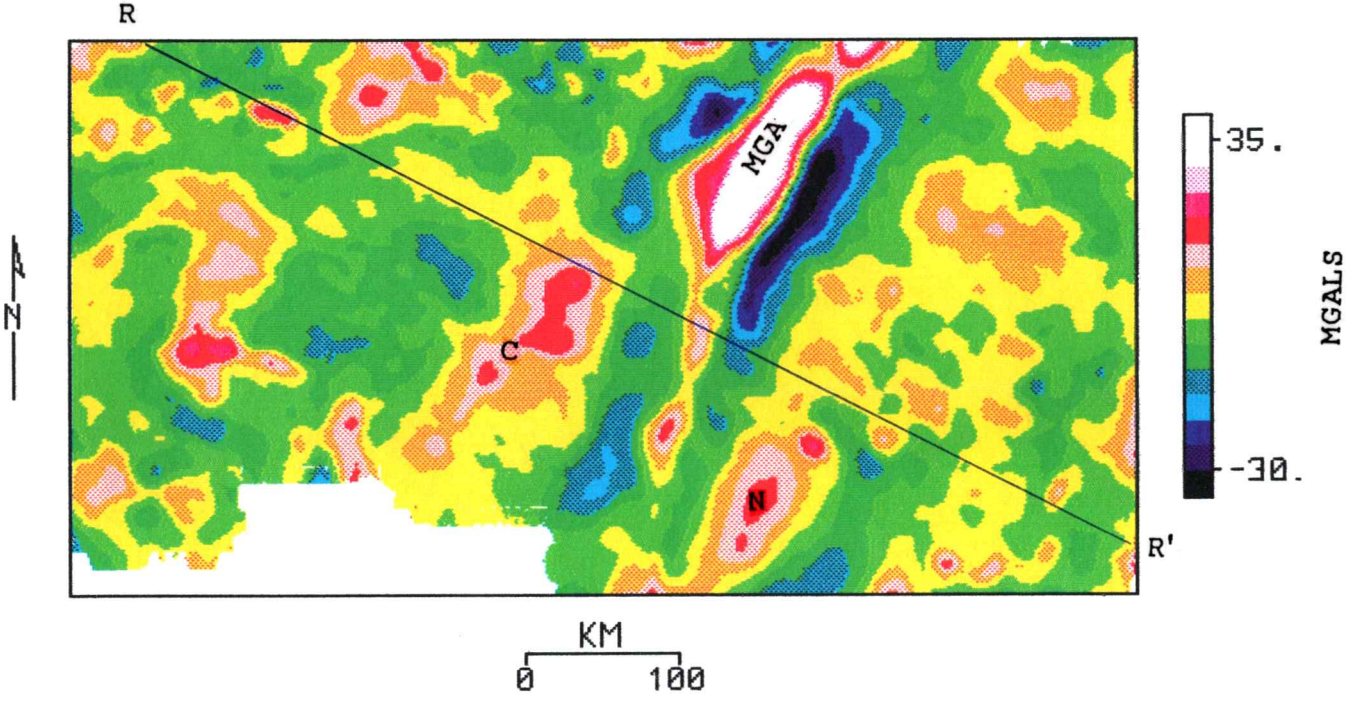

SYNTHETIC ILLUMINATION OF GRAVITY

Synthetic illumination of the Kansas Bouguer gravity grid (fig. 15) was done for azimuths at 20° intervals from 0° to 360°. This resulted in a suite of 18 reflectance maps for interpretation (figures 35 and 36 are examples).

The sun horizon was chosen by trial and error. For sun angles too high above the horizon, many interesting patterns are suppressed by high reflectances throughout map. Similarly low sun angles produce a map dominated by low reflectances. The gravity values were scaled such that the steepest gravity gradient in the data would have a pseudo topographic slope of about 1. A sun horizon of 30° and scale of 1.2 mgal/mi (0.75 mgal/km) was found to be optimal.

The reflectance map with the sun azimuth at 120°, as shown in figure 35, highlights the northeasterly trend in the gravity data. This map reveals the extent of the rift zone. I estimate the eastern and western apparent fault boundaries of the rift to be located at QQ' and PP' (fig. 35). QQ' coincides approximately with the Humboldt fault zone (see also figure 1). No major fault zone has been mapped along the trend of PP'.

Figure 36 shows a reflectance map with the sun azimuth at 180 degrees, which stresses the east-west trends in the gravity data. It reveals an east-west boundary, TT', separating the state into a northern and southern region. TT' follows approximately a chain of high reflectances, and truncates the northeastern trending high reflectance associated with the MGA in central Kansas. South of TT' in eastern Kansas, the reflectance patterns exhibit longer

Figure 35. Synthetically illuminated gravity map of Kansas. Sun horizon = 30°, azimuth = 120°, and gravity to vertical distance scale = 0.75 mgal/km.

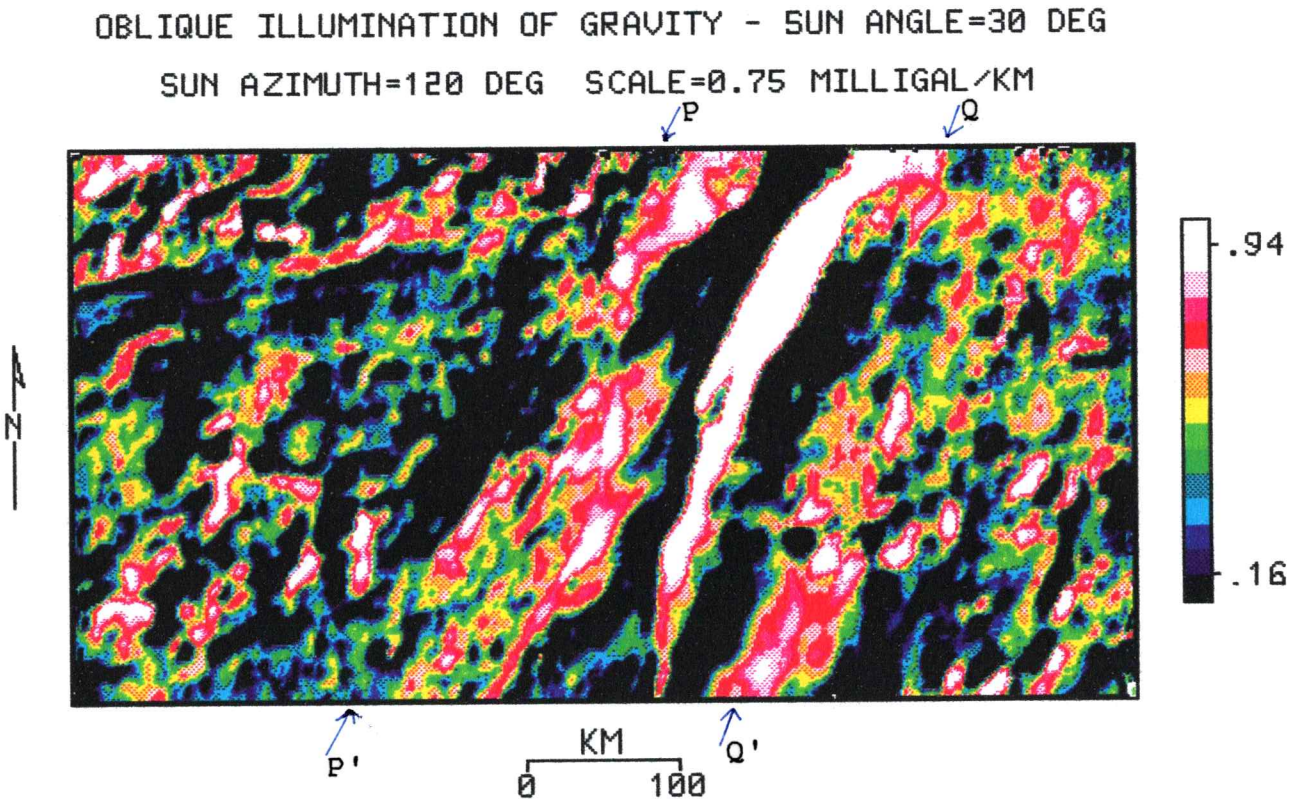
OBLIQUE ILLUMINATION OF GRAVITY - SUN ANGLE=30 DEG
SUN AZIMUTH=120 DEG SCALE=0.75 MILLIGAL/KM
P
Q
.94
.16
N
P'
Q'
KM
0
100

Figure 36. Synthetically illuminated gravity map of Kansas. Sun horizon = 30°, azimuth = 180°, and gravity to vertical distance scale = 0.75 mgal/km.

OBLIQUE ILLUMINATION OF GRAVITY - SUN ANGLE=30 DEG

SUN AZIMUTH=180 DEG SCALE=0.75 MILLIGAL/KM

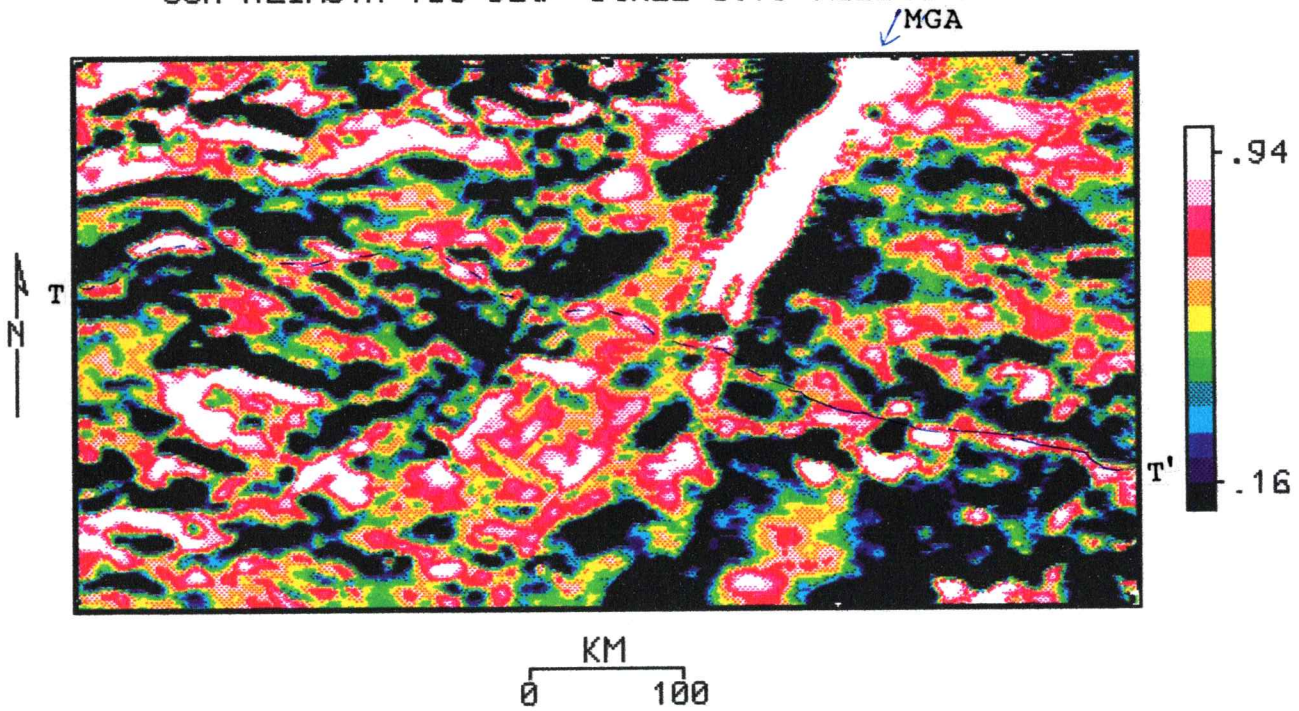

wavelengths, lower reflectance values (black), and sharper edges than those in northeastern Kansas. These distinctions are not as apparent in western Kansas. The portion of TT' indicated by a dashed line is less obvious.

A summary of the many gravity lineaments identified on the 18 reflectance maps at different azimuths appear in figure 37. The criteria I used in identifying lineaments were that it must be at least 20 km long and a straight line resulting from a change of reflectance or color. The lineaments shown in figure 37 were identified on more than one map, although the exact location of a line may vary slightly on different illumination azimuths. This is due to the width of the linear feature in the original data.

For the following discussion of figure 37, please refer to figure 2 for basement provinces and use plastic overlay with county boundaries (in the back pocket of this volume). Most of the lineaments in figure 37 are trending northeast or northwest. Two prominent lineaments, labelled A and B in figure 37, extend southwesterly to central Kansas, and are flanked in the west by another rather long lineament, labelled C, of almost the same strike. Lineament B coincides with the crest of the central gravity high of the MGA. Lineaments A and C are at the minima of the flanking gravity lows. A few shorter lineaments in south-central Kansas near 98 degree longitude are a continuation of A, B, and C. They are marked in red and blue corresponding to the central gravity high and the flanking lows respectively. The shorter and less aligned lineaments in southcentral Kansas indicate a less developed rift basin.

Figure 37. Gravity lineaments in Kansas.

GRAVITY LINEAMENTS IN KANSAS

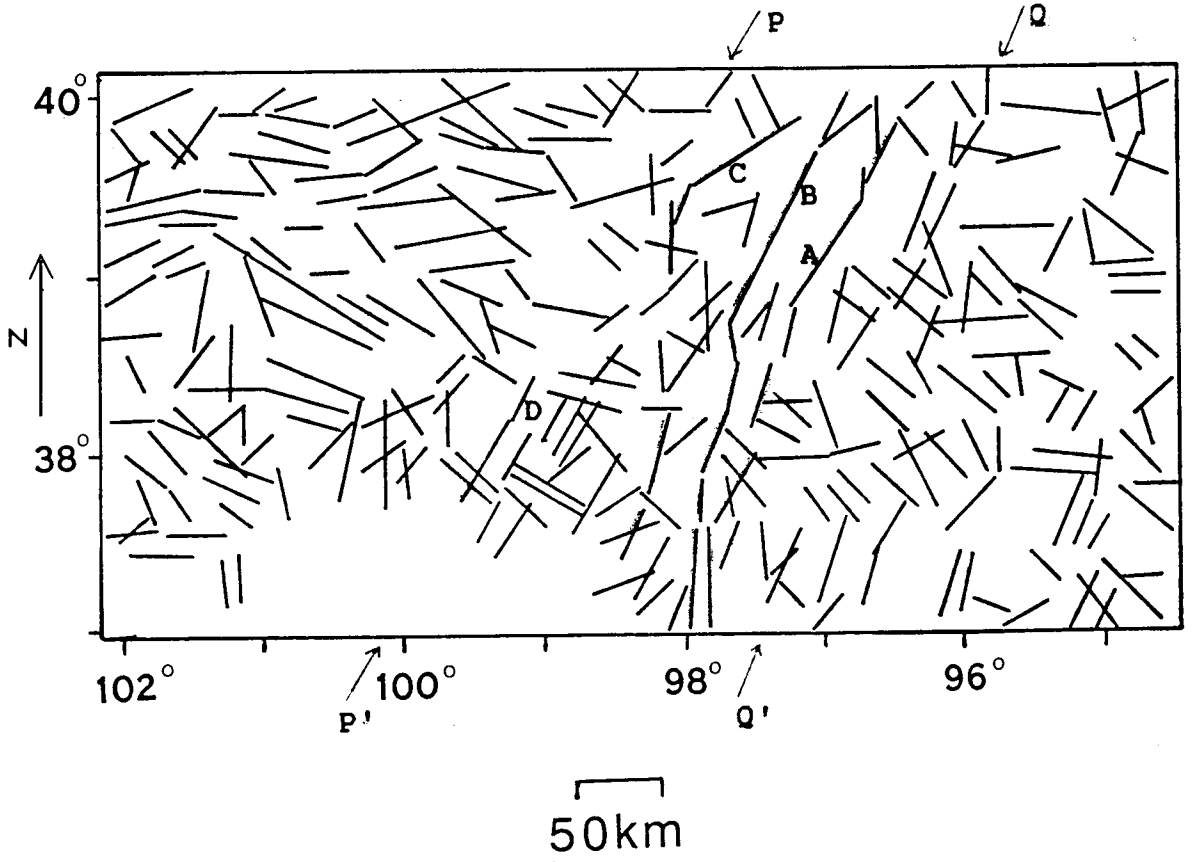

There is a swarm of near-parallel northeast trending lineaments, labelled D in figure 37, near the southeastern end of the Central Kansas uplift. These lineaments could be the gravity signature of intrusive dikes or block faulting, which are associated with the late Precambrian rift. PP' and QQ' (fig. 35) define the boundaries of the rift zone because most of the northeast lineaments in figure 37 are within these bounds. Although the northeast lineaments along PP' and QQ' are relatively short and interrupted in many places, their continuation across the state is quite evident. The rift seems to widen slightly from north to south, such that the divergent angle made by PP' and QQ' is about 17 degrees. Within the rift zone, defined by PP' and QQ', there are more northeast lineaments in southcentral Kansas than in northcentral Kansas, suggesting more extensive fractures or faulting in southcentral Kansas. On the other hand, gravity signals from any northeast trending faults in the granitic crust in northcentral Kansas would be attenuated by the thick layer of overlying Precambrian sediments.

Many northwest trending lineaments are found in figure 37. Although they are interrupted in many places, they are more or less aligned. These lineaments are interpreted as gravity expressions of pre-rift fractures in the basement because of their cross cutting relationship with the northeast lineaments. (The relative ages of two sets of intersecting lineaments/faults are determined by the assumptions that the older lineaments are interrupted by the younger lineaments.) Since there are no apparent offsets of these lineaments (see also RR' on the seventh order residual gravity map in fig. 34)

across the rift zone, it implies that no strike slip movement has taken place along the rift. The accumulated lineament length in eastern and western Kansas are plotted against the lineament azimuth (fig. 38). Peaks which correspond to both the northeast and northwest trending lineaments, are present in both histograms. The northwest trending lineaments in western Kansas appear to have rotated, relative to northwest trending lineaments in eastern Kansas, 5 to 10 degrees clockwise. This suggests that the crustal extension due to rifting was progressively larger from north to south. The rift boundaries at the beginning stage of rifting may have been parallel. A larger amount of extension in southern Kansas resulted in the divergent rift boundaries PP' and QQ' observed. Alternatively, the final geometry of the rift observed now could be the result of a wider initial rift zone in the south to begin with.

I next estimate the crustal extension and the initial width of the rift along two east-west lines, GG' and FF', as shown in figure 39. The extension ratio (b) is defined as the final width to the initial width of the rift. I assume a constant extension ratio (b) throughout the rift. The first line, GG' in northern Kansas, overlaps the COCORP seismic profile. Serpa and others (1984) estimated that the central main rift basin in northcentral Kansas has widened from an initial width of 50 km to the present width w=79 km. That means b is 79/50 or 1.58 for this portion of GG'. Assuming the same b for the entire length of GG', the beginning width of the rift zone is 106 km (the present width of the rift, 167 km, divided by 1.58). Therefore the extension along GG' is 61 km.

Figure 38. Histograms of cumulative length of gravity lineaments in eastern and western Kansas.

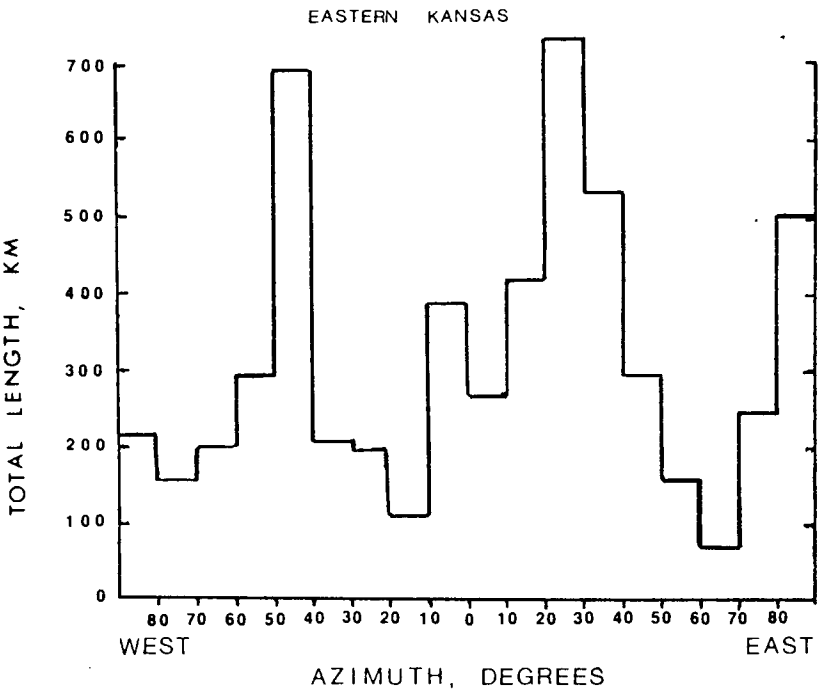
EASTERN KANSAS
TOTAL LENGTH, KM
700
600
500
400
300
200
100
0
80 70 60 50 40 30 20 10 0 10 20 30 40 50 60 70 80
WEST
EAST
AZIMUTH, DEGREES

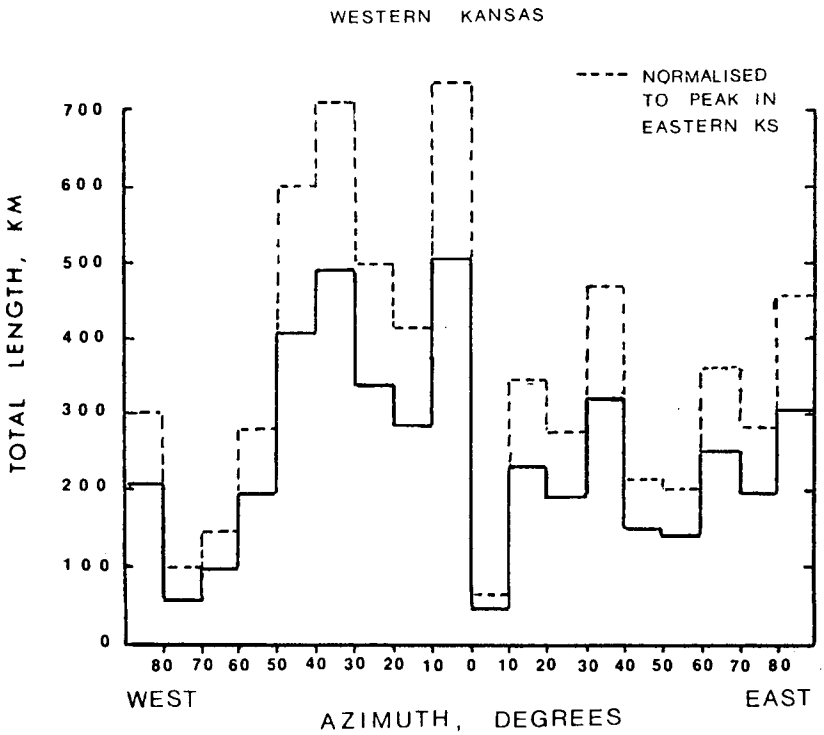
WESTERN KANSAS
NORMALISED TO PEAK IN EASTERN KS
TOTAL LENGTH, KM
700
600
500
400
300
200
100
0
80 70 60 50 40 30 20 10 0 10 20 30 40 50 60 70 80
WEST
EAST
AZIMUTH, DEGREES

Figure 39. Map of Kansas showing the boundaries of the rift zone. The extensions and initial widths of the rift were estimated along FF' and GG'. GG' overlaps partially with the COCORP seismic line 1. 'W' is the width of the central basalt filled basin which is approximately 79 km wide in the east-west direction.

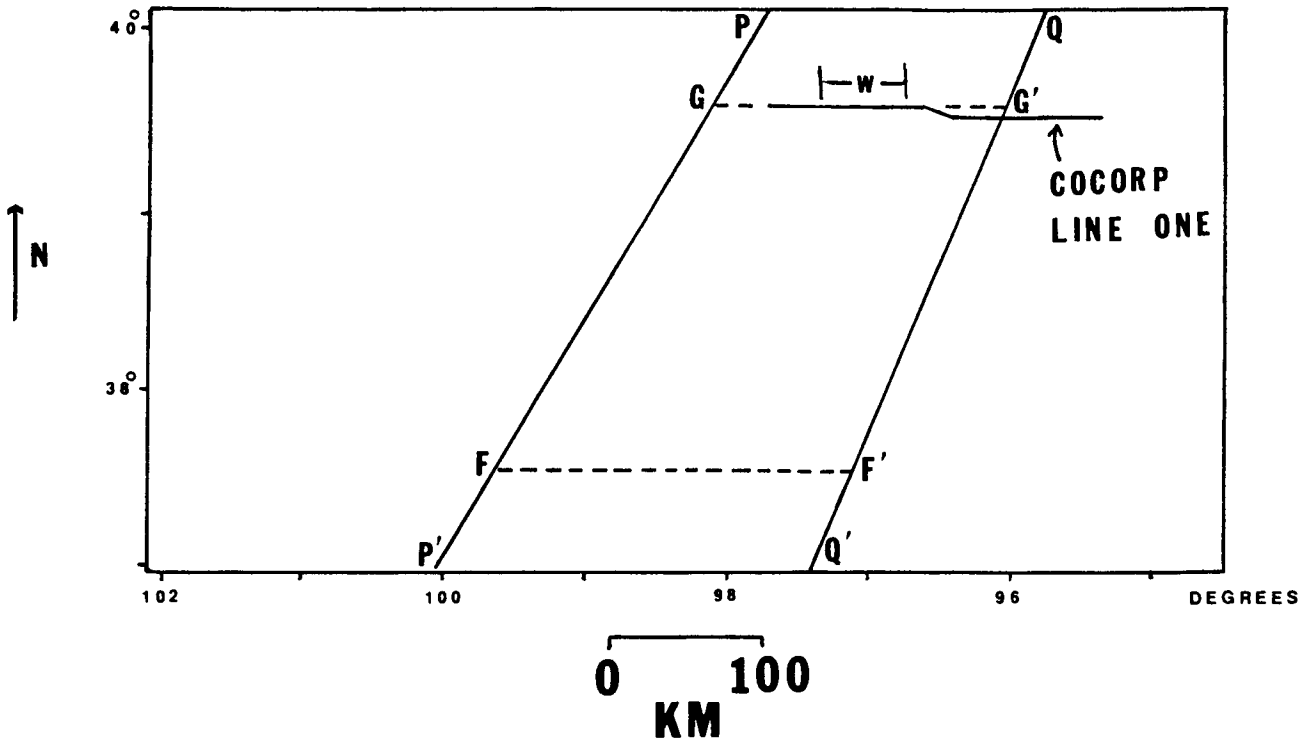
40°
38°
N
P
Q
G
W
G'
COCORP
LINE ONE
F
F'
P'
Q'
102
100
98
96
DEGREES
0
100
KM

The present width of the rift zone along FF' is 205 km. This implies an extension of 76 km along FF', using the same extension ratio as before.

The constant b model discussed above predicts a 4° rotation of the northwest lineaments. It is based on the facts that the extension along FF' is 15 km more than that along GG' ,and the perpendicular distance between GG' and FF' is 200 km. The inverse tangent of 15/200 is 4°.

Southern Kansas is quite different from northern Kansas in the amount of extension across the rift, amplitudes of the MGA central gravity and magnetic high (figs. 15 and 29), reflectance patterns on synthetically illuminated gravity maps, and the amount of northeast trending gravity lineaments. This division into northern and southern terranes has been observed by Bickford and others (1981) in radiometric dating and petrologic study of basement core samples, and by Yarger (1983) based on aeromagnetic data. The younger southern granitic terrane probably overlies a thinner crust and/or lithosphere, a higher geothermal gradient, and consequently a more ductile crust/lithosphere. The more ductile lithosphere resulted in a wider rift zone in southern Kansas (this is equivalent to the locked or resistance zone in Courtillot's (1982) propagating rift model). The attenuated gravity and magnetic signature of the MGA in southern Kansas could be related to this change in lithospheric character. Since the more ductile lithosphere did not actually rupture in southern Kansas, a major central rift basin was not formed. Injection of igneous material was of a smaller scale,

limited to the infantile central rift basin and fissures between tilted fault blocks. Whereas in northern Kansas, the more brittle lithosphere was ruptured and a central rift basin was developed on the Precambrian surface. This depression was filled with upwelling basalt that gives rise to the observed pronounced central gravity and magnetic highs of the MGA.

According to the crustal extension model of Artemjev and Artyushkov (1971), the lithosphere is divided into a brittle upper layer and a more ductile lower layer. Block faulting and rotation occur in the upper layer during crustal extension. While the lower layer is extended by ductile creeping. The northeast lineaments are related to faults or fractures in the brittle upper layer of the lithosphere. Larger extension in southern Kansas resulted in more northeast lineaments.

SPECTRAL FILTERING

I discuss in this section the general characteristics of filters and gravity anomalies in the frequency domain. Discussions and interpretations of the filtered gravity map will be presented in the next section.

The frequency spectrum of an anomaly depends on the size, depth, shape and density contrast of the causative body. A large, deep body gives rise to a very long wavelength dominated spectrum. Either a large shallow body or a deep body may produce a spectrum dominated by long wavelengths. A small shallow body gives rise to a short wavelength spectrum. It is possible therefore, if there is a small population of large dimension shallow bodies, to use band pass filters to separate gravity signals from bodies of different depths. Since the gravity signal of any body covers the entire spectrum, anomaly separation using band pass filtering is never clear cut. For example, a high pass filtered gravity map will contain mostly signals that are due to small shallow bodies. It nevertheless has a small contribution from sources at greater depth, or of a larger size. A low pass filtered gravity map will cut off most of the signals caused by small shallow sources, and retain most of the contributions of a deep or large shallow body.

Continuation filters calculate the gravity field at a higher or lower level. It is assumed that there is no mass density (or magnetic moment), i.e. a free space, between the two levels of continuation. Because of the inverse squared dependency of the gravity field on distance, the upward continuation filter will

attenuate signals due to shallow sources much faster than those due to deeper sources. It stresses the long wavelength anomalies caused by deep sources. On the other hand, the downward continuation filter, in effect, amplifies shorter wavelengths at the expense of longer wavelengths. It is a very noisy operation because random noise mixed in the signal also get enhanced. Sometimes an anomalous body is present between the two levels, invalidating the assumption of free space. Thus, downward continuation should be used with great care. Sometimes it is good practice to low pass filter the input gravity grid before applying the downward continuation filter. This precaution will get rid of the very short wavelength noise and the contributions due to shallow bodies. For example, a gravity survey with a data spacing greater than 1.6 km should detect no signal with a wavelength shorter than 3.2 km (see Brigham (1976) under Nyquist sampling rate). Therefore, a low pass filter with a cut-off wavelength larger than 3.2 km is appropriate for 1.6 km spacing data.

The continuation filter differs from the band pass filter in that the continuation filter is based on the physical law of potential fields. The continuation filter is essentially the re-calculation of the gravity field at a higher (or lower) level based on the gravity field at the original observation plane. An upward continuation filter is similar to a low pass filter, while a downward continuation filter resembles a high pass filter. While a band pass filter has a rather sharp threshold frequency (a step function, a Guassian, or a Hanning function etc.), the frequency

content of the output spectrum of a continuation filter depends more on the input gravity data.

Since the reduced to the pole magnetic field is linearly related to the first vertical derivative of gravity (see section on Poisson analysis in Chapter 5), the first vertical derivative gravity map is a form of pseudo magnetic map. The first vertical derivative gravity map provides better definition of the size of an anomalous body. It attenuates long wavelength effects and enhances vertical or near-vertical density contrasts.

The second vertical derivative filter is similar in function to the first vertical derivative filter. It does a better job of isolating anomalies and identifying vertical density contacts. It is a more noisy operation and requires good quality data. It is sometimes necessary to smooth the data before applying the vertical derivative filter in order to reduce the noise and to improve the appearance of the output map. Vertical derivative filters always level the output grid about zero, and thus generate unrealistic lows around positive closures, and vice versa. Furthermore, these filters become unstable at the map boundary and give rise to undesirable edge effects. The data boundary can be padded with a ribbon of estimated gravity values to alleviate this problem.

Strike pass filters enhance the anomalies with strike in the desired direction. It can reveal the directional patterns of anomalies in the map, hence may reflect on the geologic structural characteristics of an area.

SPECTRALLY FILTERED GRAVITY MAPS

The input gravity grid for spectral filtering was prepared as follows. The 1.28 km upward continued gravity grid (fig. 17) used for isostatic calculations was supplemented with the Defense Mapping Agency gravity data in the area surrounding Kansas to generate a padded gravity grid with a ribbon of grid nodes around the state. This helps to cut down on the edge effects caused by some filters. A second order trend was then subtracted from this padded grid, resulting in the residual grid in figure 40 which was used as input grid in the following filter operations.

A low pass filtered gravity map with cutoff wavelength at 40 km (fig. 41) was generated using a Guassian tail threshold function. This low pass filtered map resembles the input gravity grid in figure 40, which has a higher (about 10 mgals) average amplitude. The resemblance is because most of the energy of the gravity frequency spectrum is concentrated in the longer wavelength (lower frequency) region and the Guassian tail threshold function used here has a gentle slope.

The 20 km cutoff high pass filtered gravity map (fig. 42) stresses the shallow sources. A circular positive anomaly (labelled 's') in eastern Sumner county lies within the northeast trending gravity high that overlies the Nemaha ridge in southcentral Kansas (see also fig. 41). It probably is caused by a shallow pluton.

The broad positive anomaly at the southeastern end of the central Kansas uplift, CKU ('C' in fig. 41), has considerable fine structure in the 20 km high pass filtered map (fig. 42). A northeast

Figure 40. Bouguer gravity map of Kansas leveled at 1.28 km above sea level. Second order trend removed.

GRAVITY MAP OF KANSAS

LEVELED AT 1.28 KM ABOVE SEA-LEVEL

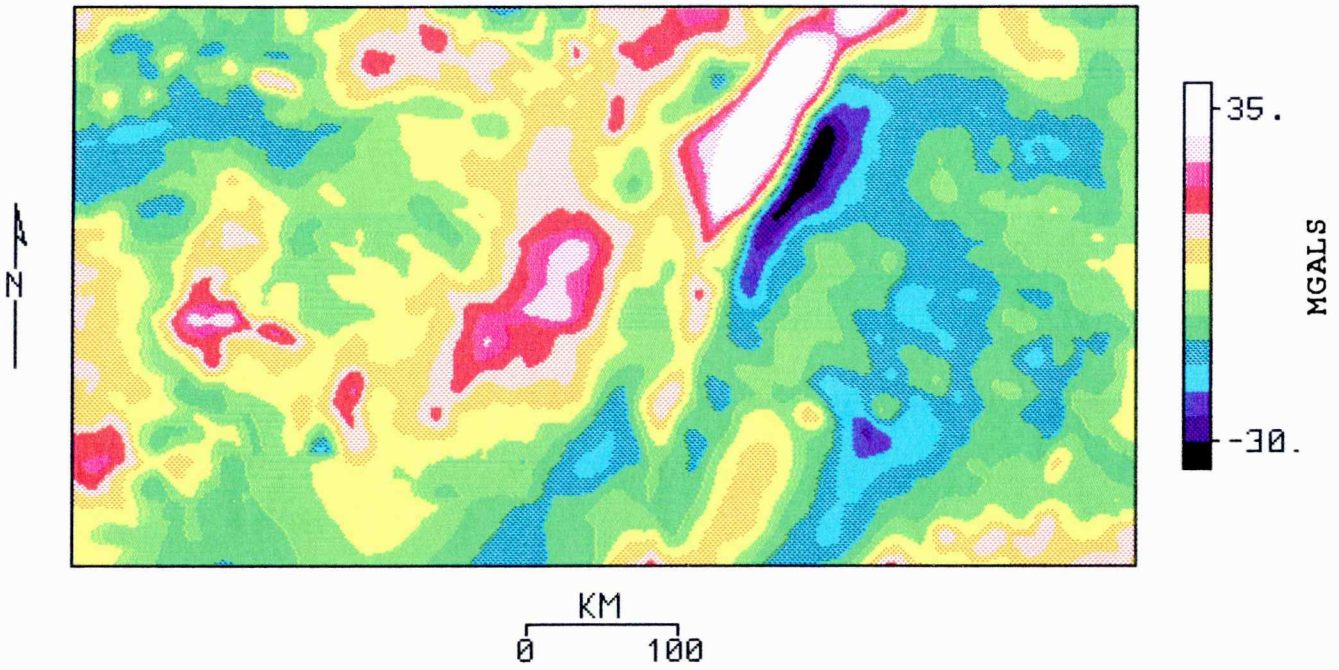

Figure 41. Low pass filtered gravity map of Kansas, cutoff wavelength at 40 km.

LOW PASS FILTERED, CUTOFF AT 40 KM

BOUGUER GRAVITY MAP

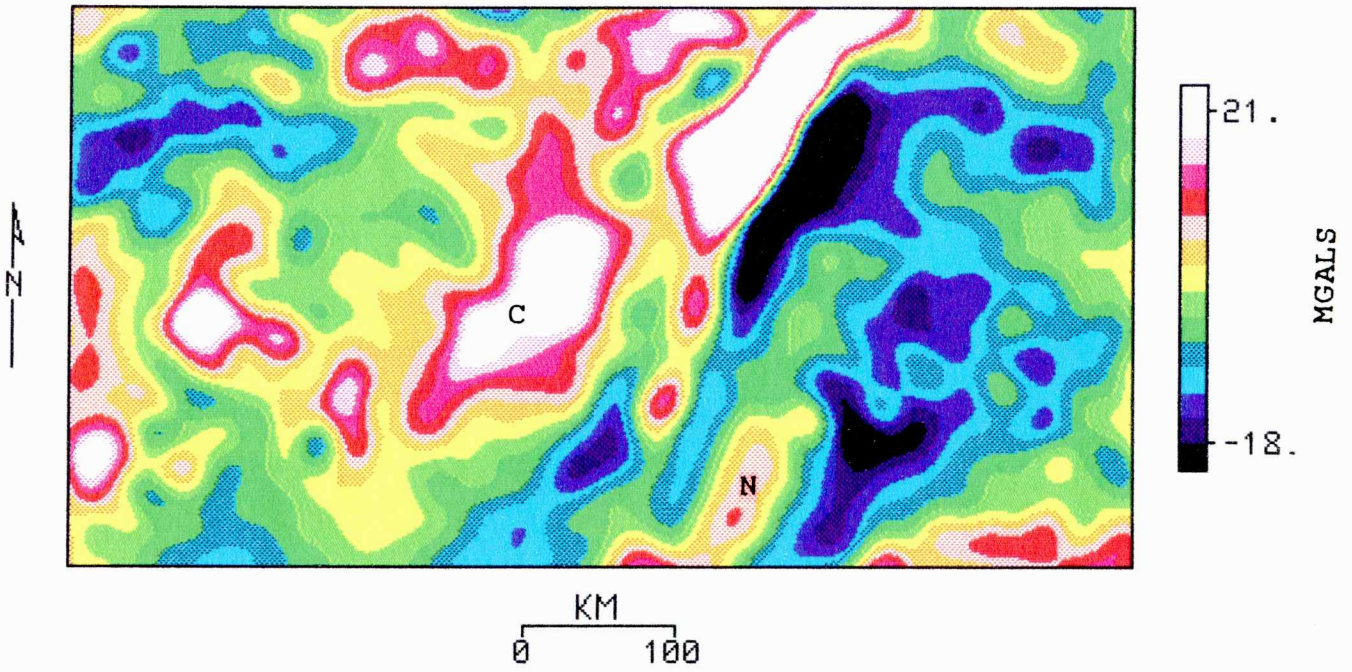

Figure 42. High pass filtered gravity map of Kansas, cutoff wavelength at 20 km.

BOUGUER GRAVITY MAP OF KANSAS

HIGH PASS FILTERED, CUTOFF = 20 KM

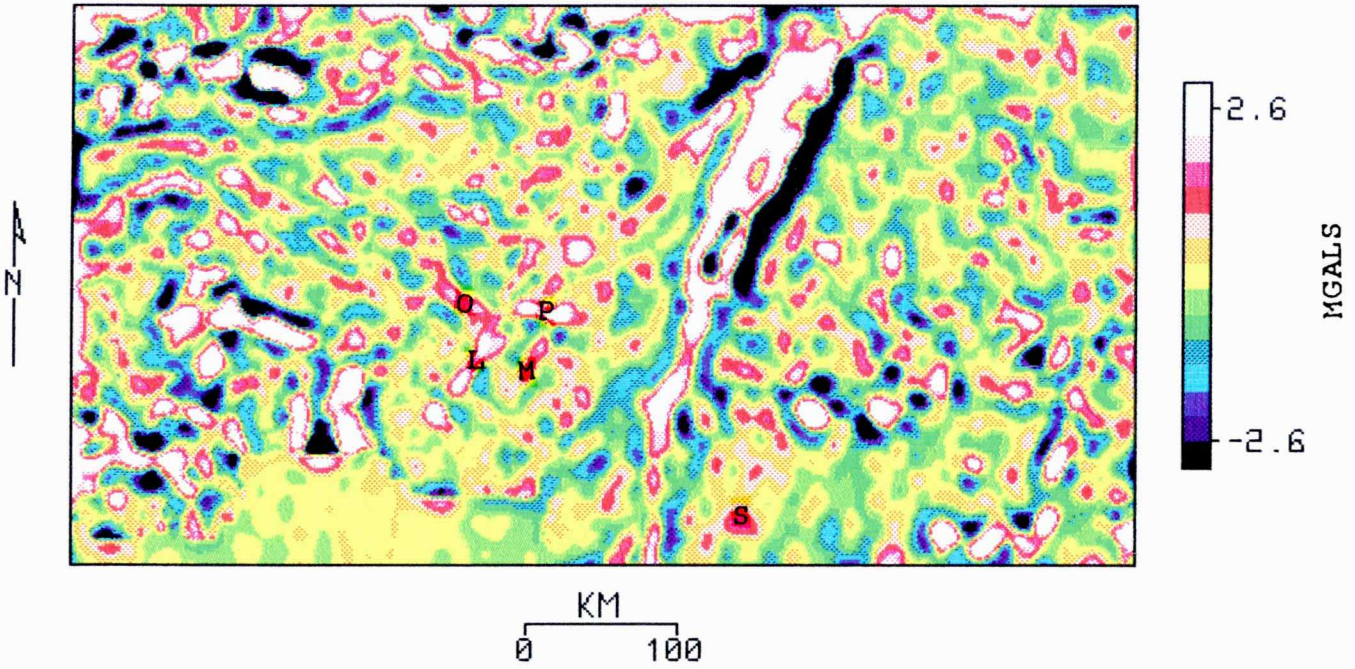

trending positive anomaly ('L' in fig. 42) from Pawnee to Barton county may be due to an intrusive dike. It appears to extend further north to Osborne county. A similar but less evident anomaly is also found in Stafford county ('M' in fig. 42). Two northwest trending anomalies orthogonal to 'L' and 'M' in south Barton ('O' in fig. 42) and central Rush counties ('P' in fig. 42) is parallel to the strike of faults mapped in the area (Cole, 1976).

The 10 km upward continued gravity map (fig. 43) shows a broad negative anomaly in eastern Kansas, which is most likely due to a negative density anomaly in the mid-crust as discussed in an earlier section. The central gravity high (labelled 'mga' in figure 43) and the east flanking low of the MGA are apparent in the 10 km upward continued gravity map. In the 40 km upward continued gravity map (fig. 44), the central gravity is still present in northcentral Kansas but the flanking lows are no longer visible anywhere. This implies that the less dense Precambrian sediments on the flanks of the central rift basin are at a shallower depth than the more dense basalt at the central rift basin in northcentral Kansas. The disappearance of any significant MGA trend in southcentral Kansas in the 40 km upward continued gravity grid (fig. 44) means little or no volcanics were emplaced at mid to lower crustal levels. The northeast trending positive anomaly (labelled 'c' in figures 43 and 44) near the southeastern end of the central Kansas uplift appears to be deep rooted because it persists in the 40 km upward continued gravity map. It is possible that this anomaly could be a deep root of the MGA which is right laterally offset near central Kansas.

Figure 43. 10 km upward continued gravity map of Kansas.

GRAVITY MAP OF KANSAS

UPWARD CONTINUED 10 KM

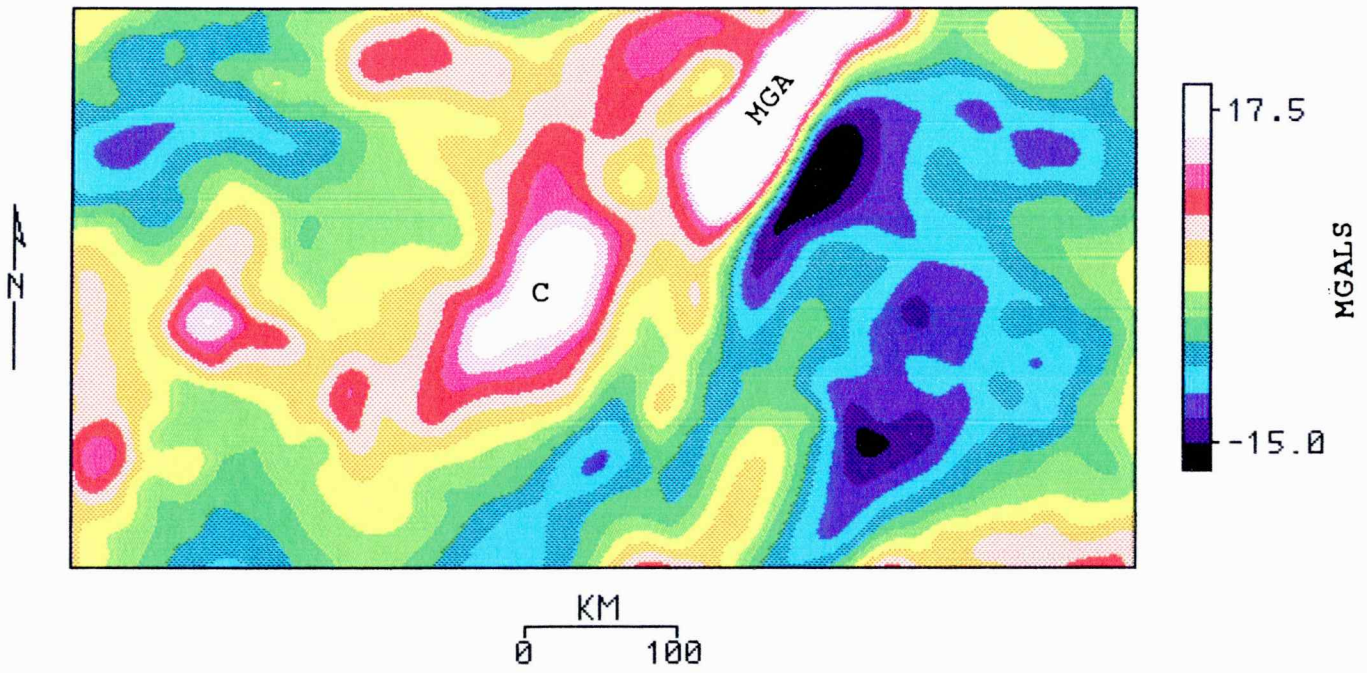

Figure 44. 40 km upward continued gravity map of Kansas.

UPWARD CONTINUED 40 KM

BOUGUER GRAVITY MAP OF KANSAS

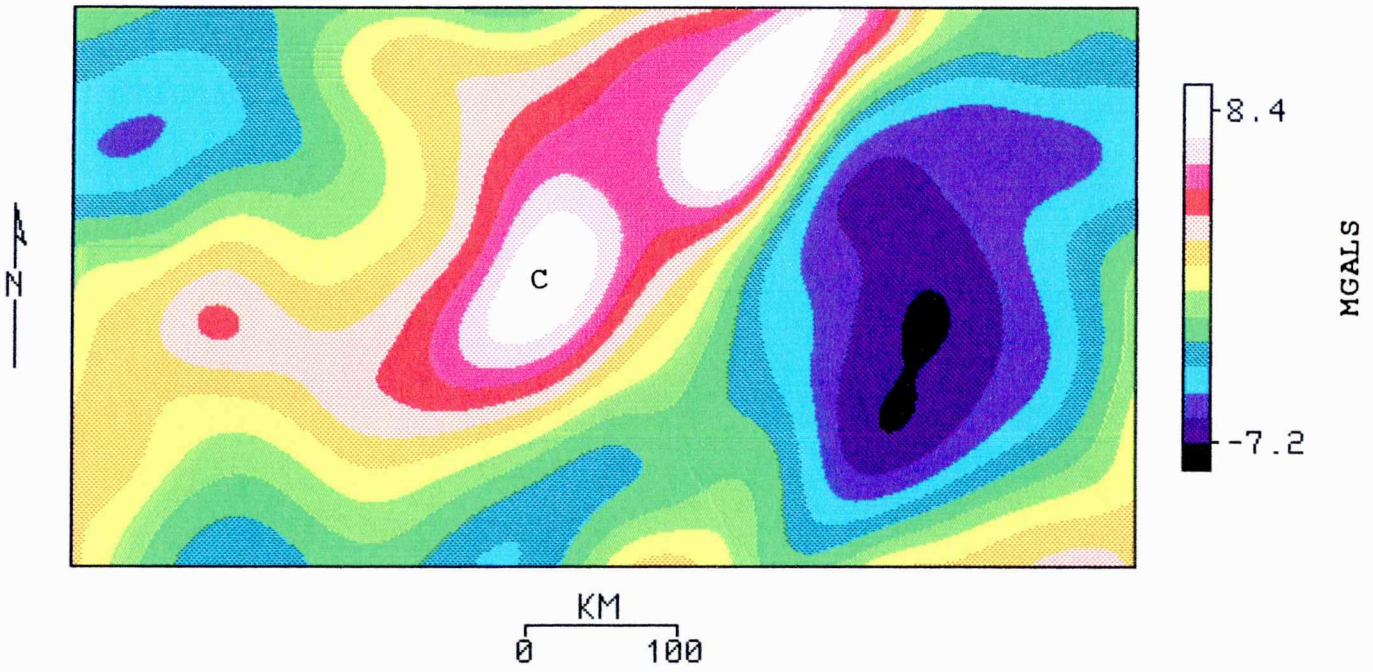

Similarly, the MGA trend has an offset just north of the Kansas/Nebraska border (not visible on Kansas gravity map) and just north of the Iowa/Minnesota border. Although the offsets in the latter cases are left lateral.

The first vertical derivative gravity map (fig. 45) helps to make individual anomalies show up better. The central gravity high and flanking lows of the MGA are even more spectacular on this map. The continuation of this anomaly to at least the Kansas-Oklahoma border is evident. The positive anomaly near the southeastern end of the central Kansas uplift (labelled 'c' in figures 43 and 44) is right laterally offset by approximately 25-30 km. The two separate parts of this anomaly are labelled 'c1' and 'c2' in figure 45. A possible interpretation of this offset is that there was strike-slip movement along a northwest trending fault zone at or shortly after the 1.1 b.y. rifting.

There is a sinuous east-west trending gravity low, approximately 300 km long, in northwestern Kansas in the counties of Sherman, Thomas, Sheridan, Graham, Rooks and Osborne (labelled 's' in figure 45). This trend consists of a series of individual negative closures. It may delineate separate basement terranes to the north and south here-to-fore unrecognized. This boundary is substantially to the north of the boundaries proposed by previous investigators (Bickford and others, 1981; Yarger, 1984), as well as the boundary TT' (fig. 36) that I have determined in the last section.

Figure 45. First vertical derivative gravity map of Kansas.

GRAVITY MAP OF KANSAS

UPWARD CONTINUED 1.28 KM ABOVE SEA-LEVEL, 1ST VERT. DERIVATIVE TAKEN

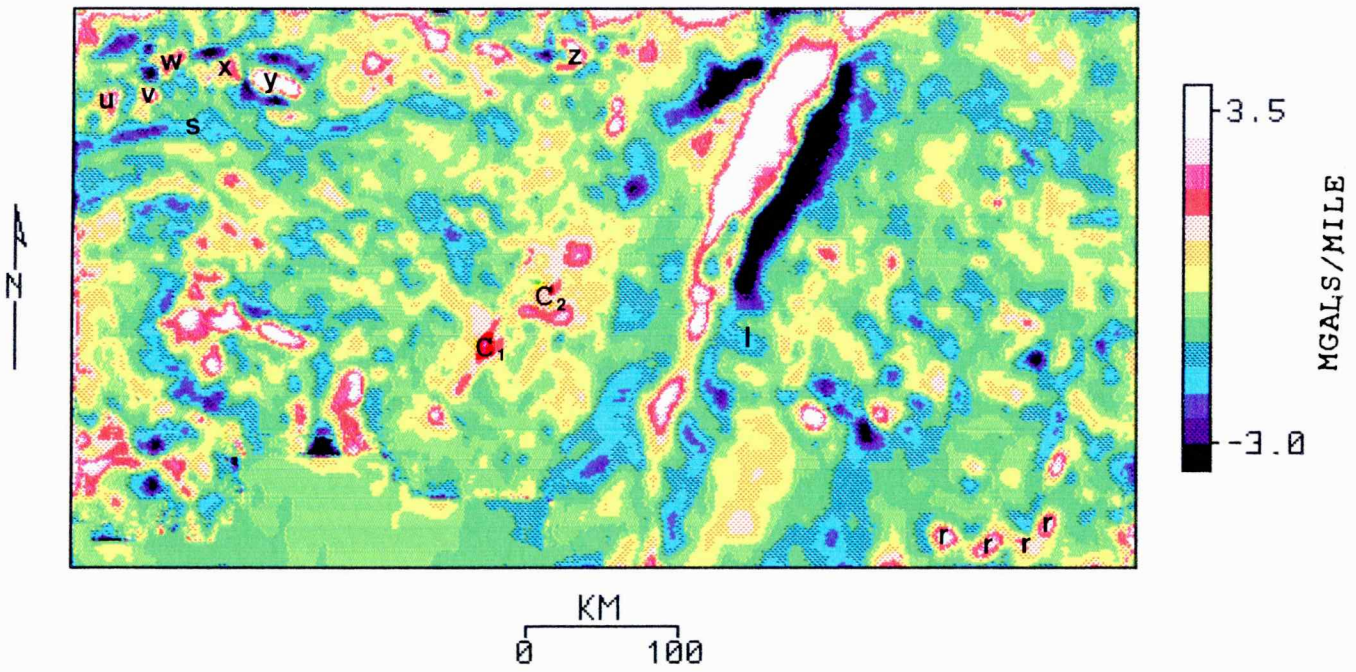

To the north of this chain of gravity lows are several positive closures in the counties of Cheyenne, Rawlins, and Decatur (labelled 'u', 'v', 'x', and 'y' in figure 45). These are interpreted as plutons at or near the basement surface. The anomalies labelled 'u', 'v', and 'y' in figure 45 approximately coincide with magnetic lows and could be emplaced when the earth's magnetic field was reversely polarized. The anomalies labelled 'w' and 'x' correspond to magnetic highs and a normally polarized earth magnetic field at the time of emplacement. The anomaly, labelled 'z' in figure 45, at the center of the Salina basin in Jewel county corresponds to a magnetic high and also has the characteristic of a shallow pluton in the basement.

The composite positive anomaly near Wichita, Scott, and Lane counties in western Kansas has a very sharp contrast on the west and northeast sides suggesting a fault controlled igneous emplacement. The positive closures in southeastern Kansas (labelled 'r' in figure 45) have exceptionally straight edges and appear to be fault bounded.

The strike pass gravity map in figure 46 enhances gravity anomalies trending N30°E, and attenuates anomalies normal to this direction. The MGA, with its central gravity high and flanking lows, extends from north to south in central Kansas. Several northeasterly trending gravity highs are present on the western flank of the main MGA gravity anomaly in southcentral Kansas (labeled 'C' in figure 46).

Another strike pass gravity map (fig. 47) stresses west northwest-east southeast trending gravity anomalies and suppresses

Figure 46. High pass filtered (cutoff at 10 km) and strike passed (N30°E ±60°) gravity map of Kansas.

BOUGUER GRAVITY MAP OF KANSAS, HIGH PASS FILTERED, CUTOFF=10 KM

N 30 E STRIKE PASS FILTERED, ANGLE BRACKET=60 DEGREES

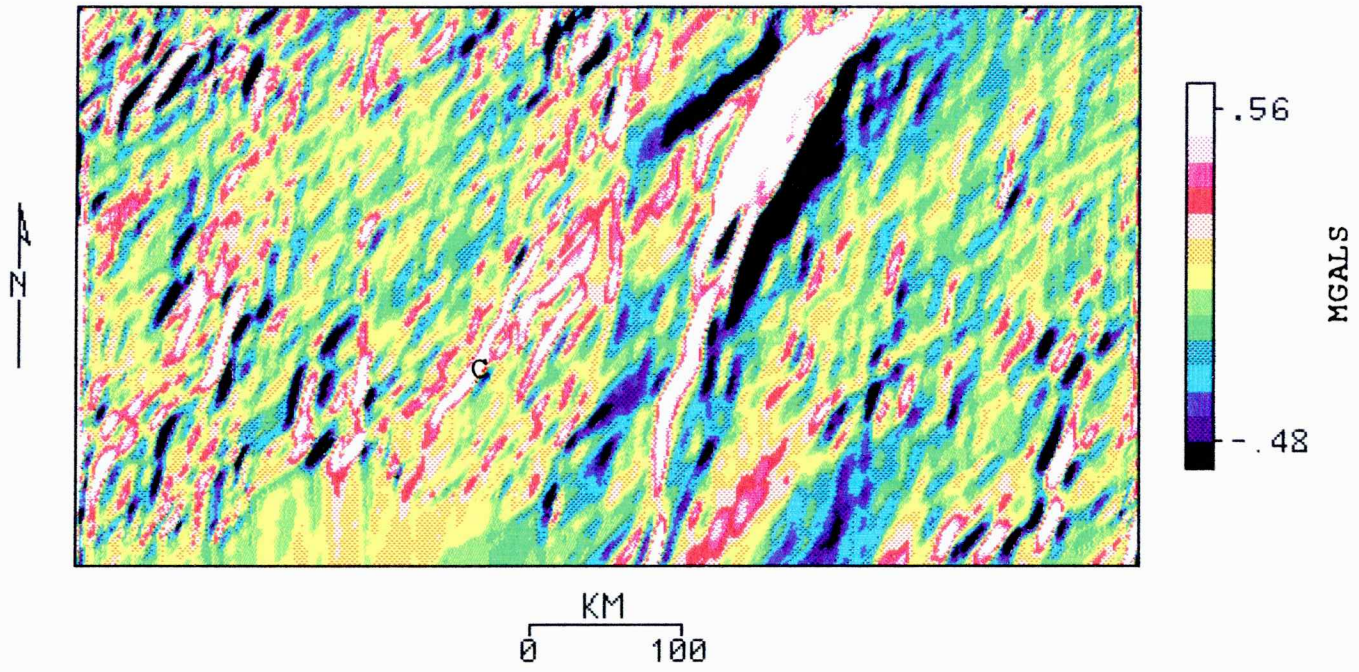

Figure 47. High pass filtered (cutoff at 10 km) and strike passed (N30°W ±60°) gravity map of Kansas.

BOUGUER GRAVITY MAP OF KANSAS, HIGH PASS FILTERED, CUTOFF=10 KM

N 60 W STRIKE PASS FILTERED, ANGLE BRACKET = 60 DEGREES

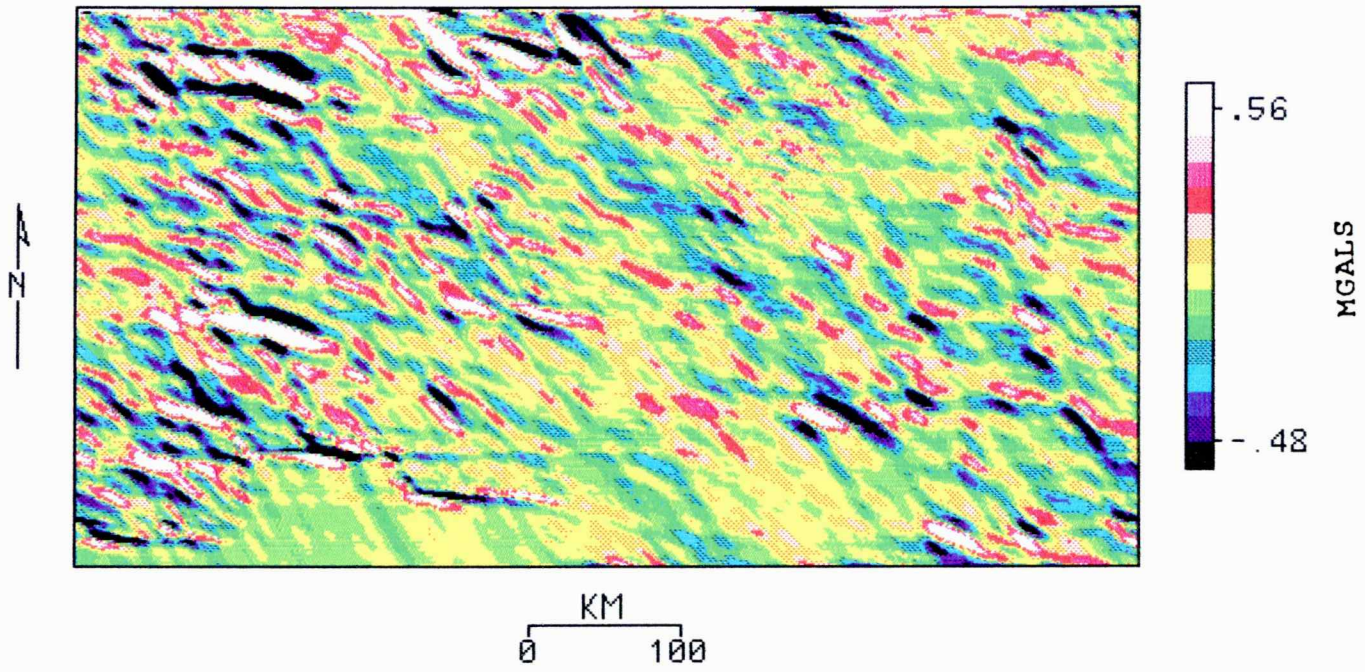

anomalies normal to this direction. There are many northwesterly trending gravity anomalies throughout the map (fig. 47), except in central Kansas along the MGA. These northwesterly trending gravity anomalies are interpreted as fractures in the granitic basement that pre-date the 1.1 b.y. MGA.

MOVING WINDOW POISSON ANALYSIS

The first vertical derivative of gravity was correlated with the reduced to the pole magnetic field using linear regression over a small moving window. Preparation of the input leveled gravity grid was discussed in the section on isostatic reduction. The second order residual gravity grid at a common datum level of 1.28 km above sea level (fig. 40) was used as input for calculating the first vertical derivative of gravity (fig. 45). Because the long wavelength regional trend is mostly due to deep sources at and below the Moho, it is appropriate to eliminate the regional trend in order to isolate shallower sources.

It was necessary to re-calculate the gravity and magnetic data grids so that they were at a common "observation" plane. This procedure removed any gravity or magnetic gradients caused by differences in the observation elevations.

It is also necessary to level the magnetic grid because the aeromagnetic survey was flown at 762 m (2500 ft), 914 m (3000 ft), and 1371 m (4500 ft) above sea level in eastern, central, and western Kansas respectively. The entire magnetic grid was continued to 1280 m (4200 ft) above sea level by reduction to the pole first (inclination = 65°, declination = 7°), and then upward continuing the eastern Kansas data by 518 m (1700 ft), the central Kansas data by 366 m (1200 ft), and downward continuing the western Kansas data by 91 m (300 ft). The resulting leveled magnetic grid is shown in figure 48.

Figure 48. Magnetic map of Kansas leveled at 1.28 km above sea level.

MAGNETIC MAP OF KANSAS, REDUCED TO POLE

LEVELED AT 1.28 KM ABOVE SEA-LEVEL

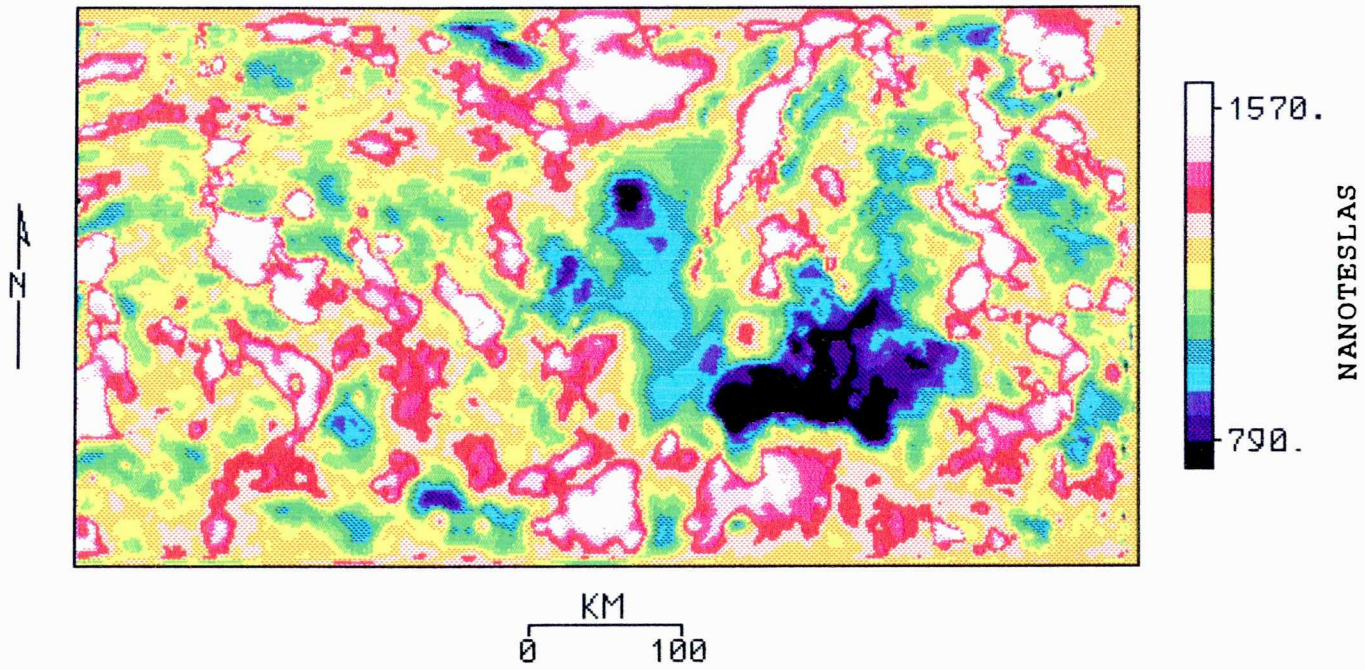

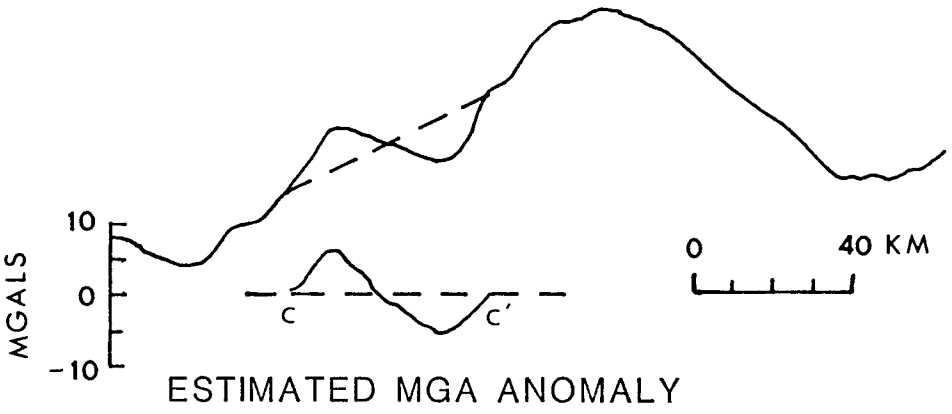

ESTIMATED MGA ANOMALY

A square window of 3-by-3 grid nodes (4.8 by 4.8 km) was found to give the optimal result in the moving window Poisson analysis, which fits a straight line between the first vertical derivative of gravity and the reduced to the pole magnetic field in the least squares sense. Smaller window sizes give unreliable fits with large root mean square value. Larger window sizes produce a smoothing effect which discriminate against smaller anomalies. Larger window sizes also increase the undefined area around the edge of the map where some interesting features are located.

Moving window Poisson analysis was performed on the 1.28 km upward continued data. The output grids of the moving window Poisson analysis are shown in figures 49, 50 and 51. The intercept (fig. 49) near the Wichita magnetic low has a very low value, indicating a regional magnetic low. The rest of the state generally has intercepts of about 1200 to 1300 nanoteslas, which is about the average value of the input magnetic map (fig. 48).

In figure 50, a large percentage of correlation coefficients are near +1 or -1, indicating good direct correlation or inverse correlation between gravity and magnetic anomalies. There are slightly more positive correlations. Incidences of non-correlation (correlation coefficient near zero) are relatively few. A striking feature of the correlation coefficient map (figure 50) is the marked difference between northern and southern Kansas, as divided by the line TT'. South of the line TT' in figure 50, the correlation coefficients are mostly near +1. An approximately 50 km wide band, bounded between TT' and the dashed line in figure 50, contains a

Figure 49. Intercept map derived from Poisson analysis of Kansas gravity and magnetic data at 1.28 km above sea level.

INTERCEPT OF POISSON ANALYSIS, IN NANOTESLAS

GRAVITY & MAGNETIC DATA AT 1.28 KM ABOVE SEA-LEVEL

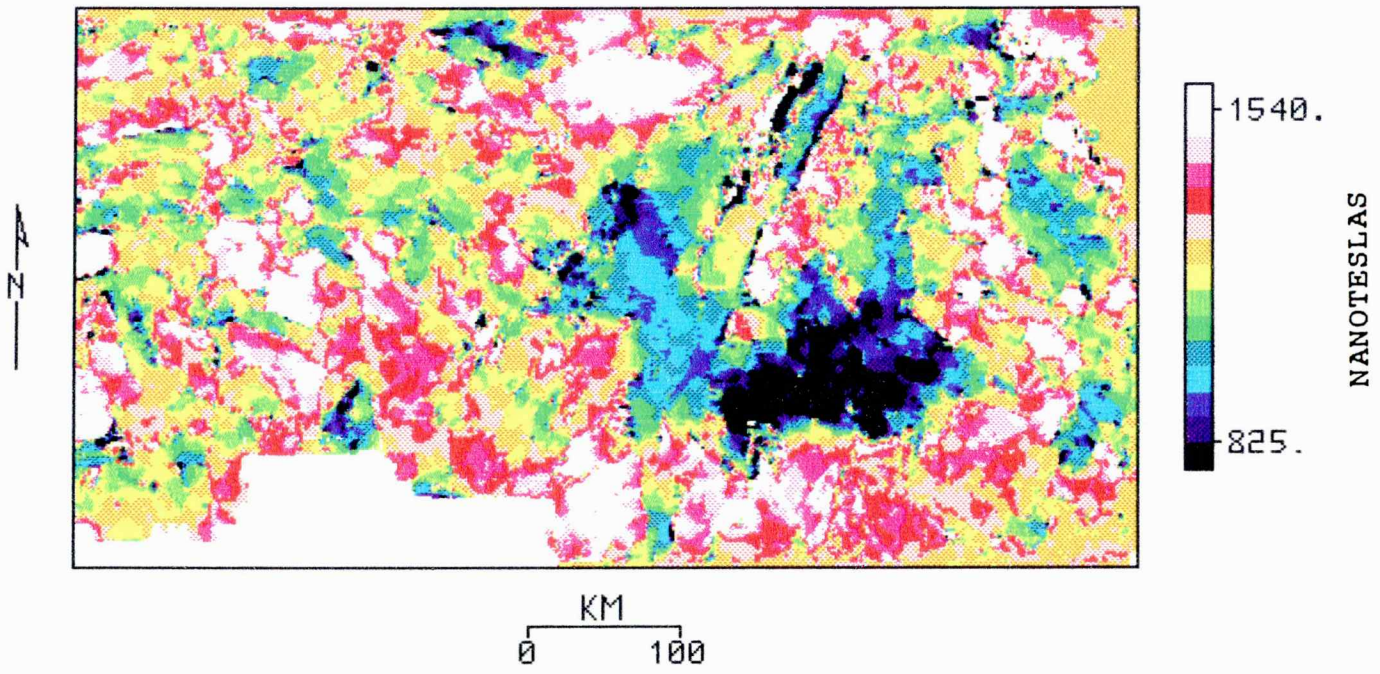

Figure 50. Correlation coefficient map derived from Poisson analysis of Kansas gravity and magnetic data at 1.28 km above sea level.

POISSON ANALYSIS OF GRAVITY AND MAGNETIC DATA

CORRELATION COEFFICIENT, DATA AT 1.28 KM ABOVE SEA-LEVEL

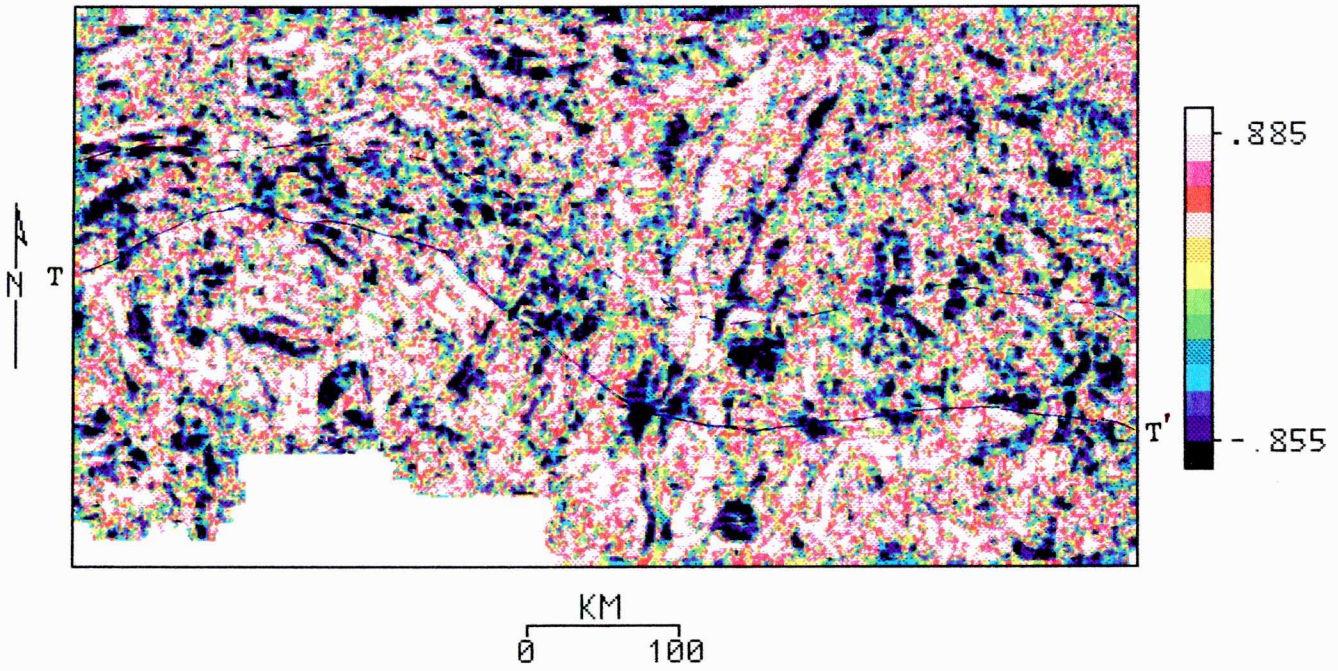

Figure 51. Magnetization contrast to density contrast ratio (m/d) map derived from Poisson analysis of Kansas gravity and magnetic data at 1.28 km above sea level.

POISSON ANALYSIS OF GRAVITY & MAGNETIC DATA AT 5 KM ABOVE SEA-LEVEL

MAGNETIZATION CONTRAST / DENSITY CONTRAST, ABS(CORR COEFF) .GT. 0.3

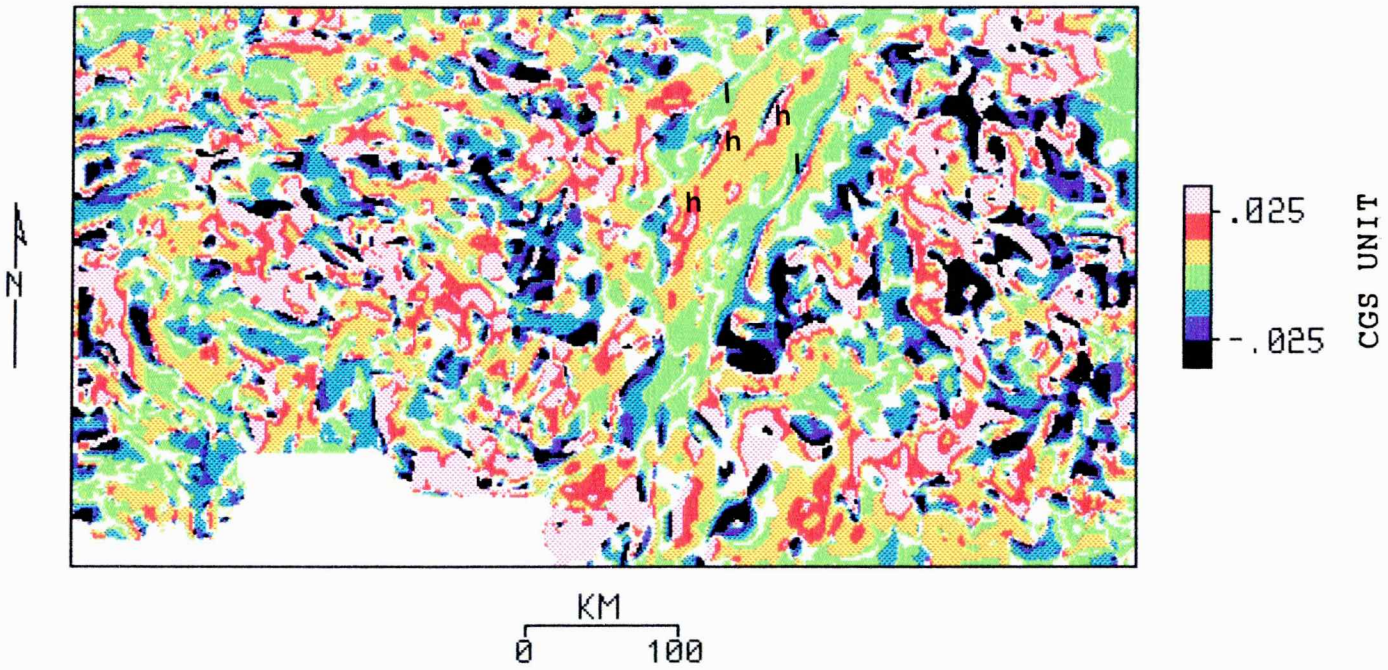

high percentage of near -1 correlation coefficients. The occurrence of high positive (white) and high negative (black) correlation coefficients north of this 50-km-wide band are approximately equal.

Similar to the correlation coefficient map (fig. 50), the magnetization-contrast to density-contrast (m/d) map in figure 51 also shows a marked difference in northern and southern Kansas, as divided by the line TT'. South of the line TT', most of the m/d values are more positive (around +0.03), corresponding to coincidence of magnetic and gravity highs. This implies that the rocks have a larger lateral magnetization contrast. In the region bounded between TT' and the dashed line in figure 51, there is a higher percentage of negative m/d value. M/d values between zero and +0.015 are common farther north. I believe that these distinctions in m/d values and correlation coefficients in northern and southern Kansas corresponds to the basement rock types as discussed by Bickford and others (1979).

Several regions in northeastern Kansas (two of these are labelled 'b' and 'm' in figure 51) have an exceptionally high m/d value of about +0.03. These are locations of plutons of the Big Springs type as discussed by Yarger (1984), and Steeples and Bickford (1981). The positive magnetic and gravity anomalies are caused by the about 2% magnetite (by weight) in the granite. Similar gravity and magnetic anomalies scattered throughout eastern Kansas are probably due to the same kind of magnetite-rich granite.

The central gravity and magnetic highs of the MGA has a m/d value of about +0.008, while the flanking lows have an m/d value of

about zero. Somanas' (1984) model of the interbedded rift basalt and Precambrian sediments have an m/d value of 0.024 and zero respectively. The discrepancy could be explained if the susceptibility contrast of the interbedded basalt was one third of the value of 0.005 used in his model and the shallower causative body was three times as large. This larger body of basalt, approximately 2 to 14 km beneath sea level, would alone account for the entire amount of observed gravity and magnetic anomalies. Because its gravitational effect would be about three times larger than that due to the smaller shallow body in Somanas' model, this in effect does away with his model's deeper sources. Serpa and others (1984) used a model of the basalt basin similar to Somanas' and found that only one third of the observed central gravity high is accounted for.

The pronounced northeasterly trend (labelled 'mga' in figure 51), which corresponds to the central gravity high of the MGA, appears to die out near the 38th parallel. The rift basin was not as well developed in southern Kansas, so the rift basalt and Precambrian sediments are not the dominant sources of the gravity and magnetic anomalies.

The Wichita magnetic low is characterized by a central area of near zero m/d values. This suggests that the Wichita magnetic low is caused by a magnetite deficient granite. A coincident circular magnetic low and gravity high in central Sumner county in southcentral Kansas produced a corresponding circular area with a m/d value of less than -0.025. This indicates a shallow mafic pluon

with a strong remanent reversed magnetization. A similar m/d anomaly is located on the Harvey and Marion county line. The first vertical derivative gravity map clearly isolates this gravity low (labelled '1' in figure 45). This gravity low is an eastern lobe on the east flanking low of the MGA, and is probably caused by a big column of Precambrian sediments, which is underlain by a magnetic pluton.

To attenuate the effect of shallow sources and to stress the contribution of deeper sources, moving window Poisson analysis was also performed on 5 km upward continued data grids. The resultant m/d map (fig. 52) is less noisy because the short wavelengths, which include most of the noise, has been filtered out.

Within the MGA there are several small regions (labelled 'h' in figure 52) which have a 0.3 m/d value. These are probably caused by the incomplete reduction to the pole operation caused by a large remanent magnetic field. The Q value of the rift basalt, which is defined as the ratio of the remanent to induced magnetic field, may be as large as one. The inclination and declination of the remanent magnetic field are quite different from the present ambient field (Somanas, 1984). Two areas (labelled '1' in figure 52) have a large negative m/d value. These are probably edge effects caused by the remanent magnetic field also.

A negative m/d anomaly (fig. 52) on the northern part of the Rawlins/Decatur county line in northwestern Kansas corresponds to a gravity high (fig. 40) and a magnetic low (fig. 48). It is probably caused by a reversely magnetized mafic pluton. A m/d low in Wichita and Scott counties in western Kansas (fig. 52) corresponds to a

Figure 52. Magnetization contrast to density contrast ratio (m/d) map derived from Poisson analysis of Kansas gravity and magnetic data at 5 km above sea level.

POISSON ANALYSIS OF GRAVITY & MAGNETIC DATA AT 1.28 KM ABOVE SEA-LEVEL

MAGNETIZATION CONTRAST / DENSITY CONTRAST, ABS(CORR COEFF) .GT. 0.3

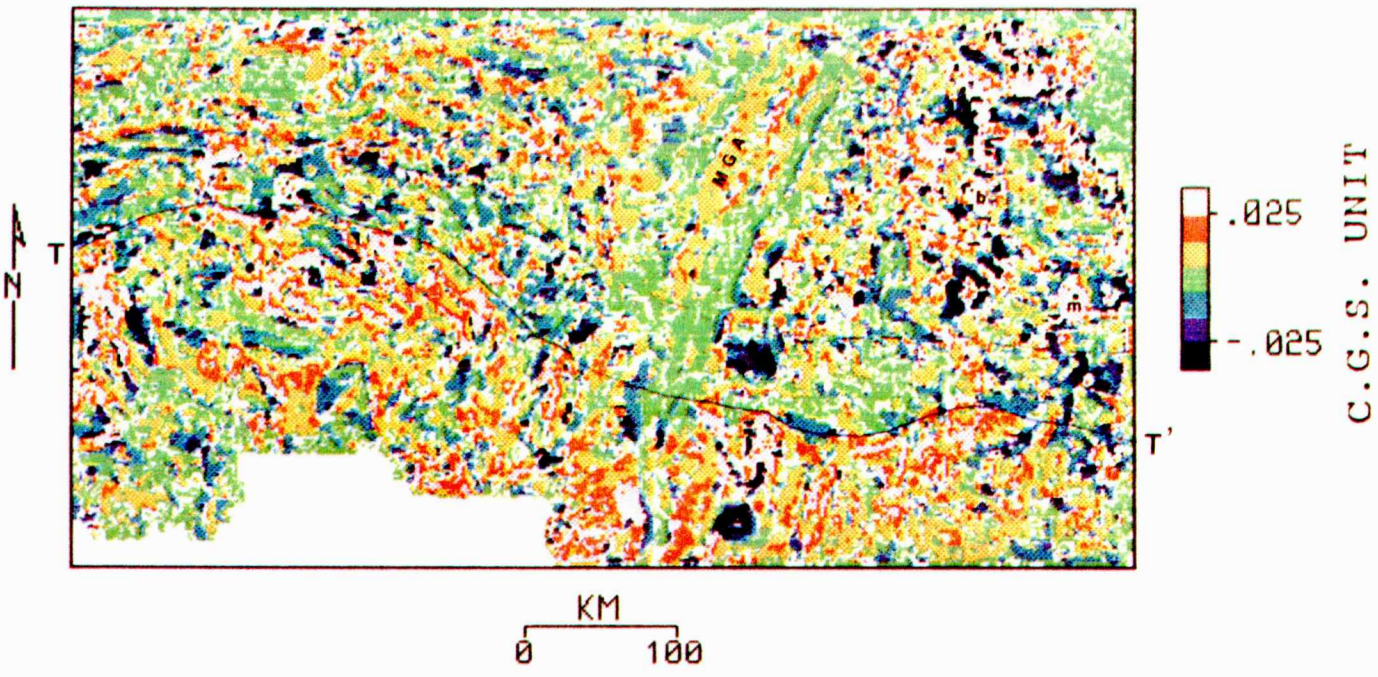

prominent gravity high (fig. 40) and a magnetic low (fig. 48). While immediately south of it in Kinney and Finney counties, there is a m/d high (orange). These are probably plutons in the basement, which occurred at two different times when the earth's magnetic field had reversed and normal polarizations.

Other m/d highs (fig. 52) corresponding to coincident gravity and magnetic highs in figures 40 and 48 are a north trending anomaly (pink and red) in western Wallace, Greely, and Hamilton counties parallel to the Colorado border, a large anomaly (pink and red) covering the entire Doniphan county in northeastern Kansas, and two 10 to 20-km-wide anomalies (orange) in Montgomery and Labett counties in southeastern Kansas. The above anomalies are probably caused by mafic plutons in the basement.

Moving window Poisson analysis was next applied to the 15-km upward continued grids to focus on the anomalous sources at greater depth. The correlation coefficient map (fig. 53) shows a similar distribution of correlation coefficients throughout the state. There is no apparent terrane boundary as in the case with the 1.28-km upward continued data grids (fig. 50). The m/d values (figure 54) also exhibit similar patterns throughout the state, showing no sign of a terrane boundary. The homogeneity of the gravity and magnetics sources beneath the shallow basement implies that the rocks at depth are laterally homogeneous. This means that the younger rocks in southern Kansas form only a thin veneer of a few kilometers thick, overlying the same 1.6 b.y. mesozonal granitic rocks found in the northern terrane. The positive m/d anomalies (fig. 54) in the Salina

Figure 53. Correlation coefficient map derived from Poisson analysis of Kansas gravity and magnetic data at 15 km above sea level.

CORRELATION COEFFICIENT OF POISSON ANALYSIS

GRAVITY AND MAGNETIC DATA UPWARD CONTINUED 15 KM ABOVE SEA-LEVEL

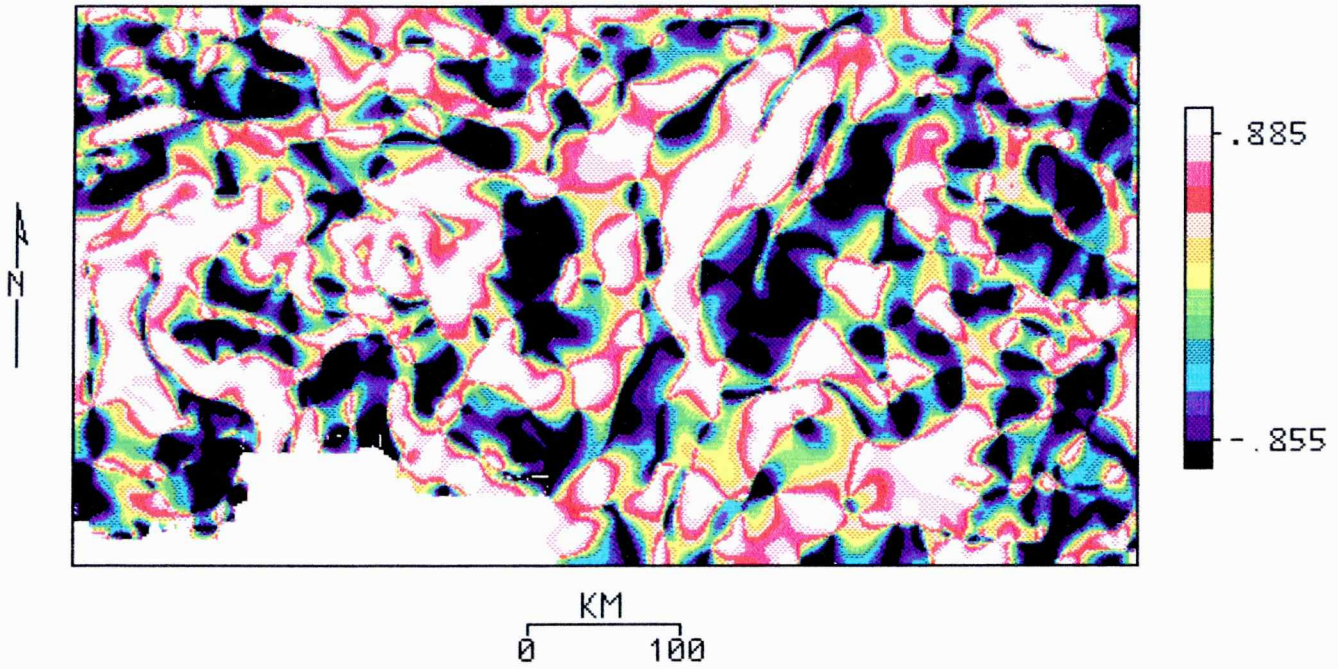

Figure 54. Magnetization contrast to density contrast ratio (m/d) map derived from Poisson analysis of Kansas gravity and magnetic data at 15 km above sea level.

POISSON ANALYSIS OF GRAVITY & MAGNETIC DATA 15 KM ABOVE SEA-LEVEL

MAGNETIZATION CONTRAST / DENSITY CONTRAST, ABS(CORR COEFF) .GT. 0.3

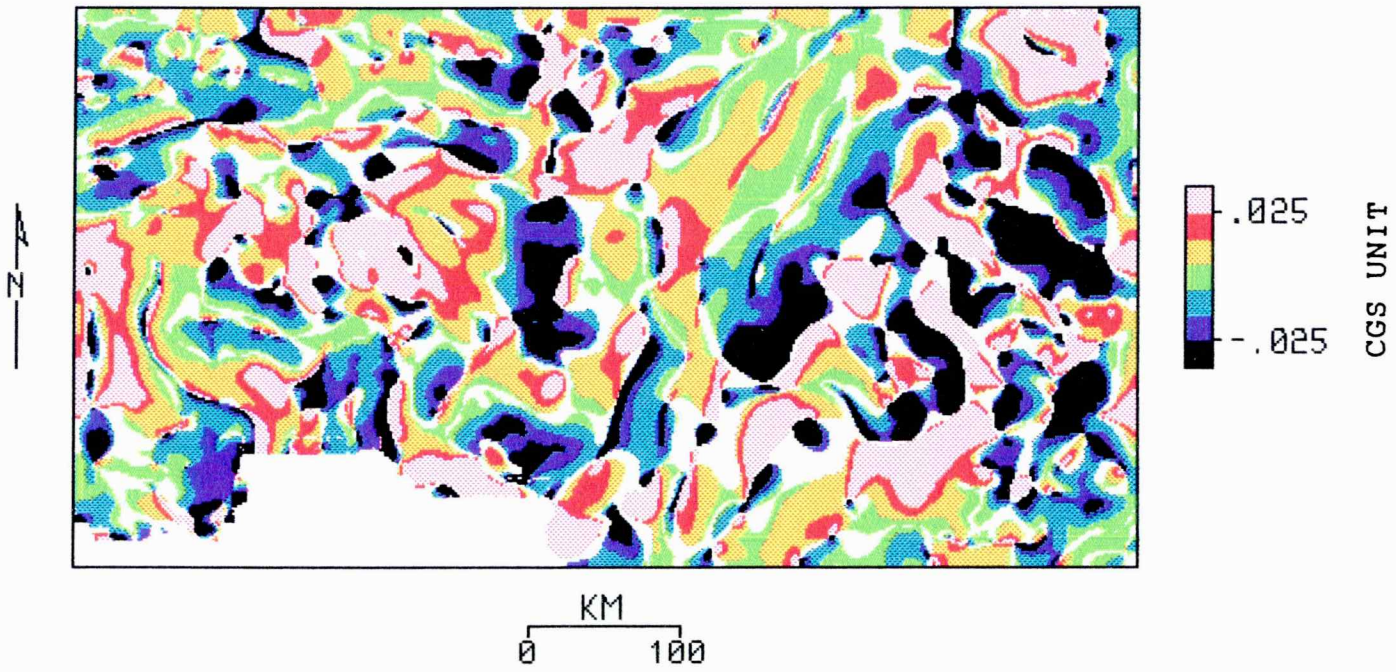

Basin and in Doniphan county are more uniform and larger that those in the 1.28-km and 5-km upward continued m/d maps (figs. 51 and 52). This is a result of the reduction of interference caused by shallow sources. It appears that both the Salina and Forest City Basins are underlain by large mafic plutons.

CHAPTER SEVEN

DISCUSSION AND CONCLUSION

In chapter six, I focused on the data enhancement methods and their resultant maps. In this chapter, I present a synthesis of last chapter's findings, and discuss their implications.

CENTRAL NORTH AMERICA RIFT SYSTEM (CNARS)

It has been shown in chapter six that the gravity trend of the MGA, which is the geophysical expression of the CNARS, extends to at least the Kansas/Oklahoma border. The amplitude of the central gravity high of the MGA in the second order residual gravity map (fig. 27) abruptly decreases from more than +60 mgals to +20 mgals near Saline county in central Kansas. This sudden change is caused by a resistance or locked zone of more ductile crust/lithosphere in southern Kansas. The more ductile crust/lithosphere was due to an elevated geothermal gradient which was caused by the igneous activity that produced the 1.4 b.y. granite/rhyolite in the shallow basement in southern Kansas.

It has been speculated (for example, Van Schmus and Hinze, 1985) that the continued extension of the incipient rift, CNARS, was halted by a east-west compressional stress some 1.1 b.y. ago. Because rifting or crustal extension is usually accompanied by normal faulting in the upper crust (for example, Wernicke and Burchfiel, 1982), it was therefore surprising to find reverse faults along the CNARS in the lake Superior region (Hinze and others, 1982)

These reverse faults could be the result of a post-rift compressional event that moved the crustal blocks along the normal faults associated with rifting. Hinze and others (1982) also reported a thicker crust beneath the rift in Minnesota/Wisconsin, which is clear evidence of crustal shortening and compressional stress. It appears that in the northern portion of the rift near lake Superior, the amount of crustal extension due to the CNARS was less than the amount of subsequent crustal shortening, resulting in a net effect of crustal shortening.

According to the interpretation of the geologic and geophysical data that follows, a different scenario developed at the southwestern end of CNARS in Kansas. Serpa and others (1984) reported normal faulting in an asymmetrical basalt filled basin some 4 km below the present Precambrian surface along COCORP seismic line 1 in northeastern Kansas. Base on a east-west seismic refraction line in western Kansas, Steeples (1976) found a thinner crust (38 versus 44 km) in central Kansas. The change from reverse faulting and crustal shortening near lake Superior to normal faulting and crustal thinning in Kansas may be due to a stronger compression in the northeastern end of CNARS. Post-rift compression was probably less pronounced in the southwestern end in Kansas. Alternatively, it is possible that the crustal extension was larger in the southwestern end than the northeastern end of the CNARS. However, this is not probable because the amplitude of the gravity trend is actually larger in the northeastern end, which rather indicates a more developed basalt basin near Wisconsin/Minnesota.

It was shown in chapter six that central Kansas is isostatically partially compensated at and below the Moho. The low velocity body observed by Hahn (1982) at about 125 km depth is a prime candidate for the low density body below the Moho. Assuming this body is a northeast trending prism having a rectangular cross-section, and is about 2% lighter than the normal upper mantle density of 3.35 gm/cc (i.e. -0.06 gm/cc), this prism needs to be about 45 km thick in order to maintain isostatic equilibrium. If we further assumes the width of the rectangular prism is 60 km and its center of mass is 125 km below sea level in central Kansas, then the negative gravity anomalies caused by this body are 9 and 30 mgals near the Kansas/Colorado border and at central Kansas respectively. Therefore, the 9 mgal unexplained difference between the isostatic correction grid and the second order trend of the Bouguer gravity grid near the Kansas/Colorado border discussed in chapter six could be attributed to this deep body.

PRECAMBRIAN BASEMENT TERRANES

Although many investigators (for example Bickford and others, 1982; Yarger, 1984) have identified an east-west Precambrian basement terrane boundary in Kansas, the origin of the 1.4 b.y. granite/rhyolite terrane in southern Kansas is still unknown. Van Schmus and others (1986) and Bickford and others (1986) favor an anorogenic intrusive event, while Emslie (1978) and Anderson (1983) propose an incipient continental rift as its cause. It is also possible that this 1.4 b.y. terrane was accreted to the continental

crust to the north in a process similar to the present day Pacific continental margin of north America.

Nelson and DePaolo (1985), based on Nd isotopic evidence, found that westcentral United States is made up of continental crust that was separated from the mantle 1.7-1.9 b.y. ago, which is considerably older then the 1.4 and 1.6 b.y. U-Pb, Rb-Sr, and K-Ar crystallization age. (The ages determined from U-Pb, Rb-Sr, and K-Ar isotopic studies give the date when the igneous rock solidified or underwent a re-crystallization event, while the Nd date is the crust formation time or the time when the magma was initially separated from the mantle.) They believe that the undeformed 1.4 b.y. granite/ rhyolite were derived from a mixture of magma from the mantle and the isotopically heterogeneous continental crust, and the rocks with a later crystallization age only make up of a thin layer several kilometers thick. These younger rocks cover an older 1.9 b.y. continental crust and is probably the inland anorogenic consequence of a subduction zone associated with formation of the ~1.4 b.y. Llano crust in southern United States.

The results of the moving window Poisson analyses of gravity and magnetic data in chapter six strongly support the above model. Potential fields data indicate that the shallow basement rocks are distinct in northern and southern Kansas, having different correlation coefficients and derived magnetization-contrast/density-contrasts. Upward continued gravity and magnetic data show a more homogeneous distribution of correlation coefficients and m/d ratios, indicating a homogeneous crust at depth.

CROSS SECTIONS OF LITHOSPHERE IN KANSAS

Plate 1 through 5 (in back pocket of this volume) are five east-west cross sections showing the structure and rock types from the surface down to ~200 km below sea level. Gravity and magnetic data along these profiles are also displayed on top of the cross section. The uppermost line is the measured magnetic field, followed by the second order residual gravity, and then the Bouguer gravity values. The surface elevation is based on the NOAA data, and the top of Mississippian and Precambrian basement were digitized from Merriam (1963) and Cole (1976). The depth to the Moho is constrained by seismic refraction results from Steeples (1976) and Stewart (1965). Deeper structures were interpreted from gravity and magnetic data and teleseismic study (Hahn, 1982).

Plate 2 is an east-west profile at latitude 39.59° that overlaps the COCORP seismic line 1 in northcentral Kansas. The intrusive dike on the eastern flank of the MGA is based on Somanas' (1984) interpretation. The mafic body on the extreme east end of the profile is related to the formation of the Forest City basin.

Plate 3 is an east-west profile at latitude 38.68° that transects the southeastern end of the Central Kansas uplift. The basalt intrusion at mid-crust level is the probable source of the observed gravity high. Dike intrusions trending northeasterly are present at shallow basement. On the east end of the profile is a Big Spring type epizonal granite intrusion near the basement surface.

Plate 4 is an east-west profile at latitude 38.24° that transects the northern edge of Wichita magnetic low. The Wichita

magnetic low is underlain by a non-magnetic granitic body at mid-crust. The Rice formation at the Precambrian surface is underlain by a northeast trending mafic body which gives rise to the positive gravity anomaly. There are two epizonal granitic plutons in southeastern Kansas and two mafic intrusions in western Kansas. The two positive spikes on the Precambrian surface in central Kansas are related to dike intrusion or faults.

Plate 5 is an east-west profile at latitude 37.81° that cuts through the central part of the Wichita magnetic low. There is a reversely magnetized mafic intrusion near the basement surface.

Plate 6 is an east-west profile along latitude 37.11°. There is no gravity data in the western half of the profile. The shallow basement in southeastern Kansas is made up of 1.36 b.y. granite/rhyolite. The Humboldt fault is less apparent on the structural profiles. Neither is there any obvious gravity signature. The positive gravity anomalies in southeastern Kansas are caused by intrusions that lie below the granite/rhyolite layer.

CONCLUSION

The new Kansas gravity data reveal many previously unidentified anomalies and basement trends. This regional survey should be followed up with more detailed surveys of local anomalies such as the Wichita magnetic low, the positive anomalies in southeastern Kansas, and the MGA near Saline county in central Kansas where the gravity signal decreases abruptly.

REFERENCES

Anderson, J.L., 1983, Proterozoic anorogenic plutonism of North America, in Medaris, L.G. and others, eds.: Proterozoic geology: Selected papers from an international Proterozoic symposium: Geol. So. Am. Memoir 161, p. 133-154.

Artemjev, M.E., and E.V. Artyushkov, 1971, Structure and isostasy of the Baikal rift and the mechanism of rifting: Jour. Geophys. Res., v. 76, p.1197-1211.

Baranov, W., 1975, Potential fields and their transformations in applied geophysics: Geopublication Associates, 121 page.

Batson, R.M., K. Edwards, and E.M. Eliason, 1975, Computer-generated shaded-relief images: Jour. Research, U.S. Geol. Survey, v. 3, no. 4, p. 401-408.

Bhattacharyya, B.K., 1964, Magnetic anomalies due to prism-shaped bodies with arbitrary polarization: Geophysics, v. 29, no. 4, p. 517-531.

Bickford, M.E., W.R. Van Schmus, and I. Zietz, 1986, Proterozoic history of the midcontinent region of North America: Geology, v. 14, p. 492-496.

Bickford, M.E., K.L. Harrower, W.J. Hoppe, B.K. Nelson, R.L. Nusbaum, and J.J. Thomas, 1981, Rb-Sr and U-Pb geochronology and distribution of rock types in the Precambrian basement of Missouri and Kansas, Part 1: Geol. Soc. Amer. Bull., v. 92, p. 323-341.

Bickford, M.E., K.L. Harrower, R.L. Nusbaum, J.J. Thomas, and G.E. Nelson, 1979, Preliminary geologic map of the Precambrian basement rocks of Kansas: Kansas Geological Survey Map M-9.

Bickford, M.E., D.G. Mose, G.W. Wetherill, and P.C. Franks, 1971, Metamorphism of Precambrian granite xenoliths in a mica peridotite at Rose Dome, Woodson County, Kansas: Part 1, Rb-Sr isotropic studies: Geol. Soc. Am. Bull., v. 82, p. 2863-2868.

Bird, P., 1984, Laramide crustal thickening event in the Rocky mountain foreland and Great Plains: Tectonics, v.3, p. 741-758.

Brigham, E.O., 1974, The fast Fourier transform: Prentice Hall, 255 page.

Brookins, D.G., 1970, The kimberlites of Riley county, Kansas: Kansas Geological Survey Bulletin 200, 32 page.

Brookins, D.G., H.O.A. Meyer, 1974, Crustal and upper mantle stratigraphy beneath eastern Kansas: Geophys. Res. Letters, v. 1, p. 269-272.

Brown, L., L. Serpa, T. Setzer, J. Oliver, S. Kaufman, R. Lillie, D. Steiner, and D.S. Steeples, 1983, Intra-crustal complexity in the U.S. midcontinent: preliminary result from COCORP surveys in N.E. Kansas: Geology, v. 11, p. 25-30.

Chandler, V. W., J. S. Koski, W. J. Hinze, and L. W. Braile, 1981, Analysis of multisource gravity and magnetic anomaly data sets by moving-window application of Poisson's theorem: Geophysics, v. 46, no. 1, p. 30-39.

Chandler, V. W., P. L. Bowman, W. J. Hinze, and N. W. O'Hara, 1982, Long-wavelength gravity and magnetic anomalies of the Lake

Superior region: in Geology and tectonics of the Lake Superior Basin, Wold, R. J., and Hinze, W. J., eds., Geol. Soc. Am. Memoir 156, 280 page.

Chase, C.G. and T.H. Gilmer, 1973, Precambrian plate tectonics,the Midcontinent gravity high: Earth and Planetary Science Letters, v. 21, p. 70-78.

Clark, S. P., ed., 1966, Handbook of physical constants : Geol. Soc. Am. Memoir 97, 548 page.

Cole, V. B., 1976, Configuration of the top of the Precambrian rocks in Kansas: Kansas Geological Survey Map M-7, scale 1:500,000, 1 sheet.

Cooley, J. W., and J. W. Tukey, 1965, An algorithm for machine calculation of complex Fourier series: Math. Computation, v. 19, p. 297-301.

Coons, R.L., G.P. Woollard, and G. Hershey, 1967, Structural significance of the mid-continent gravity high: Bull. Am. Assoc. Pet. Geol., v. 51, no. 12, p. 2381-2399.

Courtillot, V., 1982, Propagating rifts and continental breakup: Tectonics, v. 1, no. 3, p. 239-250.

Denison, R.E., E.G. Lidiak, M.E. Bickford, and E. Kisvarsanyi, 1984, Geology and geochronology of Precambrian rocks in the central interior region of the United States: U.S. Geol. Survey, Prof. Paper 1241-C, 20 page.

Emslie, R.F., 1978, Anorthosite massifs, rapakivi granite, and late Proterozoic rifting of North America: Precambrian Research, v.7, p. 61-98

Fleitout, L., and C. Froidevaux, 1983, Tectonic stresses in the lithosphere: Tectonics, v. 3, p. 315-324.

Garland, G.D., 1979, Introduction to Geophysics-Mantle, Core, and Crust: W.B. Saunders Company, 494 page.

Goodacre, A. K., 1973, Some comments on the calculation of the gravitational and magnetic attraction of a homogeneous rectangular prism: Geophys. Prospecting, v. 21, p. 66-69.

Gunn, P.J., 1974, Linear transformation of gravity and magnetic fields: Geophys. Prospecting, v. 23, p. 300-312.

Guinness, E.A., R.E. Arvidson, J.W. Strebeck, K.J. Schulz, G.F. Davies, and C.E. Leff, 1982, Identification of a Precambrian rift through Missouri by digital image processing of geophysical and geological data: Jour. Geophys. Res., v. 87, no. B10, p. 8529-8545.

Hahn, R.K., 1982, Upper mantle velocity structure in eastern Kansas from teleseismic P-wave residual: M.S. thesis, Department of Geology, University of Kansas, Lawrence, Kansas, 84 page.

Heiskanen, W.A., and F.A. Vening Meinesz, 1958, The earth and its gravity field: McGraw-Hill Book Company.

Hinze, W.J., ed., 1985, The utility of regional gravity and magnetic anomaly maps: Soc. Exploration Geophys.

Hinze, W.J., R.J. Wold, and N.W. O'Hara, 1982, Gravity and magnetic anomaly studies of Lake Superior: In Wold R.J. and W.J. Hinze, eds., Geology in Tectonics of the Lake Superior Basin, Geol. Soc. Am. Memoir 156, p. 203-222.

Horn, B. K. P., 1981, Hill shading and the reflectance map: Proceedings of the IEEE, v. 69, no. 1, p. 14-47.

International Association of Geodesy, 1967, special publication, no. 3., Geodetic reference system.

Jackson, J.D., 1963, Classical electrodynamics, John Wiley, 641 page.

Kane, M.F., 1962, A comprehensive system of terrain corrections using a digital computer: Geophysics, v. 27, p. 455-462.

Karki, P., L. Kivioja, and W.A. Heiskanen, 1961, Topographic-isostatic reduction maps for the world for the Hayford zones 18-1, Airy-Heiskanen system, T = 30 km: Publications of the isostatic Institute of the International Association of Geodesy, no. 35, 5 page.

Kellogg, O.D., 1954, Foundations of potential theory: Dover, 384 page.

King, E.R., and I. Zietz, 1971, Aeromagnetic study of the midcontinent gravity high of the central United States: Geol. Soc. Am. Bull., v. 82, p. 2187-2208.

Lambert, W.D., 1930, The reduction of observed value of gravity to sea level: Bull. geod., no. 26, p.128-130.

Longman, I. M., 1959, Formulas for computing the tidal acceleration due to the moon and the sun: Jour. Geophys. Res., v. 64, p. 2351-2356.

McGinnis, L.D., 1970, Tectonics and the gravity field in the continental interior: Jour. Geophys. Res., v. 75, p. 317-331.

McGinnis, L.D., M.G. Wolf, J.J. Kohsmann, and C.P. Ervin, 1979, Regional free air gravity anomalies and tectonic observations in the United States, Jour. Geophys. Res., v. 84, p. 591-601.

McKenzie, D., 1978, Some remarks on the development of sedimentary basins: Earth and Planetary Science letters, v. 40, p. 25-32.

McLelland, J.M., 1986, Pre-Grenvillian history of the Adirondacks as an anorogenic, bimodal caldera complex of mid-Proterozoic age, Geology, v. 14, p. 229-233.

Merriam, D.F., 1961, Structural contour map of the Mississippian rocks in Kansas: Kansas Geological Survey map series M-11.

Merriam, D. F., 1963, The geologic history of Kansas: Kansas Geological Survey Bulletin 162, 317 page.

Mittermayer, E., 1969, Numerical formulas for the Geodetic Reference System 1967: Bullentino di Geofisca Teorica ed Applicata, v. 11, p. 96-107.

Morelli, C., C. Ganter, T. Honkasalo, R.K. McConnell, J.G. Tanner, B. Szabo, V. Votila, and C.T. Whalen, 1974, The International Gravity Standardization Net 1971 (IGSN71): Publ. Spec. Bur. Cent. Assoc. Int. Geod., Paris, No. 4.

Nelson, B.K. and D.J. DePaolo, 1985, Rapid production of continental crust 1.7-1.9 b.y. ago: Nd and Sr isotopic evidence from the basement of the North American midcontinent: Geol. Soc. Am. Bull., v. 96, p. 746-754.

Nettleton, L.L., 1976, Gravity and magnetics in oil prospecting: McGraw Hill Book Company, 464 page.

Ocola, L.C., and R.P. Meyer, 1973, Central north American rift system:1. Structure of the axial zone from seismic and gravimetric data: Jour. Geophys. Res., v. 78, p. 5173-5194.

Parker, P.L., 1972, The rapid calculation of potential anomalies: Geophysical Journal of the Royal Astronomical Society, v. 31, p. 447-455.

Paterson, N.R., and C.V. Reeves, 1985, Applications of gravity and magnetic surveys: The state-of-the-art in 1985: Geophysics, v. 50, no. 12, p. 2558-2594.

Poisson, S.D., 1826, M moire sur la th du magn tisme: M moires de l' Acad mie Royale des Sciences de l' Institut de France, p. 247-348.

Sampson, R.J., 1978, Surface II graphics system: Kansas Geological Survey series on spatial analysis number 1.

Sawyer, D.S., 1985, Total Tectonic Subsidence: A parameter for distinguishing crust type at the U.S. Atlantic continental margin: Jour. Geophys. Res., v. 90, p. 7751-7769.

Serpa, L., T. Setzer, H. Farmer, L. Brown, J. Oliver, S. Kaufman, J. Sharp, and D. W. Steeples, 1984, Structure of the southern Keweenawan Rift from COCORP surveys across the Midcontinent Geophysical Anomaly in northeastern Kansas: Tectonics, v. 3, p. 367-384.

Simpson, R.W., R.C. Jachens, and R.J. Blakely, 1983, AIRYROOT : A FORTRAN program for calculating the gravitational attraction of an Airy isostatic root out to 166.7 km, USGS open file report, 83-883, 65 page, Menlo Park, California.

Simpson, R.W., R.C. Jachens, R.J. Blakely, and R.W. Saltus, 1986, A new isostatic residual gravity map of the conterminous United States with a discussion on the significance of isostatic residual anomalies: Jour. Geophys. Res., v. 91, p. 8348-8372.

Singleton, R. C., 1969, An algorithm for computing the mixed radix fast Fourier transform: Institute of Electrical and Electronics Engineers Transactions on Audio and Electroacoustics, vol. AU-17, no. 2, p. 93-100.

Somanas, C, 1984, A comprehensive geophysical interpretation of the midcontinent geophysical anomaly in northeastern Kansas: M.S. Thesis, Department of Physics, University of Kansas, 88 page.

Stavnes, S. and D. W. Steeples, 1982, Geothermal resources of Kansas- map showing areas of geothermal potential: Kansas Geological Survey special map.

Steeples, D.W., 1976, Preliminary crustal model for northwest Kansas (abstract): EOS (Am. Geophys. Union Trans.), v. 57, no. 12, p. 961.

Steeples, D.W., 1980, Micro-earthquake recorded by the Kansas Geological Survey: Kansas Geological Survey Journal, v. 2, no. 3, p. 14.

Steeples, D.W., 1981, Kansas earthquakes - 1979: Earthquake Notes, v. 52, no. 2, p. 42-48.

Steeples, D.W., and M.E. Bickford, 1981, Piggyback drilling in Kansas: An example for the continental scientific drilling program: EOS (Am. Geophys. Union Trans.), v. 62, no. 18, p.473-476.

Steeples, D.W., and S. Stavnes, eds., 1982, Assessment of the geothermal resources in Kansas: Kansas Geological Survey open file report 82-22.

Stewart, S.W., 1968, Crustal structure in Missouri by seismic refraction methods: Bulletin of Seismological Society of America, v. 58, p. 291-323.

Thomas, J.J., R.D. Shuster, and M.E. Bickford, 1984, A terrane of 1350- to 1400-m.y.-old silicic volcanic and plutonic rocks in the buried Proterozoic of the midcontinent and in the Wet Mountains, Colorado: Geol. Soc. Am. Bull., v. 95, p. 1150-1157.

Van Schmus, W.R., M.E. Bickford, and I. Zietz, 1986, Early and middle Proterozoic provinces in the central United States: in Am. Geophys. Union Geodynamic Series, v. 15: A. Kroner, ed.

Van Schmus, W.R., and W.J. Hinze, 1985, The midcontinent rift system: Ann. Rev. Earth Planet. Sci., v. 13, p. 345-383.

Van Voorhis, G.D., and T.M. Davis, 1964, Magnetic anomalies north of Puerto Rico: trend removal with orthogonal polynomials: Jour. Geophys. Res., v. 69, p. 5363-5371.

Vargas, J., 1983, Deterministic deconvolution model for high resolution seismic data in Kansas: M.S. Thesis, Department of Physics, University of Kansas, 80 page.

Wernicke, B. and B.C. Burchfiel, 1982, Modes of extensional tectonics: Journal of Structural Geology, v. 4, no. 2, p. 105-115.

Wise, D.U., R. Funiciello, M. Parotto, and F. Salvini, 1985, Topographic lineament swarms: clues to their origin from domain analysis of Italy: Geol. So. Am. Bull., v. 96, p. 952-967.

Wold, R.J. and W.J. Hinze, eds., 1982, Geology and Tectonics of Lake Superior Basin: Geol. Soc. Am. Memoir 156, Boulder, Colorado.

Woollard, G.P., 1959, The relation of gravity to geology in Kansas: in Hambleton, W.W., ed.: Symposium on geophysics in Kansas: Kansas Geological Survey Bulletin 137, p. 63-103.

Woollard, G.P., 1963, An analysis of the reliability of gravimeter measurements: Hawaii Institute of Geophysics scientific report number 3, University of Hawaii.

Woollard, G.P., 1966, Regional isostatic relations in the United States: in J.S. Steinhart and T.J. Smith, eds.,: The earth beneath the continents, Geophys. Monograph 10, p. 557-594, Am. Geophys. Union, Washington, D.C.

Yarger, H.L., 1981, Aeromagnetic survey of Kansas: EOS (Am. Geophys. Union Trans.), v. 62, no. 17, p. 173-178.

Yarger, H.L., 1983, Regional interpretation of Kansas aeromagnetic data: Kansas Geological Survey Geophysics Series 1.

Yarger, H.L., 1985, Kansas basement study using spectrally filtered aeromagnetic data: in Hinze, W.J., ed., The utility of regional gravity and magnetic anomaly maps: Soc. Exploration Geophys., p. 213-232.

Yarger, H.L., 1986, Kansas aeromagnetic data: Steeples, D.W., ed., Symposium of Geophysics in Kansas- a 25 year update, Kansas Geological Survey Bulletin.

Yarger, H.L. and C. Lam, 1982, Gravity measurements in Kansas: in Steeples, D.W. and S. Stavnes, eds.: Assessment of the geothermal

resources of Kansas, Kansas Geological Survey open file report 82-22.

Zeller, D.E., ed., 1968, The stratigraphic succession in Kansas: Kansas Geological Survey Bulletin 189, 81 page.

PLATE 1

BOUGUER GRAVITY MAP OF KANSAS

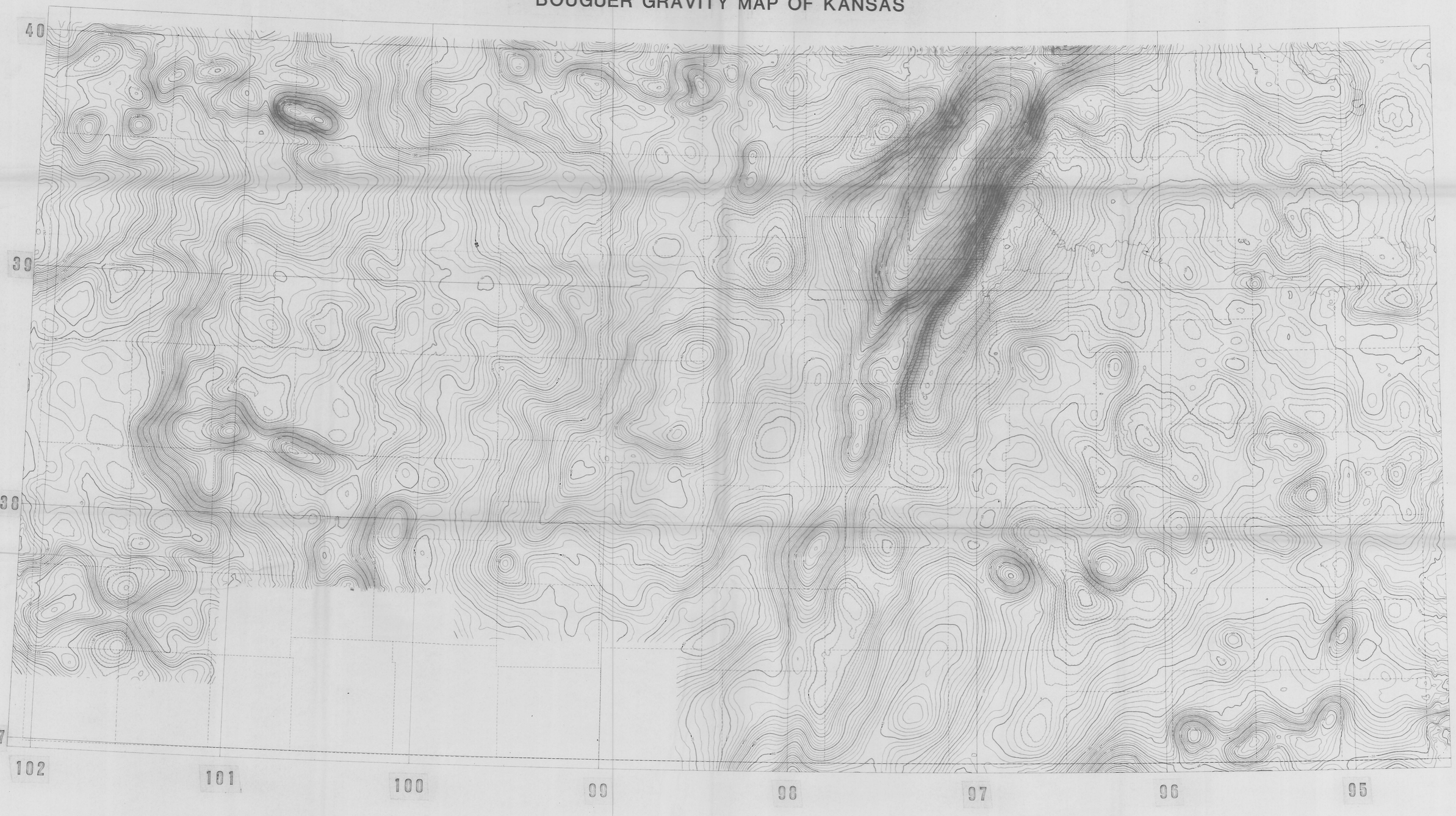

PLATE 2

LATITUDE = 39.59°

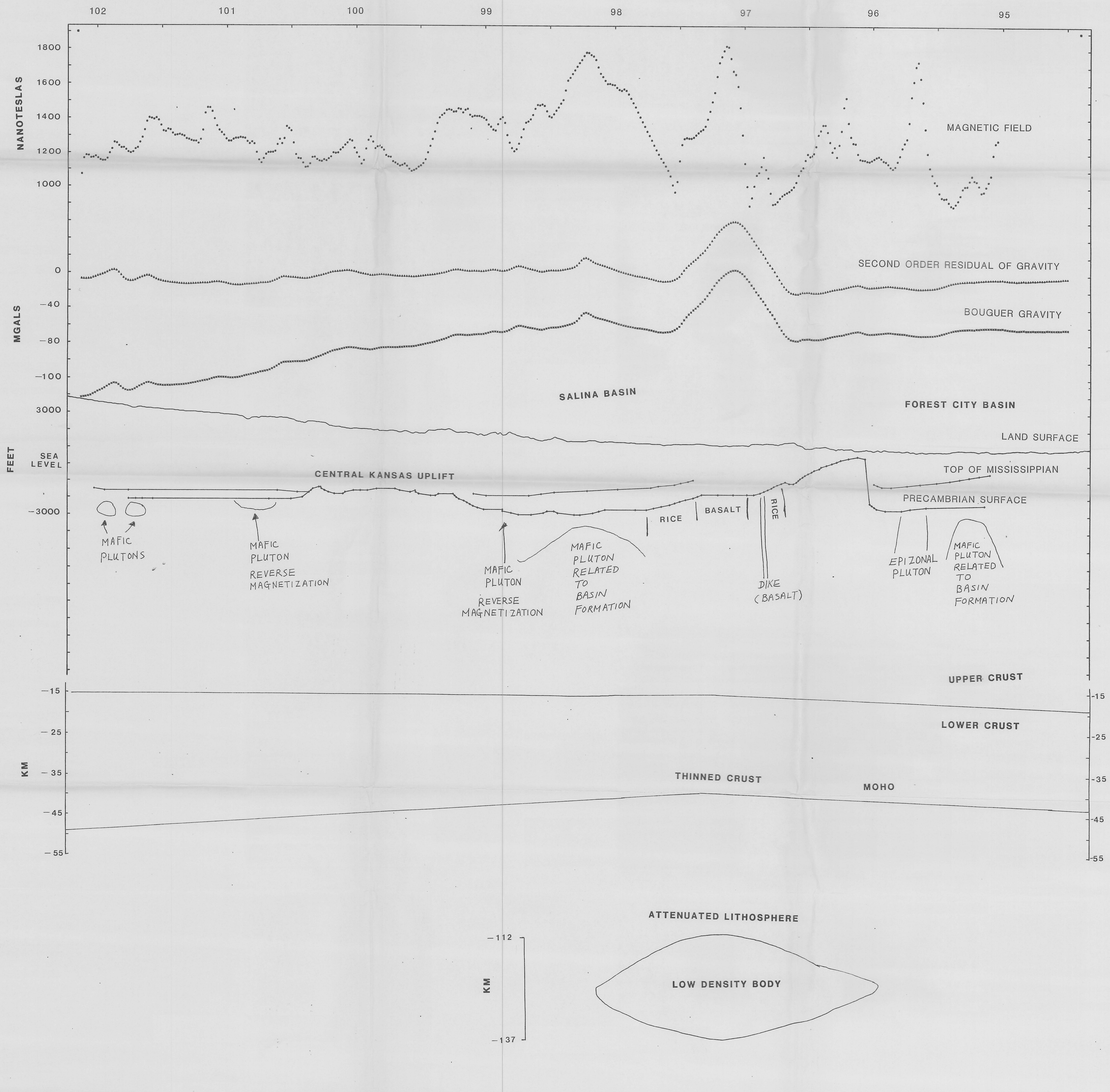

PLATE 3

LATITUDE = 38.68°

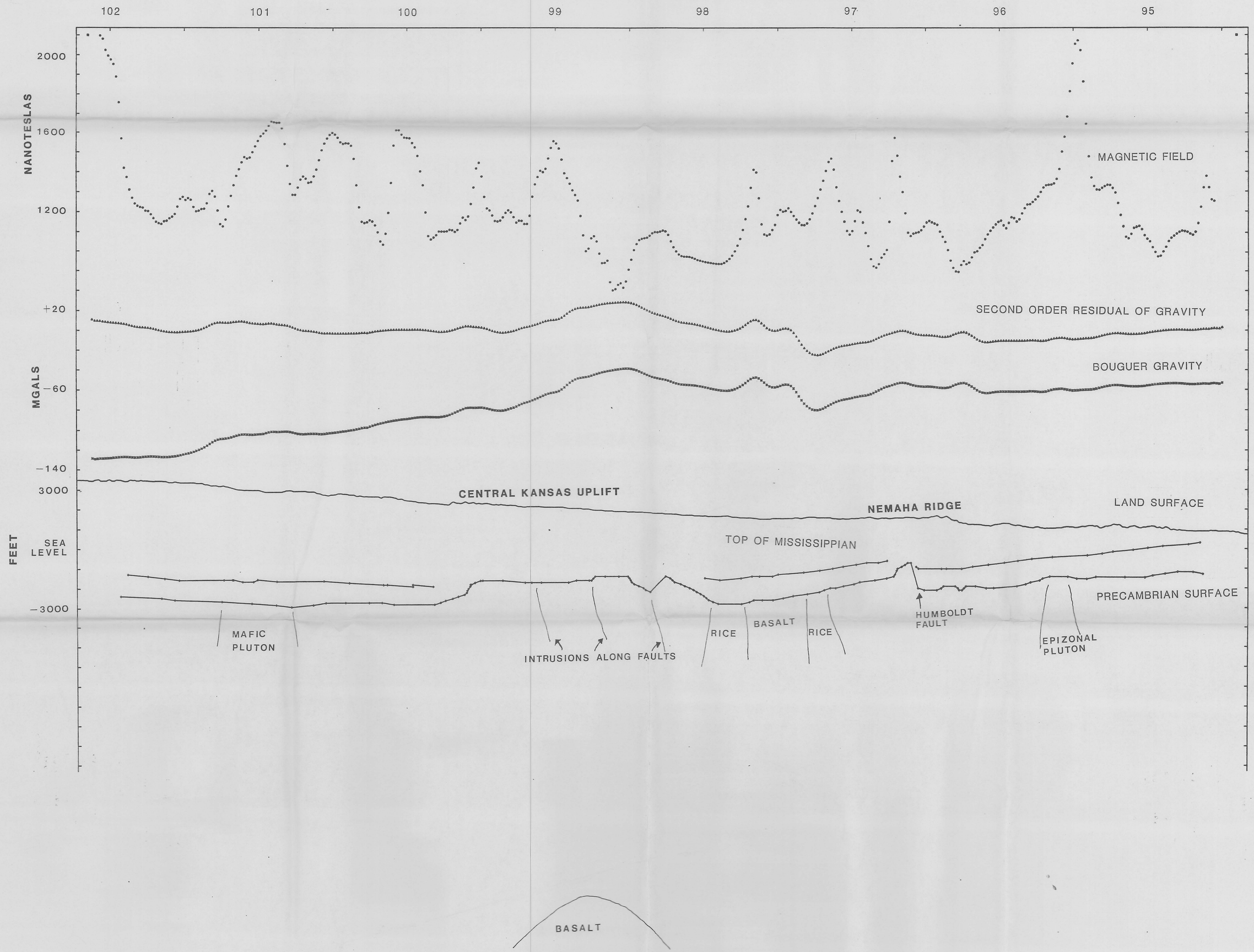

PLATE 4

LATITUDE = 38.24°

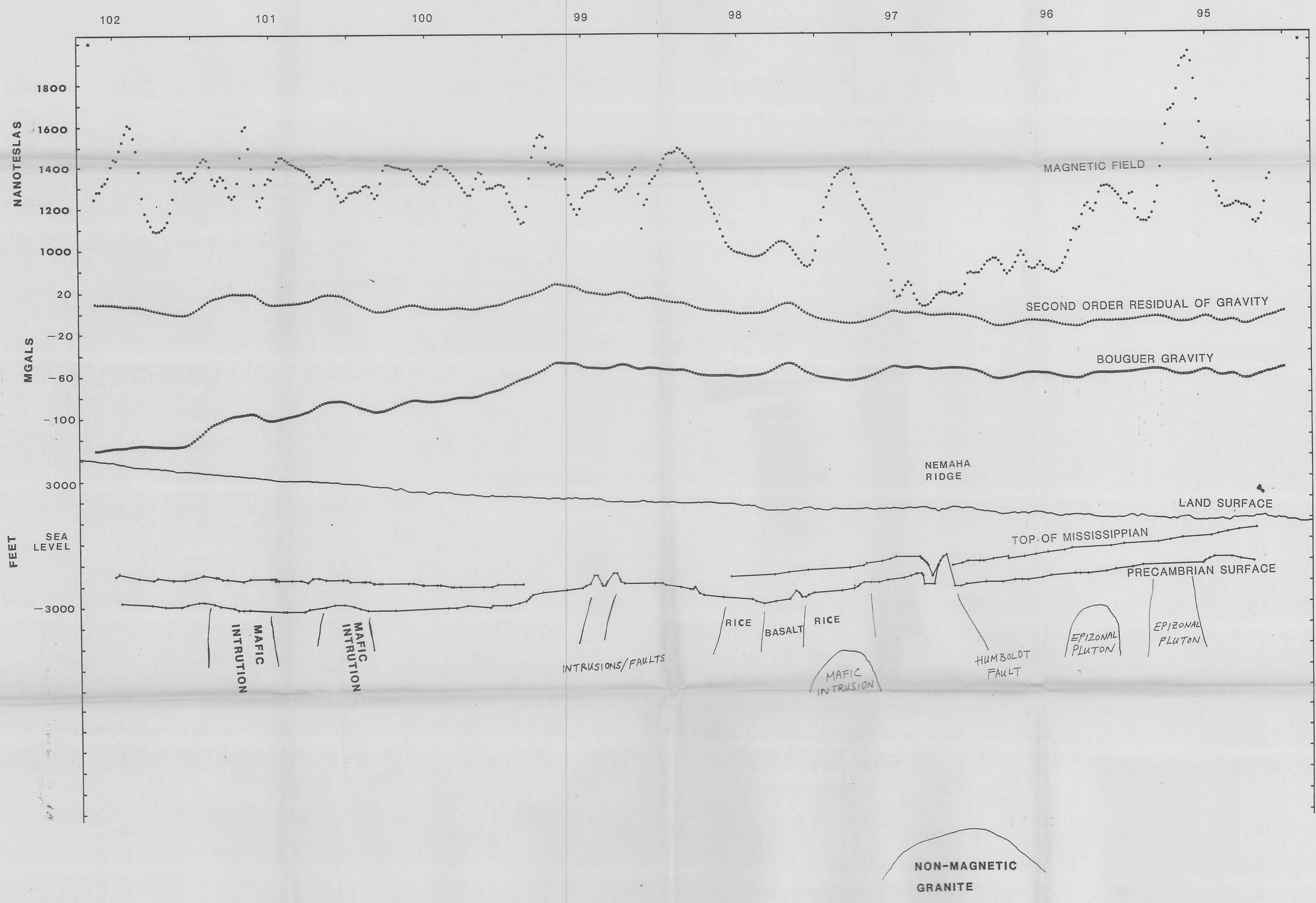

PLATE 5

LATITUDE = 37.81°

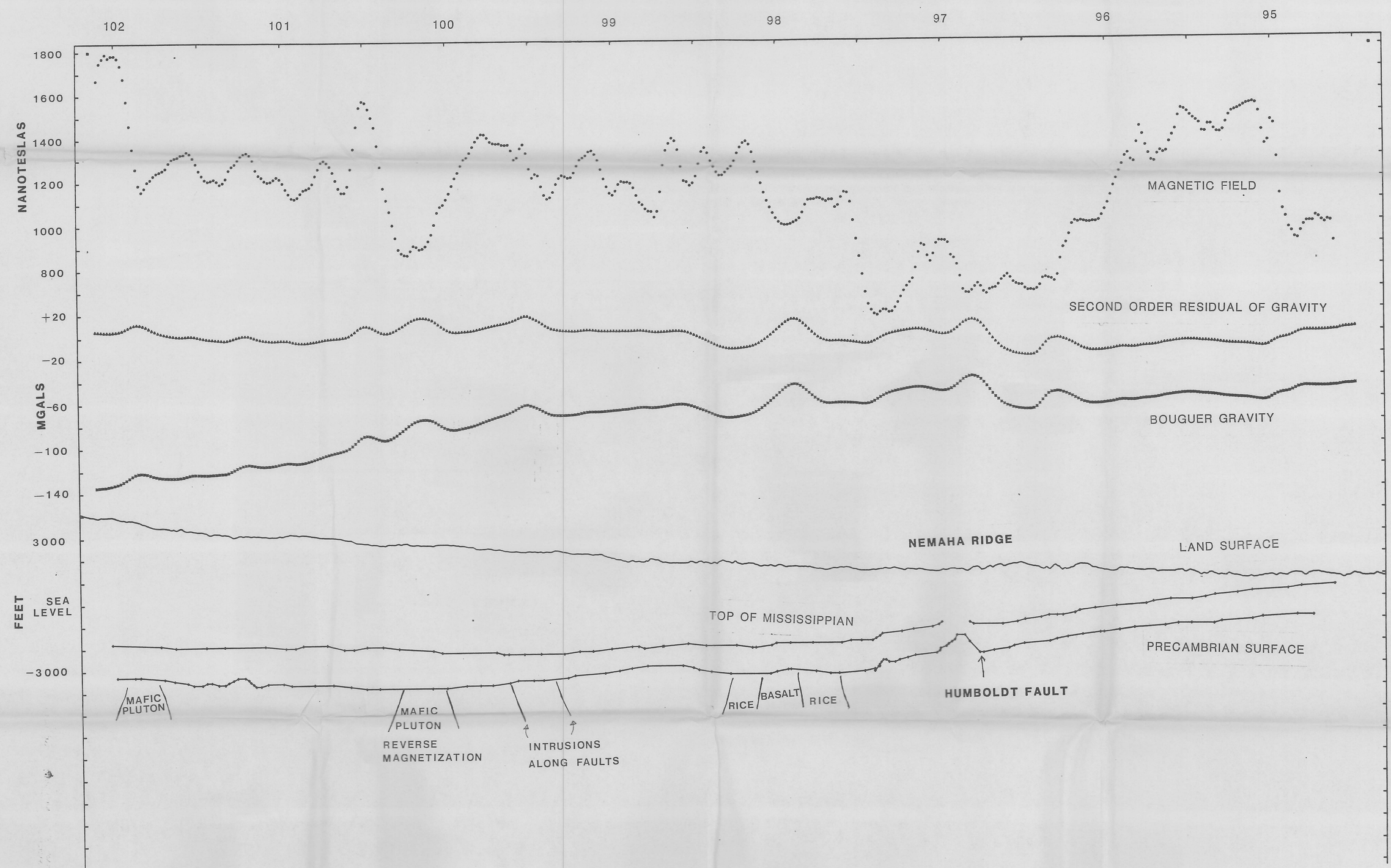

PLATE 6

LATITUDE= 37.11°